

ELECTRONIC PROPERTIES OF BIOLOGICALLY IMPORTANT MOLECULES

THE UNIVERSITY
OF ALABAMA
BIRMINGHAM
LIBRARY

23 OCT 1968

11200 | 113848

547.52

BUR

Foreword

This thesis, entitled "Electronic properties of biologically important molecules", which is being submitted to the University of Aston in Birmingham for the degree of Doctor of Philosophy, is an account of the work done under the supervision of Professor F. M. Page, B.A., Ph.D., Sc.D., and Dr. A. C. M. Finch, B.Sc., Ph.D. It has not been submitted for an award of any other academic institution and except where references are given in the text the work described is original and has not been done in collaboration.

I should like to express my gratitude to Professor F. M. Page for his guidance and encouragement in the development of this thesis and to the many other members of the University of Aston for their helpful discussions and suggestions on particular aspects of the work.

I should also like to thank the Department of Pharmacy for the Research Assistantship which enabled the research to be done.

Marion Burdett, B.Sc.

June 1968

S U M M A R Y

The magnetron technique, which had been developed for the measurement of gaseous electron affinities from observations on the equilibrium between atoms electrons and ions at a heated metal surface, was applied to the measurement of electron affinities of some classes of aromatic compounds which show biological activity. The stabilities of a number of anions derived from molecules and radicals were obtained, but it was found that the limitations of the method precluded useful measurements from being made on large polyatomic molecules. Methods were therefore considered which would enable relative electron affinities of these larger molecules to be estimated, and which would also give values for the molecules studied successfully by the magnetron technique. These could then be used as reference values.

It has been claimed that an electron capture detector developed for use in gas chromatography could be used to measure electron affinities. After some preliminary experiments to determine the optimum operating conditions of such a detector the compounds which have been previously investigated in the magnetron were introduced into the carrier gas stream flowing through an electron capture detector. The attenuation in electron concentration produced by a known number of acceptor molecules was measured and the results analysed. It was found however that the detector response was proportional to the total collision cross section of the molecules rather than the electron affinity and it was not therefore possible to compare the results from the two methods.

Finally some other methods which have been used to estimate electron affinities were considered. The results obtained by these techniques i.e. charge transfer spectroscopy and polarography, together with some calculated values are discussed and compared with the results obtained in the magnetron.

TABLE OF CONTENTS

	Page
Chapter 1 - <u>Introduction</u>	... 1
Chapter 2 - <u>The magnetron technique</u>	
2.1 Introduction	... 6
2.2 Emission of electrons from clean metal surfaces	... 7
2.3 Emission of electrons and negative ions in the presence of a gas	... 9
2.4 Theory of the magnetron	... 11
2.5 Design of the magnetron	... 14
2.6 Ancillary equipment	... 16
2.7 Measurement of filament temperature	... 17
2.8 Measurement of the apparent electron affinity	... 18
2.9 Calculation of electron affinities from the measured energies	... 20
2.10 Summary	... 26
Chapter 3 - <u>Application of the magnetron technique to the measurement of the stability of some negative ions</u>	
3.1 Introduction	... 27
3.2 Experimental observations on hydrocarbons	... 27
3.3 Discussion of observations on hydrocarbons	... 34

Table of Contents (continued) ...	Page
3.4 Experimental observations on fluorocarbons ...	44
3.5 Discussion of observations on fluorocarbons ...	50
3.6 Experimental observations on quinones ...	60
3.7 Discussion of observations on quinones ...	65
Chapter 4 - <u>The electron capture cell</u>	
4.1 Introduction ...	71
4.2 The electron capture cell and ancillary apparatus ...	79
4.3 Preliminary experiments with the electron capture cell ...	83
4.4 Experimental studies on various compounds using the electron capture cell ...	94
4.5 Discussion of results obtained in the electron capture cell ...	108
Chapter 5 - <u>Values of electron affinities obtained by other methods</u>	
5.1 Introduction ...	118
5.2 Calculated values of electron affinities ...	120
5.3 Charge transfer spectra and electron affinities ...	125
5.4 Polarographic half wave reduction potentials and electron affinities ...	128
5.5 Dipole moments and electron affinities ...	131
5.6 Conclusion ...	136
References ...	138

TABLE OF FIGURES

Figure		Following Page No:
<u>CHAPTER 2.</u>		
2.1	Forces on an electron in a magnetic field	11
2.2	Design of the magnetron	14
2.3	Needle valve	15
2.4	Sample container	15
2.5	Heated sample container	15
2.6	Pumping system	16
2.7	Design of magnet	16
2.8	Electrical circuit for magnetron	17
2.9	Filament calibration graph	18
2.10	Electron work function graph for iridium	18
<u>CHAPTER 3.</u>		
3.1	Log-log plot for benzene on iridium	28
3.2	Ratio plot for benzene on iridium	28
3.3	Ratio plot for naphthalene on platinum	29
3.4	Log i_1 against $10^4/T$ for naphthalene on iridium	29
3.5	Ratio plot for naphthalene on iridium	30
3.6	Ratio plot for anthracene on iridium	30
3.7	Ratio plot for azulene on iridium	31
3.8	Log i_1 against $10^4/T$ for some polycyclic hydrocarbons	31

Figure		Following Page No:
3.9	Ratio plot for perfluorobenzene on iridium 44
3.10	Ratio plot for pentafluorobromobenzene on iridium 44
3.11	Ratio plot for pentafluorochlorobenzene on iridium 45
3.12	Ratio plot for 1,2,3,4-tetrafluoro- naphthalene on iridium 45
3.13	Log i_i against $10^4/T$ for perfluoro- cyclohexane on iridium 47
3.14	Ratio plot for perfluorodecalin on iridium 47
3.15	Heats of adsorption on platinum against those on iridium 54
3.16	Ratio plot for benzoquinone on iridium 60
3.17	Ratio plot for naphthaquinone on iridium 60
3.18	Ratio plot for anthraquinone on iridium 61
3.19	Ratio plot for chloranil on iridium 61
3.20	Ratio plot for fluoranil on iridium 62
3.21	Ratio plot for chloroquinone on iridium 62
3.22	Ratio plot for 2,6 dichlorobenzoquinone on iridium 62

CHAPTER 4.

4.1	The electron capture detector 79
4.2	Electrical circuit for electron capture detector 79
4.3	Gas line for electron capture detector 81

Figure		Following Page No:
4.4	Saturator 81
4.5	Bridge network for oven thermostat 83
4.6	Amplifier circuit diagram 83
4.7	Graph of detector current against applied D.C. voltage 85
4.8	Graph of detector current against applied pulsed voltage 87
4.9	Graph of detector current against pulse duration 88
4.10	Graph of electrons per pulse against pulse interval 88
4.11	Graph showing effect of rate of gas flow on detector current 91
4.12	Graph of detector current against excess pressure 92
4.13	Graph showing effect of temperature on detector current 92
4.14	($\epsilon_0/\epsilon - 1$) against concentration of naphthalene 102
4.15	($\epsilon_0/\epsilon - 1$) against concentration of anthracene 102
4.16	($\epsilon_0/\epsilon - 1$) against concentration of perfluorodecalin 103
4.17	($\epsilon_0/\epsilon - 1$) against concentration of perfluorocyclohexane 103

Figure		Following Page No:
4.18	($\epsilon_0/\epsilon - 1$) against concentration of benzoquinone 104
4.19	($\epsilon_0/\epsilon - 1$) against concentration of anthraquinone 104
4.20	($\epsilon_0/\epsilon - 1$) against concentration of chloranil 105
4.21	($\epsilon_0/\epsilon - 1$) against concentration of oxygen 105
4.22	Log K against $1/T^0K$ for several compounds 107
4.23	Log K against log area of molecule 116

Chapter 1 - Introduction

The properties of molecules depend to a large extent on their outer electronic structure. Elements which belong to the same group of the periodic table, and have different core structures but the same outer electronic configuration, are very similar in their chemical behaviour. The reactivity of molecules is also affected by the enthalpies involved in the addition or removal of outer electrons, that is by their electron affinities and ionisation potentials respectively.

A knowledge of these energies would therefore be extremely useful in predicting the chemical behaviour of molecules. Apart from the field of pure chemistry, the science of biochemistry, which is more specifically concerned with reactions occurring in living organisms, is becoming increasingly involved in attempts to explain phenomena at a submolecular level in terms of electron interaction. A great deal of progress has been made on the molecular scale in unravelling the complex cycles of intermediary metabolism which are involved in preparing foodstuffs for their final oxidation. This oxidation of reduced pyridine nucleotides, is done by a series of reactions, known as the electron transport chain, where the initial substrate is oxidised, and the resulting electron is passed on down a series of intermediates of successively lower redox potentials, until, finally, molecular oxygen is reduced. The mechanism for the transfer of the electrons is not known but Szent Gyorgyi⁽¹⁾ has considered several possible methods. In order adequately to explain these types of reactions it is necessary to know the energies involved in the addition or removal of electrons to the molecules which make up the chain.

Electron transfer is also important in understanding the mode of action of some drugs (2-5) and in explaining the causes of some diseases. It was suggested on theoretical grounds (6-7) that the carcinogenicity of some aromatic hydrocarbons may be due to their electron accepting properties and this is supported by the evidence of Allison and Lightbrown (8) who showed that an important step in carcinogenesis, by a variety of compounds was their ability to disturb mitochondrial electron transport. Thus it can be seen that a knowledge of the energies with which electrons are bound to molecules is important in any theoretical attempt to rationalise their properties.

Biological systems are, however, extremely complex and electron transfer is affected by many parameters other than the ionisation potential and electron affinity of the donating and accepting molecules respectively. Enzymes lower activation energies, and many reactions take place in a lipid matrix where energy values may be very different from any measured in aqueous solution, or in the gas phase. However, in the absence of a method for measuring electron affinities in biological media a knowledge of the gas phase values would be a useful guide.

The energy required to remove one electron from the highest filled orbital of a molecule or atom to infinity is its ionisation potential, and the work done in bringing an electron from infinity to the lowest unfilled orbital is its electron affinity. There are considerable data on ionisation potentials obtained by various methods, experimental and theoretical (9)-(13) but there are very few reliable measurements of electron affinities. Several direct experimental techniques have been

applied such as electron impact ⁽¹⁴⁾; measurements on equilibria between electrons, ions and molecules ⁽¹⁵⁻¹⁷⁾; and, photodetachment studies ⁽¹⁸⁻¹⁹⁾. Until recently, however, these methods have been applied mainly to simple molecules such as the halogens. Electron affinities have also been found theoretically from lattice energy calculations ⁽²⁰⁻²¹⁾, and by applying Hückel M.O. theory to the calculation of molecular orbital energies for some organic compounds, in particular aromatic hydrocarbons ⁽²²⁻²⁵⁾. Most of the experimental methods mentioned earlier for measuring electron affinities are very limited in their application and could not be applied to large polyatomic molecules such as are found in biological systems. One of the techniques however - using equilibrium measurements made in a magnetron - originally described by Sutton and Mayer ⁽¹⁷⁾ and developed by Page has been used to measure the gas phase electron affinities of many polyatomic species ⁽²⁶⁻⁴⁰⁾.

This technique was applied to the measurement of the electron affinities of aromatic hydrocarbons in an attempt to correlate their electron affinities with carcinogenic activity. Benzene naphthalene and anthracene were studied but since the higher, polycyclic, hydrocarbons some of which are known to have carcinogenic properties, had very low vapour pressures it was not possible to maintain a high enough concentration of these molecules in the magnetron to give meaningful results. Besides hydrocarbons a series of quinones was studied in the magnetron. Recently a review has been published on the biological activity of these compounds ⁽⁴¹⁾ which quotes as

examples - vitamin K, 2 methyl-napthaquinone with a 3 phytyl side chain, and the more recently discovered ubiquinones which are substituted benzoquinones and which form part of the electron transport chain. The electron affinities of benzoquinone, naphthaquinone, anthraquinone, and some substituted benzoquinones were measured but the substituted napthaquinones and anthraquinones did not have sufficiently high vapour pressures even when the sample was heated.

Recently an electron capture detector, developed for gas chromatography ⁽⁴²⁾ has been used to obtain electron affinities ⁽⁴³⁾ and this offered a method which could be applied to large, relatively involatile, molecules. After a preliminary study of the operating conditions of the cell, the compounds which had been previously studied in the magnetron were introduced into the detector and the resulting electron attenuation measured. This was to enable a comparison to be made between the electron affinities obtained by the two methods. Alternatively, if the detector gave only relative values it would be possible to extrapolate from data obtained by both methods to the electron affinity of molecules such as naphthalene, which is predicted to be of the order of a few tenths of an eV, and below the limit which could be measured in the magnetron. In order to obtain a more reliable comparison it was desirable to have additional values of electron affinities measured by both methods.

Fluorocarbons were therefore studied since their relatively high volatility, and expected higher electron affinities, ~~by a~~ compared ~~on~~ with the hydrocarbons were likely to enable comparative data to be obtained from the two methods.

Finally some other methods such as charge transfer spectroscopy and polarography, which have been applied to the measurement of electron affinities, were considered together with some calculated values and compared with the results obtained in the present work.

CHAPTER 2 - THE MAGNETRON TECHNIQUE2.1 Introduction

The magnetron technique for the measurement of electron affinities in the gas phase was originally developed by Sutton and Mayer⁽¹⁷⁾ and was subsequently modified by Page⁽²⁶⁾. The apparatus is essentially a triode valve, the cathode of which is an electrically heated metal filament. The electrons emitted by this filament are drawn across to a concentric anode by means of an applied voltage, and the resulting current is measured. In the presence of gas molecules which can capture electrons part of the measured anode current will be due to the negative ions formed by electron attachment at the filament. In order to measure the fraction of the total current which is carried by the negative ions, a solenoidal magnetic field is applied. The electrons describe helical paths around the filament and are caught by the third electrode, a squirrel cage grid between the filament and the anode. The negative ions, which are much heavier than the electrons will be virtually unaffected by the magnetic field and will be collected at the anode. The resulting ion current may therefore be measured.

From measurements of the electron and ion currents, and a knowledge of the concentration of the acceptor molecules it is possible to calculate the equilibrium constant for the reaction leading to ion formation. The enthalpy of this reaction is the electron affinity of these molecules. It is therefore necessary to study the factors which affect the emission of electrons and ions from heated metal surfaces.

2.2 Emission of electrons from clean metal surfaces

The rate of electron emission from a heated metal surface is described by Richardsons equation for thermionic emission. It may be derived by consideration of the equilibrium existing between electrons leaving and returning to the surface of the metal. The following derivation is after Moelwyn-Hughes⁽⁴⁵⁾. It is based on the assumption that the electrons in the vacuum are in equilibrium with those in the metal. The molecular thermodynamic chemical potential μ may be expressed in terms of the free energy A, and the total number of particles in a system N, by :

$$\mu = \left(\frac{\delta A}{\delta N} \right)_{TV} \dots \dots \dots (2.1)$$

The free energy may be expressed in terms of the partition function per mole, f, as :

$$A = -NkT \ln f \dots \dots \dots (2.2)$$

Where k is the Boltzman constant.

Differentiating equation 2.2 with respect to N at constant temperature and volume one obtains :

$$dA/dN = -kT \left[\ln f + (d \ln f / d \ln N) \right] = \mu \dots \dots (2.3)$$

The partition function for a particle of mass m_e and degeneracy g, moving freely in a system containing N particles of the same kind at temperature T and total volume V is

$$f = g(2\pi m_e kT)^{3/2} V e/h^3 N \dots \dots \dots (2.4)$$

Where h is Planck's constant and e is the exponential factor.

Therefore

$$\mu = -kT \ln \left[g(2\pi m_e kT)^{3/2} / h^3 n \right] \dots \dots \dots (2.5)$$

where n is the number concentration.

The chemical potential μ of the electrons in the gas is given by

$$\mu = -kT \ln \left[g (2\pi m_e kT)^{3/2} / h^3 n \right] + u_g \dots \dots (2.6)$$

where u_g is the potential energy of the electrons in the gas.

The chemical potential of the electrons inside the metal μ_m is

$$\mu_m = \epsilon_0 - u_m \dots \dots \dots (2.7)$$

where ϵ_0 is the Fermi energy and u_m is the potential energy of the electrons in the metal.

By equating the chemical potentials of the electrons in the gas and in the metal the equilibrium concentration of the electrons in the gas is obtained as

$$n = g (2\pi m_e kT)^{3/2} / h^3 \exp - \left[(u_g - u_m) - \epsilon_0 \right] / kT \dots (2.8)$$

The saturation current emitted from unit area of the metal surface is

$$i = n \bar{\omega} (e) \dots \dots \dots (2.9)$$

where n is the total number of electrons ^{per sec} and $\bar{\omega}$ the average velocity in the direction perpendicular to and towards the metal surface and e is the electronic charge.

$$\text{Since } \bar{\omega} = (kT/2\pi m)^{1/2} \text{ and } g = 2$$

and if a fraction of the electrons r is reflected back into the gas the saturation current emitted per unit area is

$$i = \frac{(1-r) 4\pi m_e e (kT)^2}{h^3} \exp - (\epsilon_a - \epsilon_0) / kT \dots (2.10)$$

where $\epsilon_a = (u_g - u_m)$, the difference in the potential energies of the two phases ($\epsilon_a - \epsilon_0$) is known as the thermionic work function, and is the energy required to remove an electron from

the metal to infinity.

Equation (2.10) is known as Richardson's equation and may be used to calculate the number of electrons emitted by a filament at a known temperature and of known work function. Hence the current flowing between the filament and anode of the magnetron may be calculated. This derivation of equation (2.10) has assumed an equilibrium existing at the surface of the filament between electrons evaporating from, and condensing on to, the surface. This implies that the external voltage applied between the filament and anode to draw the electrons across does not affect the rate of evaporation. Since the voltages used are small the Schottky effect will not be appreciable and the assumption will be valid.

2.3 Emission of electrons and negative ions in the presence of a gas

The equation describing thermionic emission from clean surfaces has been derived above. If the work function χ of the filament material is not greatly altered by a sparse layer of molecules absorbed on the surface⁽²⁶⁾, and if the fraction of the surface covered is θ , electron emission will occur from an area $(1 - \theta)$, and Richardson's equation may be written as

$$i_e = A(1-r)(1-\theta)4\pi m_e k^2 T^2 / h^3 \exp - \chi / RT \dots \dots \dots (2.11)$$

$$\text{or } i_e = BA(1-\theta)T^2 \exp - \chi / RT \dots \dots \dots (2.12)$$

Where $B = (1-r)4\pi m_e k^2 / h^3 = 120 \text{ amps cm}^{-2} \text{ degree}^{-2}$, assuming a transmission factor of unity.

If the gas molecules adsorbed on the surface form negative ions by electron attachment, an equilibrium will be set up between the

molecules, electrons, and negative ions. The energy involved in the formation of a negative ion may be regarded as the algebraic sum of the energies required to remove an electron from the metal (the work function of the metal filament) and the energy released on bringing an electron from infinity to the lowest unoccupied orbital of the molecule. If adsorption on to the filament occurs, the exothermic energy of adsorption will also be included in the total energy of negative ion formation.

Hence the ion current derived from an area $A \text{ cm}^2$ of the filament is

$$i_i = CAT^m \theta \exp \left[(E - q_A - \chi')/RT \right] \quad \dots \quad (2.13)$$

where E is the electron affinity of the acceptor molecule, q_A is its activation energy for adsorption on to the filament and χ' is the work function of the filament in the presence of adsorbed molecules. If θ is small, χ' may be taken to be the same as χ (26).

Combining equations 2.12 and 2.13, one obtains

$$i_e/i_i = \frac{BT^{2-m}}{C} \frac{1-\theta}{\theta} \exp \left[(q_A - E)/RT \right] \quad \dots \quad (2.14)$$

The Langmuir relationship for the fraction of the surface covered is given (46) by

$$= \frac{\alpha u}{v + \alpha u} \quad \dots \quad (2.15)$$

where u is the number of molecules striking one cm^2 of the surface per second and is proportional to the pressure p of the gas. α is the proportion which adhered and v is the rate constant for evaporation. Therefore equation (2.14) may be rewritten

$$i_e/i_i = \frac{BT^{2-m}}{C} \frac{v}{\alpha u} \exp \left[(q_A - E)/RT \right] \quad \dots \quad (2.16)$$

v may be written in its exponential form as $k_1 \exp(-W/RT)$ where W is the heat of adsorption of the gas. This may be resolved⁽⁴⁷⁾ into

$$W = q_A + q_r - D \quad \dots \quad \dots \quad (2.17)$$

where D is the energy of the bond broken in producing the two species A , and the fragment r , which have heats of adsorption q_A and q_r respectively.

Hence equation 2.16 may be rewritten

$$i_e/i_i = BT^{2-m}/C \propto uk_1 \exp \left[(-q_r + D - E)/RT \right] \quad \dots \quad \dots \quad (2.18)$$

Taking logarithms of equation 2.18 and differentiating with respect to $1/T$ at constant pressure, one obtains

$$\frac{d \log i_e/i_i}{d \log 1/T} = - (2-m) T - (E - D + q_r)/RT \quad \dots \quad \dots \quad (2.19)$$

Therefore if $\log (i_e/i_i)$ is plotted against $1/T$ the sum of the energies $(E - D + q_r)$ may be obtained from the negative slope. This sum is the apparent electron affinity, E' , from which the actual electron affinity may be calculated if the appropriate bond energies and heats of adsorption are known.

2.4 The theory of the magnetron

We may now consider the forces acting on an electron emitted from the filament. The original paper on the operation of the magnetron was published by Hull⁽⁴⁸⁾. The discussion given here⁽⁴⁹⁾ illustrates the theory of the operation of the instrument. Figure 2.1 shows the forces acting on an electron emitted from the hot central filament placed in a uniform magnetic field of flux density B , running parallel to the length of the filament. The electrostatic and electromagnetic forces acting on the electron are respectively

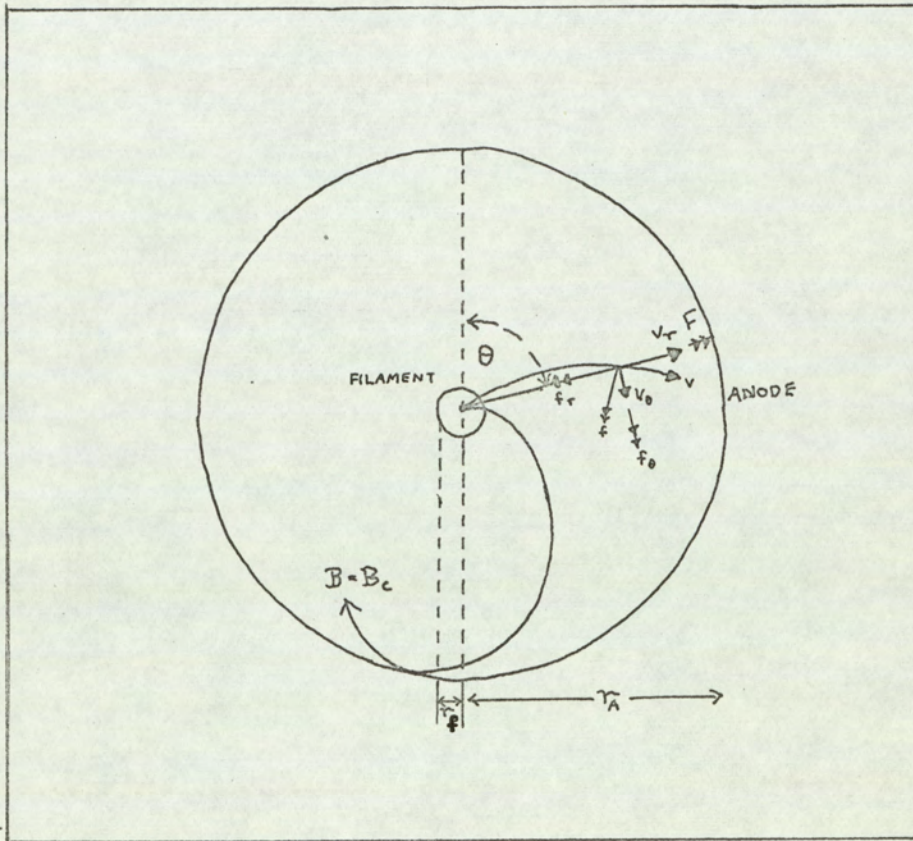


Fig. 2.1 Forces on an electron in a magnetic field.

$$F = -e E = e \frac{dV}{dr} \quad \dots \quad \dots \quad (2.20)$$

$$\text{and } f = Bev \quad \dots \quad \dots \quad (2.21)$$

where e is the electronic charge, E is the strength of the electrostatic field, V is the potential at a distance r from the filament, and v is the velocity of the electron at this point.

If the velocity is resolved into components v_r and v_θ along, and perpendicular to, the radius vector r , then the components of f will be

$$f_r = Bev_\theta$$

and $f_\theta = Bev_r$

If θ is the angle made by the radius vector with an arbitrary line in the azimuthal plane the angular velocity of the electron is

$$\omega = d\theta/dt = v_\theta / r \quad \dots \quad \dots \quad (2.22)$$

The equation for radial motion is therefore

$$d/dt(mdr/dt) = F - f_r = e dV/dr - Ber d\theta/dt \quad \dots \quad \dots \quad (2.23)$$

where m is the mass of the electron.

The equation for azimuthal motion is found by equating the moment of the impressed force to the rate of change of angular momentum thus:

$$rf_\theta = d/dt(mr^2 d\theta/dt) \quad \dots \quad \dots \quad (2.24)$$

$$\text{or } rBedr/dt = d/dt(mr^2 \omega) \quad \dots \quad \dots \quad (2.25)$$

Integrating each side with respect to time and using the condition $\omega = 0$ at $r = r_f$ one obtains

$$\omega = \frac{Be}{2m} \left(1 - r_f^2 / r^2 \right) \quad \dots \quad \dots \quad (2.26)$$

If the small velocities with which the electrons leave the

filament are ignored, then the speed v of an electron at a point where the potential is V , is given by

$$v = \sqrt{2e/m V} = \left[\left(\frac{dr}{dt} \right)^2 + \left(\frac{d\theta}{dt} \right)^2 + \left(\frac{dz}{dt} \right)^2 \right]^{1/2} \dots \dots (2.27)$$

At a certain critical value of the magnetic field strength B the electron will just fail to reach the anode. At this point $r = r_a$

$$V = V_a \text{ and } v_r = 0; v_\theta = v = \sqrt{2eV_a/m}; \omega = \frac{v_\theta}{r_a} = \frac{1}{r_a} \sqrt{2eV_a/m}$$

Substitution of this value of ω into equation 2.26 gives

$$\frac{B_c e}{2m} \left(1 - r_f^2/r_a^2 \right) = 1/r_a \sqrt{2eV_a/m} \dots \dots (2.28)$$

Therefore

$$8V_a/r_a^2 = \frac{e}{m} B_c^2 \left(1 - r_f^2/r_a^2 \right)^2 \dots \dots (2.29)$$

and hence if $r_a \gg r_f$

$$B_c = \sqrt{8mV_a/er_a^2} \dots \dots (2.30)$$

Equation 2.30 shows the value of B_c to be independent of the distribution of potential between the anode and the cathode so that the presence of other electrodes or space charge effects should not alter cut-off conditions. In practice the cut-off is not so sharp with the grids present, probably because of the distortion of the magnetic and electric fields by these structures⁽⁵⁰⁾.

In the magnetron triode the electrons are captured by the grid and so prevented from creating a large space charge near the filament which would affect the emission of negative ions. The magnetic field strength is usually made greater than B_c so that apogee occurs near the grid. This causes the electrons to approach it tangentially and results in greater efficiency of electron removal.

The presence of a second grid was shown by Page⁽²⁶⁾ to lead to

a greater efficiency, presumably because of its action in trapping electrons which had passed through the first grid.

2.5 Design of the magnetron

Fig. 2^{2a} shows the design of the magnetron used for the experimental observations discussed in section 3.2. The rest of the measurements were made by using the design illustrated in Fig. 2^{2b}.

The two modifications were very similar, differing only in minor detail. Both consisted of a central filament F surrounded coaxially by two grids G_1 and G_2 and an anode A which was flanked above and below by guard plates P_1 and P_2 .

The filament was attached at one end to a hook on the base plate B and the other end was wound around the 0.01" diameter tungsten wire spring. This method of support kept the filament taut when it expanded on heating. The anode and guard plates, made of 1mm thick molybdenum sheet were sprung inside the glass cylinder C in design 2^{2b}. This arrangement enabled the whole grid, filament, and anode assembly to be removed as a unit for cleaning. When the molybdenum sheets were sprung directly into the bottle as in design 2^{2a} they were very difficult to remove, and electrical connections to the guard plates and anode were difficult to make.

The grid assembly was constructed from 6 B.A. brass studding and brass formers (plates D and E) of diameters 1.1 and 1.75cm respectively, and was wound with 40 swg nickel wire. In design 2^{2b} the grids were insulated from each other by means of glass tubing

FIG 2.2 Design of the magnetron

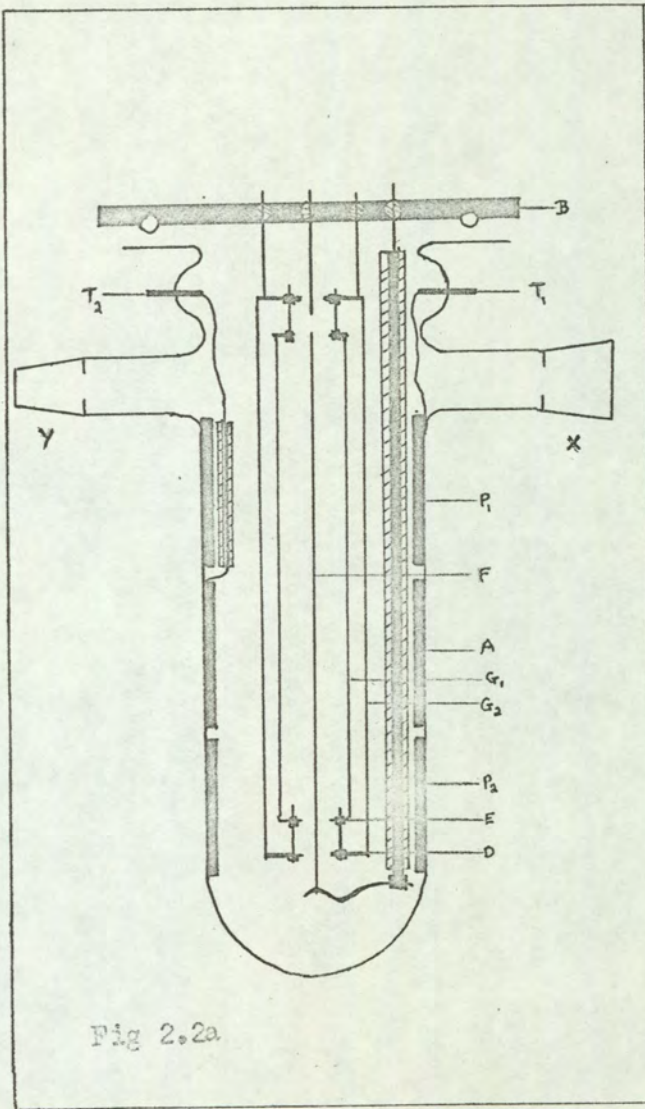


Fig 2.2a

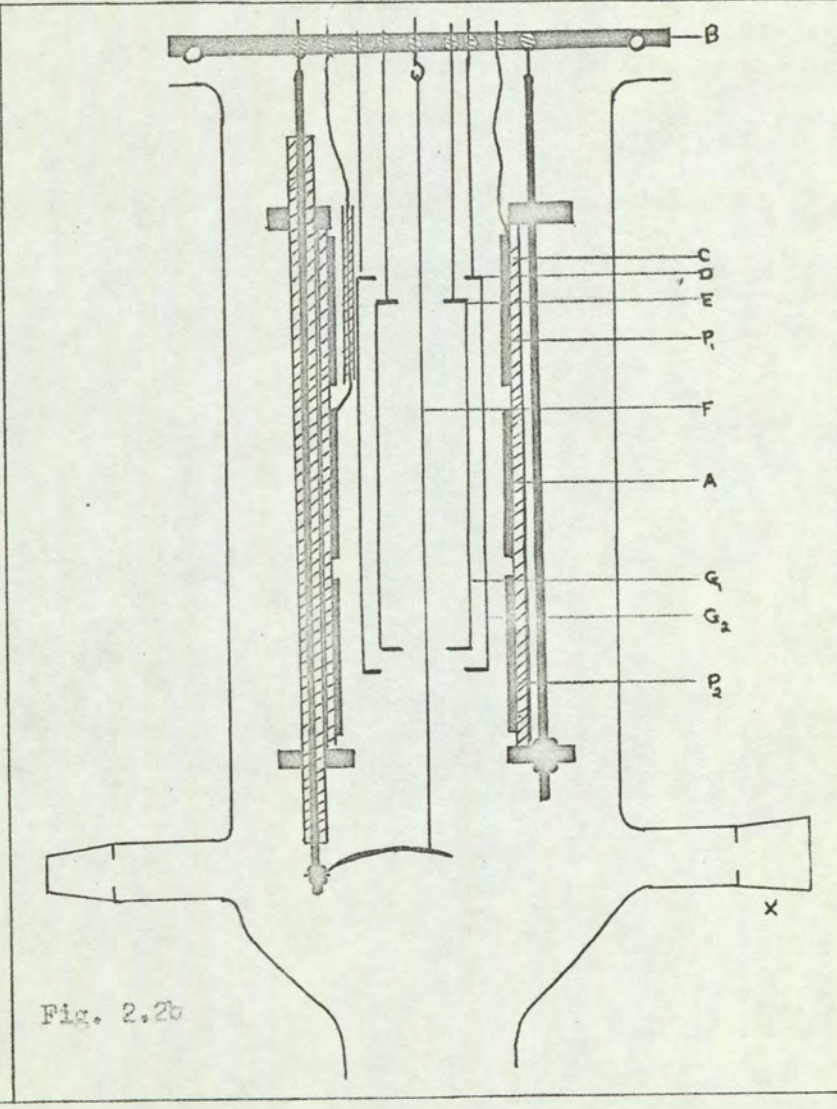


Fig. 2.2b

around the supporting brass studding. This enabled the grids to be at different potentials which could be chosen to give a more uniform potential gradient than with design 2^{2a} where both grids were at the same potential.

Electrical connections through the base plate B were made through AEI type S5 metal to glass seals on to which the filament and grid assemblies were mounted. In design 2^{2a} the electrical connections to the anode and guard plates were made through tungsten seals T₁ and T₂ by means of miniature crocodile clips. A better connection was obtained in design 2^{2b} by soldering connections inside and outside the magnetron to a metal to glass seal in the base plate B.

The base plate was sealed on to the ground glass flange of the outer vessel by means of a neoprene 'O ring', lightly coated with Apiezon N high vacuum grease, and held in a groove in the base plate. The sample was contained in the side arm (X) and admitted through a high vacuum tap. For substances with high vapour pressures finer control was obtained by introducing a linear needle valve (Fig.2.3) adjusted by an external magnet, between the sample and the magnetron. Compounds with low vapour pressures were placed in the heated sample holder in Fig. (2.5) which enabled them to be sublimed directly on to the filament.

The magnetron was evacuated through the side arm (Y) in design 2^{2a} and through the bottom of the glass vessel in design 2^{2b}.

Fig. (2.7) shows the design of the magnet. The solenoid was wire-wound, different models having between 10 and 15 layers of 900 t.

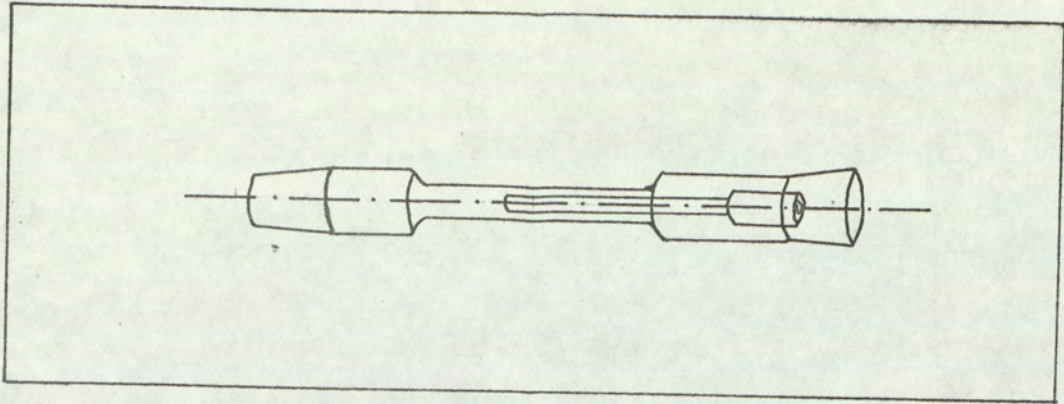


Fig. 2.3 Needle valve.

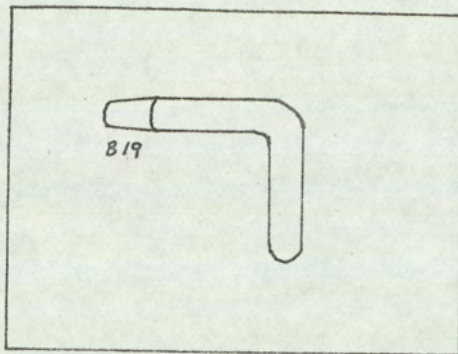


Fig. 2.4 Sample holder

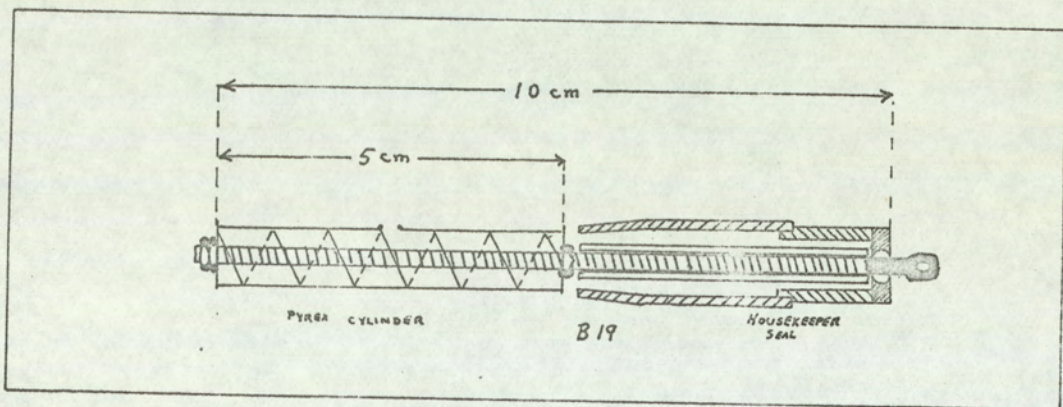


Fig 2.5 Heated sample holder.

1,500 turns of 20 swg enamelled copper wire. The brass former was cooled by water continuously flowing through it.

2.6 Ancillary equipment

The magnetron vessel was maintained at low pressures by the pumping system shown in Fig. (2.6). In design 2^{2a} the taps were of 10mm bore and the connecting tubing was of Pyrex glass. The joints were standard taper B19 and the Pirani head (Edwards 95B-2) was B14. The liquid nitrogen trap B was 1.5" diameter and 4" deep, and C was 0.75" diameter and 9" deep. The two stage mercury diffusion pump D was backed by a rotary diffusion pump and was capable of maintaining pressures of the order of 10^{-5} torr.

The electrical circuit is shown in figure (2.8). The anode currents were measured on an Avo DC amplifier (1388B) which measured currents over a range of 10^{-14} to 10^{-5} amps. For larger currents a Pye Scalamp microammeter (7906/5) with a range of 10^{-6} to 10^{-3} amps was used. The resistance across the leads, between the anode connection and earth was 4×10^4 M ohms. This was only just satisfactory for the smallest currents the lead was expected to carry. The plate and grid voltages were supplied by an Exide H1006 battery and the magnet current was supplied from a 120V stack of lead-acid accumulators.

The pressure in the system was measured by a Pirani pressure gauge model 95B-2. Since this gauge is sensitive to changes in thermal conductivity the reading it registered was to some extent dependent on the nature of the gas present. An absolute knowledge of the pressure was not, however, important since the pressure was kept constant throughout an experiment. The range of pressures used was

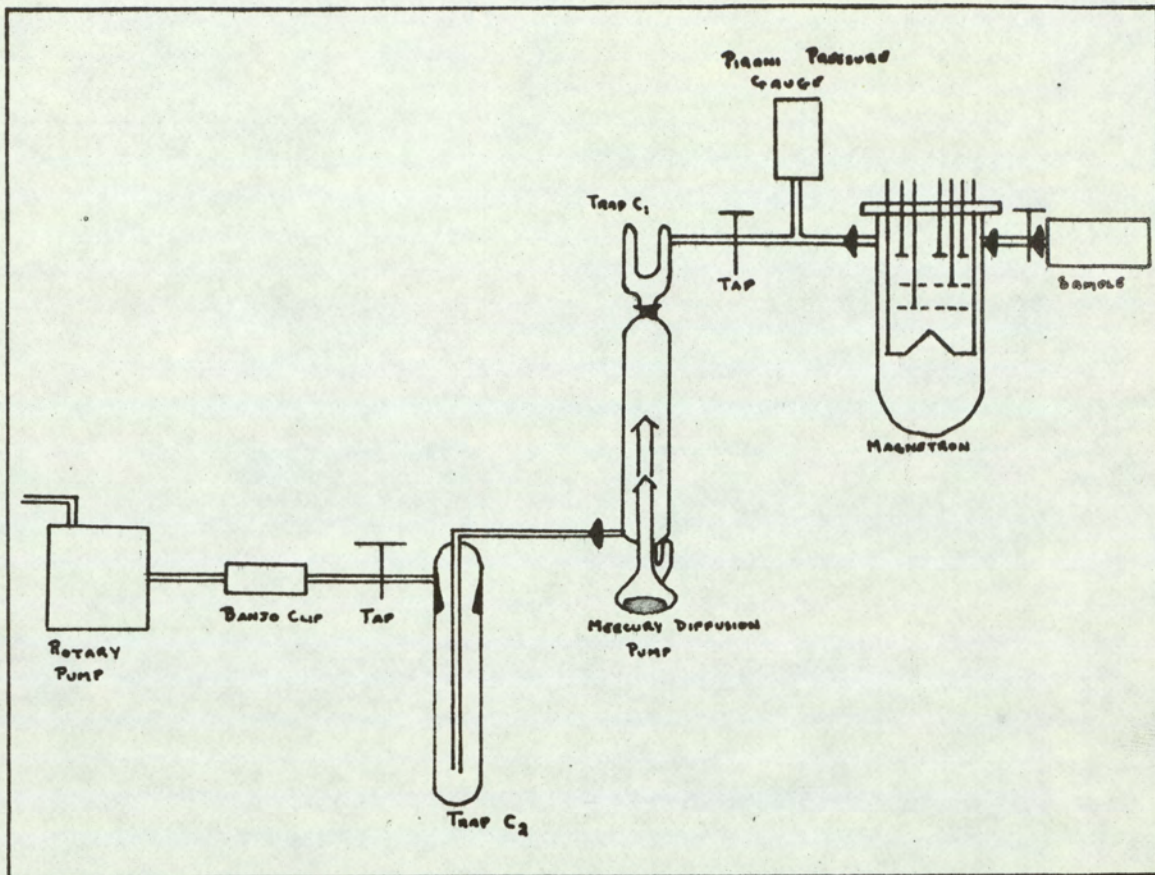


Fig 2.6 Pumping system

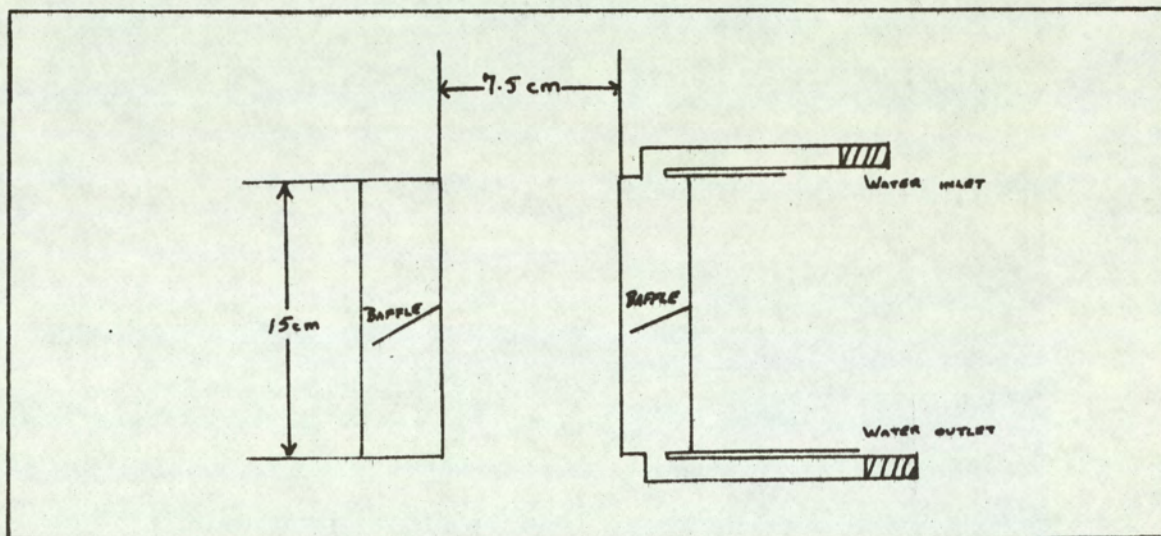


Fig 2.7 Magnet design

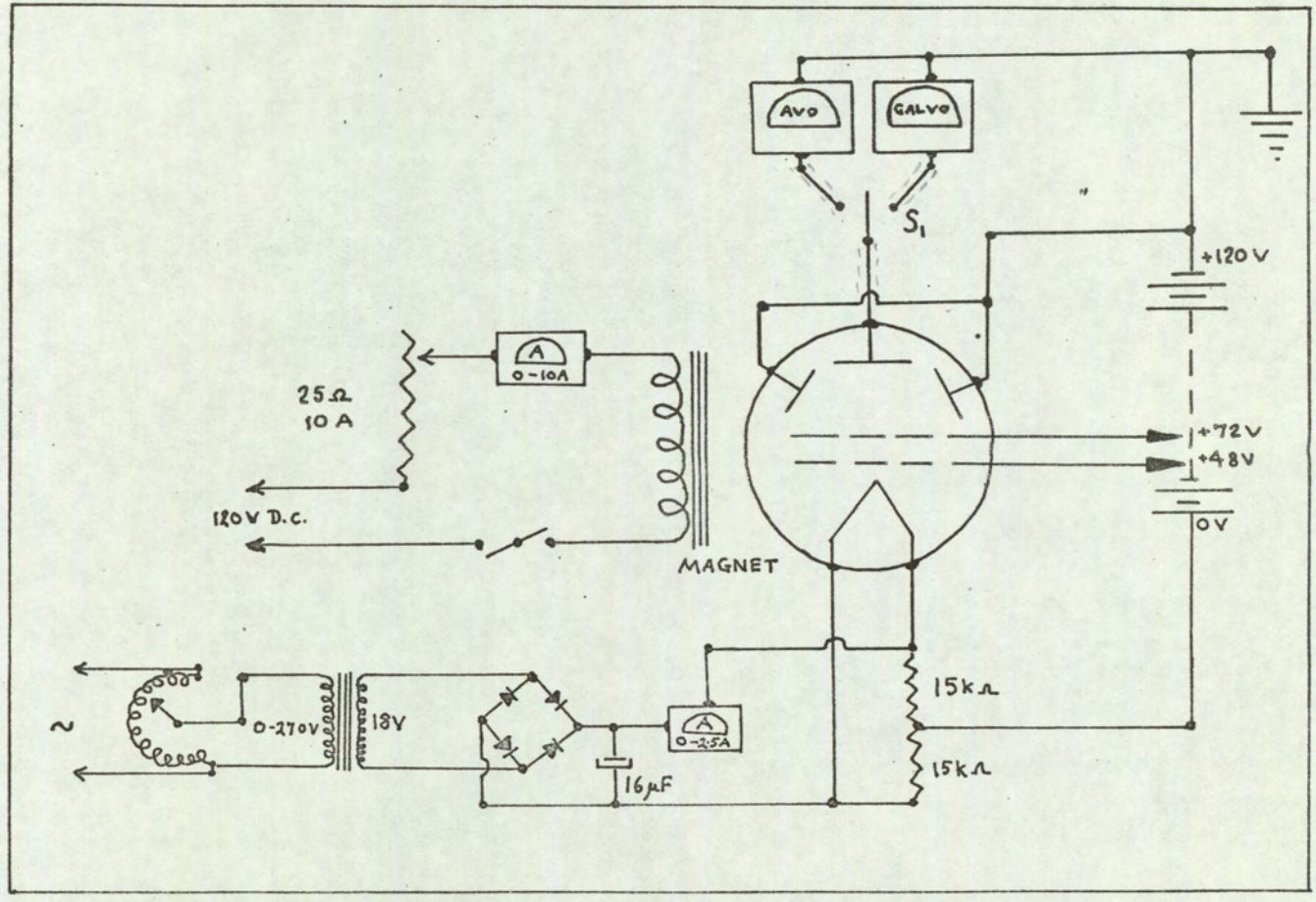
10^{-4} to 5×10^{-3} torr. At these pressures, the mean free path of the molecules exceeded the dimensions of the apparatus and so minimised the probability of collision between the negative ions and molecules.

2.7 Measurement of the filament temperature

In applying the magnetron technique to the measurement of electron affinities, a knowledge of the temperature of the filament is essential. This was measured using a Leeds and Northrup disappearing filament optical pyrometer. It has been found by various methods⁽²⁶⁾⁽⁵⁰⁾ that it is necessary to add about 300°C to the measured values of the temperature to allow for the emissivity of the glass of the vessel and for the loss of light by reflection at the surfaces of the glass.

The temperatures of the central region of the filament were measured and the corrected values plotted against the filament current, and a smooth curve drawn through the points. (This line did not, however, go through the origin when extrapolated, unless the temperature above ambient rather than absolute temperature was plotted against the filament current. This is in accordance with Newton's Law of cooling). At high temperatures, the filament will approximate to a 'black body' and will lose heat at a rate proportional to T^4 where T is the absolute temperature of the filament. Since the resistance of the wire will be relatively constant, the rate of heating is proportional to i^2 where i is the current flowing through the filament. A graph of T^2 against i should therefore be a straight line over the region of temperatures where the approximation of 'black body' radiation holds. In practice the line obtained was linear at

Fig. 2.8 Electrical circuit for magnetron



high temperatures and slightly curved at lower temperatures as shown in Fig. (2.9). The corrected temperatures were smoothed by the use of this line. Electron currents were then measured and used in conjunction with the filament temperatures obtained, Fig.(2.10), to evaluate the work function of the material of the filament using Richardson's equation (eq 2.12). This value of the work function was used to check the reliability of the temperatures measured.

Having calibrated the filament it was not necessary to measure its temperature at each electron and ion current measurement since it was possible to set the current through the filament with sufficient accuracy to reproduce the electron currents at given settings. The temperature calibration was checked periodically by a work function measurement in case the substrate had altered the surface.

2.8 Measurement of the apparent electron affinity

There are several methods for graphically analysing the measured electron and ion currents at known filament temperatures, to obtain the apparent electron affinity. Since the temperature of the filament at a given filament current varied very little over a period of time it was possible to precalibrate the temperature in terms of the filament current. The electron and ion currents were then measured at set filament current.

In making these measurements there are two possible approaches; either the electron and ion currents may be measured at each filament temperature, or, the electron currents measured for each filament temperature and then in all subsequent runs only ion currents measured.

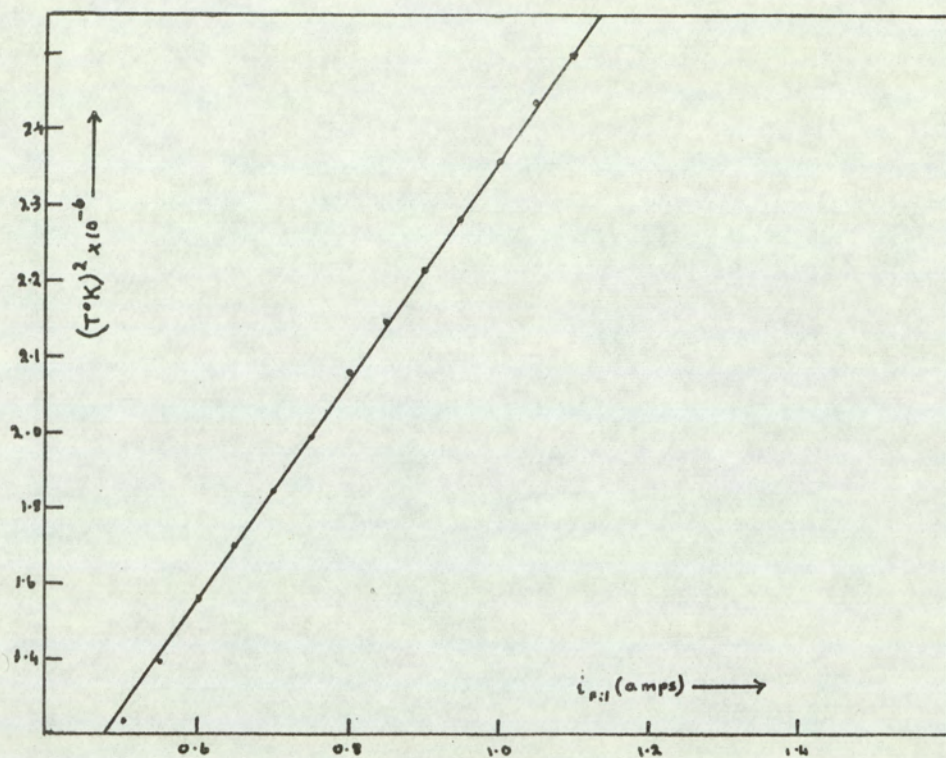


Fig. 2.9 Filament calibration graph

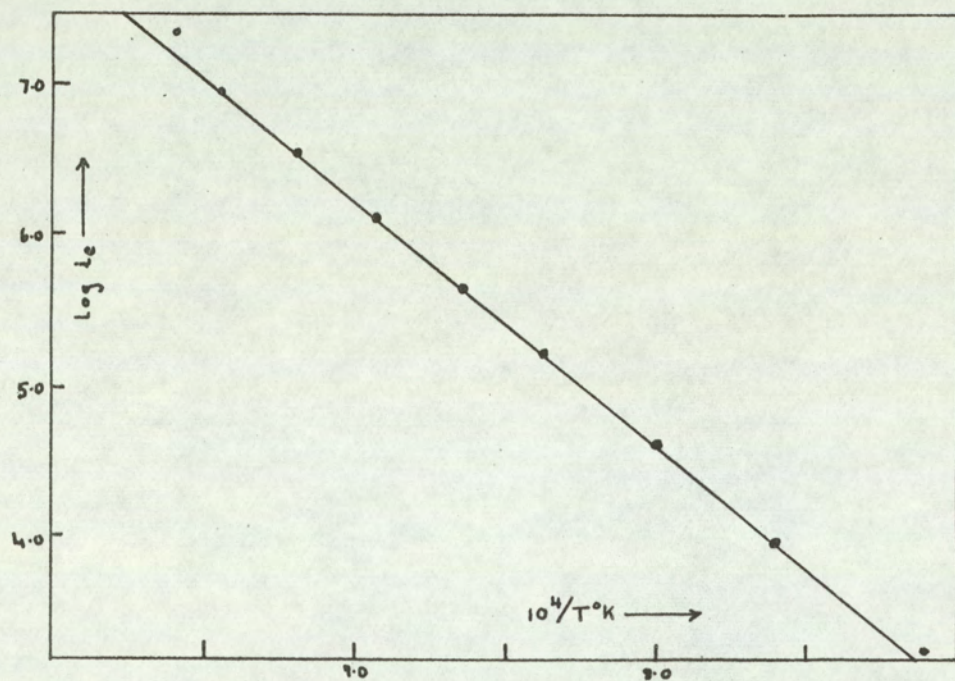


Fig. 2.10 Electron work function for iridium.

This latter method has the advantage that a series of measurements may be made very rapidly and is particularly useful if a limited amount of the compound is available. Also decomposition products are not so likely to build up if measurements are done quickly. When this second method was used the electron currents were checked after a series of ion currents measurements, for which the vapour pressure of the compound was kept constant.

It was shown earlier that the apparent electron affinity E' could be obtained from a graph of $\log i_e/i_i$ against $10^4/T$. This type will be referred to as a 'ratio' plot.

An alternative method for analysing the results has been developed by Gaines and Page⁽³²⁾.

Equation 2.18 (section 2.3) may be re-written

$$i_i/i_e p = K/T^2 \exp E'/RT \quad \dots \quad (2.31)$$

If this equation is combined with equation 2.12 one obtains

$$\log i_i = \left[(\chi - E')/\chi \right] \log i_e + \log p - \left[2(\chi - E')/\chi \right] \log T + \log K + \left[E'/\chi \right] \log BA \quad \dots \quad (2.32)$$

Variations in $\log T$ may be neglected compared with variations in $\log i_e$. Thus if the pressure is held constant throughout an experiment a plot of $\log i_e$ against $\log i_i$ should be linear and the slope of the line will be $(\chi - E')/\chi$. The work function of the filament may be found from the slope of a graph of $\log i_e$ against $10^4/T$ with measurements taken while the substrate gas is present in the magnetron. This type of analysis will be referred to as a 'log-log' plot. The advantage of this method is that it is not

necessary to know the temperature of the filament for each ion and electron current measurement and it is therefore possible to obtain many points at very small intervals of temperature. The work function may be measured in a separate experiment. The use of log-log graphs however unavoidably reduced the sensitivity of the results and it is therefore advisable to check that the same value of E' is obtained from a ratio plot.

2.9 Calculations of electron affinities from the measured energies

As was shown in section 2.3 the apparent electron affinity of a molecule E' may be obtained from the slope of a graph of $\log i_e/i_i$ against $10^4/T$, and that this energy is the overall enthalpy change between the neutral species in the gas phase and the negative ion formed, also in the gas phase. That is

$$E' = E - D + q_r \quad \dots \quad \dots \quad (2.33)$$

where E is the electron affinity of the molecule, or radical, D is the bond dissociation energy of any bond broken and q_r is the heat of adsorption of the fragment left on the surface of the filament.

Several mechanisms of negative ion formation have been found to occur in the magnetron. These are distinguished by the energy terms which contribute to the apparent electron affinity.

(a) If the neutral species adds on an electron directly, the apparent electron affinity must be equal to the actual electron affinity at the temperature of measurement since the process involves neither bond breaking nor adsorption.

(b) For dissociative reactions, the bond energy of the bond broken

must be included in E' and subtracted from it in order to find the actual electron affinity E of the acceptor radical.

That is

$$E' = E - D \quad \dots \quad \dots \quad (2.34)$$

(c) If the substrate leaves a fragment adsorbed on the filament then the heat of adsorption q_r is also included in the apparent electron affinity E' and

$$E' = E - D + q_r \quad \dots \quad \dots \quad (2.35)$$

It is possible to decide which of these processes is occurring for a given measured value of E' by consideration of the energetics of the various possibilities. Usually only one process gives a reasonable value for the electron affinity from the experimentally determined energy. Supporting evidence may be obtained for the type of reaction by calculating the change in entropy for the formation of the negative ion using transition state theory. In the model proposed by Farragher ⁽⁵⁰⁾ ions are assumed to be formed by the interaction of the electrons in the metal with the adsorbed ion-precursors resulting in the formation of a transition state which may be irreversibly desorbed as an ion. It is convenient to regard the reaction in two stages.



The first of these is the desorption of the adsorbed ion precursor $A^*(a)$ in its transition state to form the molecule in the gas phase $A(g)$. The second reaction is the dissociation of the adsorbed negative ion A^{-*} into a neutral species $A(d)^*$ and an

electron e^* each in their transition state for desorption. Farragher has shown that the ratio of the electron and ion currents may be expressed in terms of the equilibrium constants of the above reactions. If K_1 and K_2 are the concentration equilibrium constants of the reactions represented by equations 2.36 and 2.37 respectively then

$$i_e/i_i = \frac{kT}{p} K_1 K_2 \quad \dots \quad \dots \quad (2.38)$$

$$\text{or } i_e/i_i = kT/p \exp(-\Delta G_1/RT_g) \exp(-\Delta G_2/RT) \quad \dots \quad \dots \quad (2.39)$$

whereas ΔG_1 and ΔG_2 are the associated Gibbs' free energies and T_g is the gas temperature.

Since

$$\Delta G = \Delta H - T\Delta S$$

equation 2.39 may be rewritten

$$\frac{i_e}{i_i} = \frac{kT}{p} \exp(-\Delta H_2/RT) \exp(\Delta S_1 - \Delta S_2/R) \quad \dots \quad \dots \quad (2.40)$$

assuming the adsorption process to be non activated, and ΔH_1 to be zero.

Defining $\Delta S = \Delta S_1 + \Delta S_2$ one obtains

$$\frac{i_e}{i_i} = \frac{kT}{p} \exp(-\Delta H/RT) \exp(\Delta S/R) \quad \dots \quad \dots \quad (2.41)$$

Taking logarithms and differentiating with respect to T and noting

that K_1 is independent of temperature it is found that

$$\frac{d}{dT}(\log i_e/i_i) = 1/T + \frac{d}{dT} \log K_2 = 1/T + \Delta U/RT^2 \quad \dots \quad \dots \quad (2.42)$$

Where U is the internal energy of the system

Since

$$\Delta U = \Delta H + RT \text{ then}$$

$$\frac{d}{dT}(\log i_e/i_i) = 1/T + \frac{H + RT}{RT^2} = H/RT^2 \quad \dots \quad \dots \quad (2.43)$$

But

$$\frac{d}{dT} \log i_e/i_i = E'/RT \quad \dots \quad (2.44)$$

and hence the apparent electron affinity has been identified with the enthalpy of the overall reaction.

Taking logarithms of equation 2.41 and substituting $\Delta H = E'$ it is seen that

$$\Delta S = R \log i_e/i_i + R \log P + E'/T - R \log kT \quad \dots \quad (2.45)$$

The entropy change ΔS represents the sum of the entropy changes for the reactions in equations 2.36 and 2.37 with all their transition states in the standard states of one mole per cm^2 and the gas molecules in the standard state of one mole per cm^3 .

By the use of equation 2.45, the entropy changes associated with direct capture, dissociative capture, and dissociative capture with adsorption have been calculated for many compounds whose electron affinities have been measured by the magnetron technique⁽⁵⁰⁾. It has been found by constructing a histogram of the values for ΔS for the various compounds, that direct capture reactions give a change in entropy of 110 ± 17 e.u., dissociation with adsorption, a change of 82 ± 5 e.u. and dissociation without adsorption a change of 55 ± 7 e.u. The entropy units are in $\text{kcal degree}^{-1} \text{ mole}^{-1}$. The value of ΔS may therefore be used as a diagnostic test for reaction type. Although in principle the calculated entropy changes may be used as confirmatory evidence, in practice this is not very conclusive. From equation 2.45 it is seen that the quantity which determines ΔS is E' , since variations in $\log i_e/i_i$ for different types of reactions are not great enough to produce large variations in ΔS . When the apparent electron affinity is either high, of the order of 60 kcal/mole, or

negative, the process may be diagnosed by consideration of the energies involved. The former reaction most probably involves direct capture and the latter, dissociation without adsorption. It is in the intermediate range of E' that it is often difficult to interpret the results and this is the region in which the change in entropy is not definitive, usually lying between, or near to, the lower limit for direct capture and the higher limit for dissociation with adsorption.

As has been shown, the apparent electron affinity E' represents the enthalpy of the reaction for the formation of a negative ion at the temperature of the filament. This energy is in general the algebraic sum of several terms, the electron affinity of a radical, the dissociation energy of any bond broken, and the heat of adsorption of any fragment on the filament. It is therefore necessary to convert the apparent electron affinity, measured at a mean filament temperature of $T^{\circ}\text{K}$ to standard conditions at 0°K so that it may be combined with the other data to obtain the actual electron affinity. The method of correction used in the present work is that derived by Farragher⁽⁵⁰⁾ using transition state theory described earlier in this section. For direct capture reactions and simple dissociative reactions

$$\Delta H(T) = \Delta H_0 + 2RT \quad \dots \quad (2.46)$$

Where

$\Delta H(T)$ and ΔH_0 are the enthalpies of reactions at $T^{\circ}\text{K}$ and 0°K respectively.

For dissociative reactions involving adsorption of the residue

$$\Delta H(T) = \Delta H_0 + 3RT \quad \dots \quad (2.47)$$

These are approximate corrections. The exact correlation between $\Delta H(T)$ and ΔH_0 requires a more complete knowledge of the vibration frequencies of the transition state ion that is generally available, so the vibrational frequencies are assumed constant and the corrections made are only for changes in the translational degrees of freedom.

Owing to limitations of the apparatus it is not possible to measure direct capture electron affinities below a minimum value. For the most efficient production of negative ions it is desirable to have the maximum number of electrons present. As can be seen from Richardson's equation (2.11) the rate of emission is increased by lowering the work function of the filament, and raising its temperature. However, substances with low work functions, for example barium and sodium, are impractical filament materials and the metals which are used all have work functions in the region of 100 kcal/mole. Also, at high filament temperatures the dominant, ion-producing reaction tends to be dissociative rather than one of direct capture, and one is limited to relatively low temperatures of about 1200°K. A filament of the sizes used, and with a work function of 100 kcal/mole, at a temperature of 1250°K emits an electron current of 1.3×10^{-10} amps as may be calculated from Richardson's equation. The minimum current which it is possible to detect on the DC Amplifier used is of the order of 10^{-12} amps and the pressures of gas in the magnetron are of the order of 10^{-3} mm Hg.

By the use of equation 2.45 therefore it is possible to calculate the lower limit of E to give an entropy change of 110 e.u. which is the mean value for direct capture reactions. The value thus obtained is 28.7 kcal/mole and therefore, using the magnetron technique, it is unlikely to be possible to measure the stabilities of negative ions whose values lie much below this figure.

2.10 Summary

It has been shown that the apparent electron affinity E' of a molecule or radical may be found by the measurement of electron and ion currents produced by a heated filament in the presence of a capturing species. The actual electron affinity may be found by allowing for the contribution of energies of dissociation and adsorption to the total measured energy. Consideration of the entropy change for the formation of a negative ion may in theory be used as supporting evidence for the type of reaction.

Chapter 3.

Application of The Magnetron Technique to the Measurement of the Stability of some Negative Ions

3.1 Introduction

The magnetron technique was applied to the study of the stability of negative ions formed from molecules of several types of organic compounds. The results, which were obtained using these classes of compounds, namely hydrocarbons, fluorocarbons and quinones, will be discussed in turn after the section describing the experimental results. The hydrocarbons were studied using the modification of the apparatus shown in figure 2^{2a} and for the other compounds the improved design shown in figure 2^{2b} was used.

The pressure of the vapour in the system was maintained at values of the order of 10^{-3} mm Hg so that the mean free path of the gas molecules, about 15 cm, was greater than the dimensions of the apparatus. This was done by means of the sample introduction and pumping systems described earlier.

3.2 Experimental observation on hydrocarbons

3.2₁ - Benzene

"AnalaR" Benzene, dried over sodium, was put in the sample holder (figure 2.4) and freed from dissolved gasses by successive freezing and melting under vacuum. It was found that a pressure of the order of 5×10^{-3} mm Hg could be maintained by immersing the sample holder in an acetone-solid carbon dioxide slurry. The flow

of the vapour from the holder to the magnetron was controlled by means of a needle valve shown in figure (2.3). Initially a carbided tungsten filament ⁽³²⁾ was used, but the slopes of the ratio plot lines indicated experimental electron affinities scattered over a range from 20 to 40 kcal/mole. A platinum filament was tried, but it was found that an iridium filament gave the most reproducible results. The conditions of the experiment were varied to obtain the optimum conditions. The pressure of the vapour in the magnetron, and the pumping rate were varied to give pressures of benzene between 1×10^{-3} and 5×10^{-3} mm Hg. Some measurements were made with ascending and some with descending filament temperatures, but usually ratio plots still gave a scatter of points.

It was then decided to use the log-log method of analysis (fig 3.1). This method has the advantage that it is possible to obtain more points over a given temperature range. The apparent electron affinity, obtained as an average of forty log-log plots was 28.5 ± 1.4 kcal/mole at a mean filament temperature of 1300°K . The values obtained from the few ratio plots which did give reasonably straight lines were in fair agreement with those obtained from the log-log analyses. An example of a ratio plot is shown in figure 3.2 which gives an apparent electron affinity of 26.1 kcal/mole.

3.2₂ - Naphthalene

Micro Analytical Standard naphthalene was used without further purification, placed in the sample holder (figure 2.4) and introduced into the magnetron through a 5 mm bore tap. Measurements of ion and

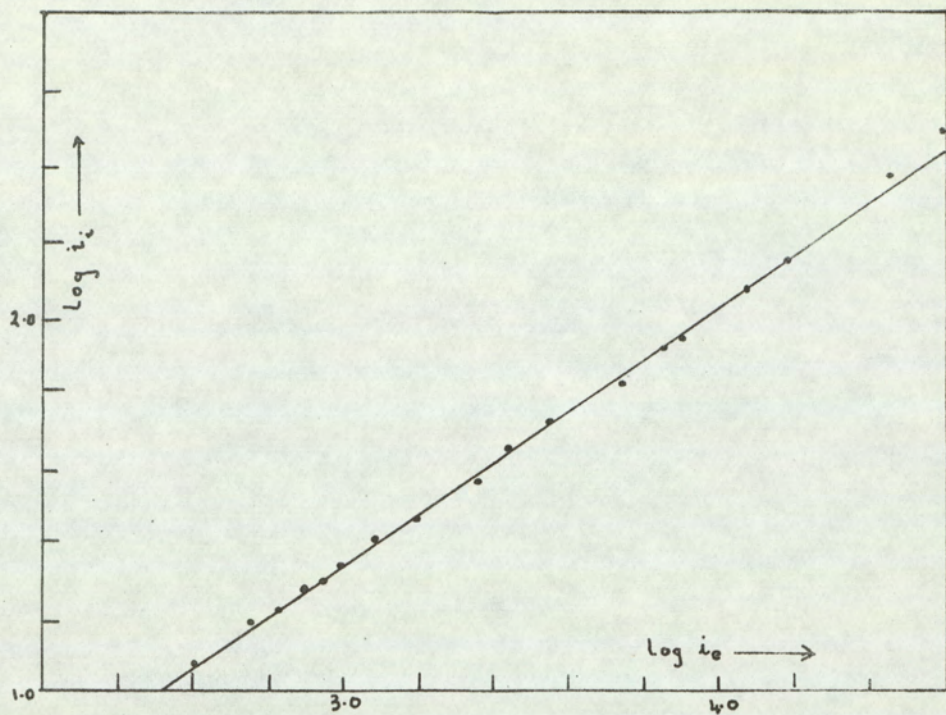


Fig. 3.1 log-log plot for benzene on iridium.

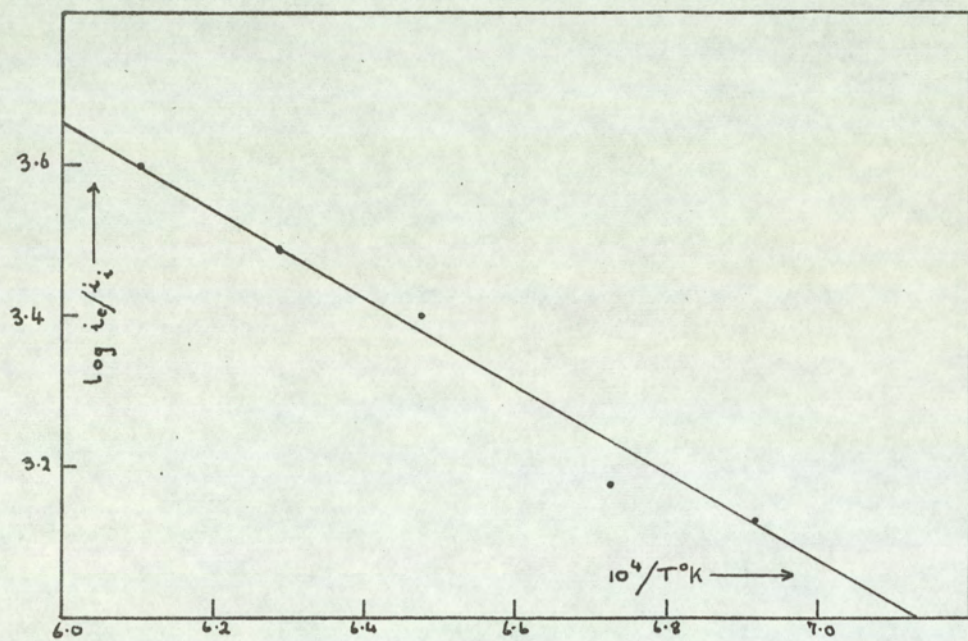


Fig. 3.2 ratio plot for benzene on iridium

electron currents were made in ascending order of filament temperatures. Ratio plots gave slopes, the mean value of which corresponded to an apparent electron affinity of 53.5 ± 7.3 kcal/mole at a mean temperature of 1200°K . At higher temperatures a curve was obtained. When the measurements were made in order of descending temperature, ratio plots gave a different slope corresponding to an apparent electron affinity of 22.2 ± 0.2 kcal/mole at a mean temperature of 1250°K (fig. 3.3). A wide scatter of points was obtained for many runs. The platinum filament was replaced by a tungsten filament which was carbided by allowing naphthalene to flow through the apparatus with the filament at about 1400°K until consistent electron currents were obtained for a given filament current. The results were plotted as two separate graphs, $\log i_e$ against $10^4/T$, and $\log i_i$ against $10^4/T$ (fig. 3.4). This method of analysis is not so sensitive as the normal ratio plots but these latter gave a scatter of points, and it was not possible to determine where the best straight line lay. The ion current plots gave better straight lines. Since the $\log i_e$ against $10^4/T$ plot line was a very good straight line with a reproducible slope, one merely needed to measure the ion current at each temperature to be able to make many more measurements and statistically decrease the error of the result. The apparent electron affinity obtained in this way was 32.5 ± 4.0 kcal/mole at a mean temperature of 1400°K . The large standard deviation is an indication of the scatter of values for the apparent electron affinity and the difficulty found in obtaining consistent results.

By using an iridium filament better straight lines were obtained on a ratio plot for the first three sets of measurements. One of

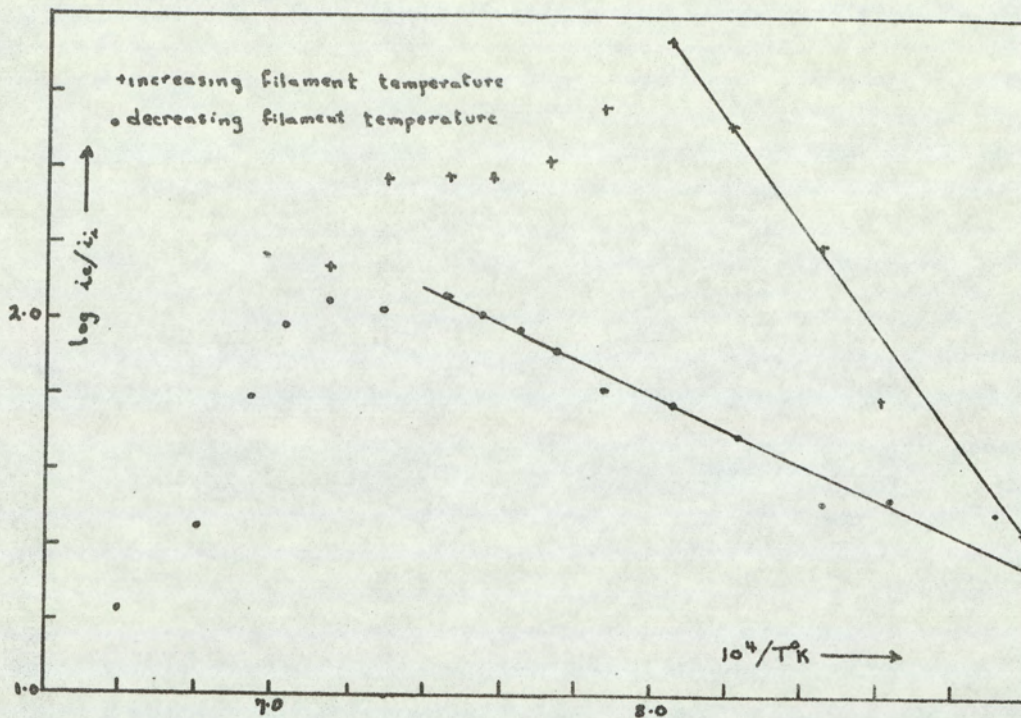
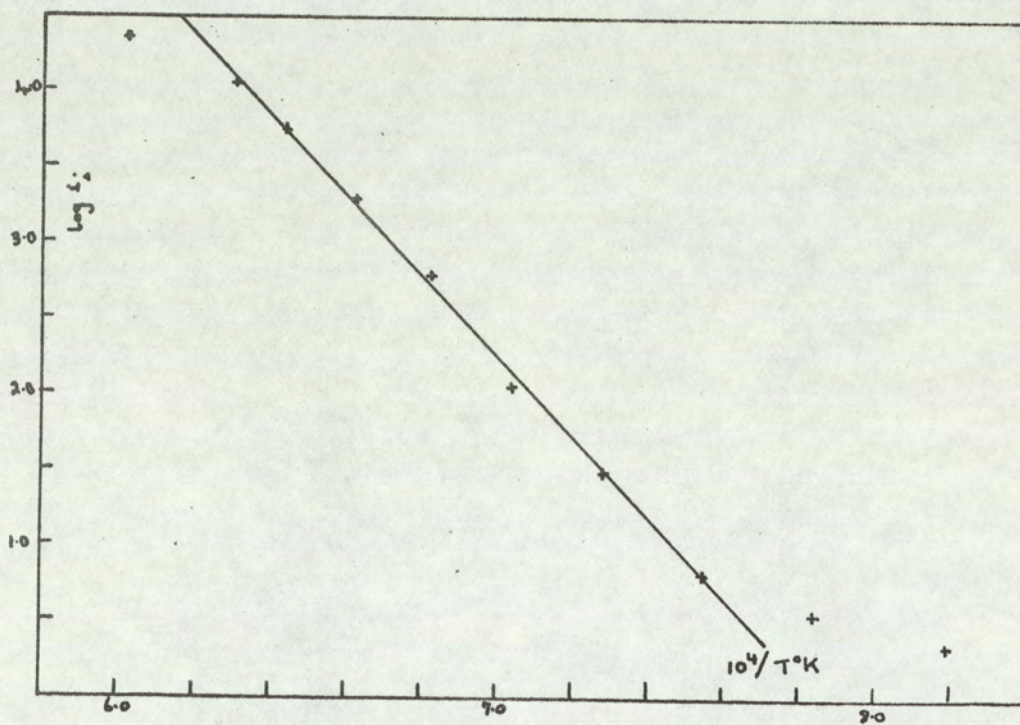


Fig. 3.3 Ratio plot for naphthalene on platinum.



these is shown in Figure 3.5. After this the points were erratic, possibly due to partial carbiding of the filament. The apparent electron affinity found from the average of the runs done on iridium was 23.0 ± 0.5 kcal/mole at a mean temperature of 1330°K .

3.2₃ - Anthracene

B.D.H. Microanalytical Standard anthracene was sublimed from the sample holder (figure 2.4) into the magnetron by immersing the holder in hot water in a dewar flask. The ion currents measured using an iridium filament were above the background level obtained in the absence of any vapour but the Pirani pressure gauge did not indicate any pressure change as the anthracene was sublimed into the magnetron. This was presumably due to the anthracene condensing onto the apparatus before reaching the Pirani head. Ratio plots (Fig. 3.6) gave two distinct slopes, the steeper one at higher temperatures, corresponding to an apparent electron affinity of 50.4 ± 3.5 kcal/mole at a mean filament temperature of 1600°K , and the other to a value of 20.9 ± 0.4 kcal/mole at a mean temperature of 1400°K . In an attempt to produce a greater vapour pressure of anthracene in the system, a modified magnetron bottle was used with a jacket of boiling xylene, but completely erratic results were obtained. Anthracene was also studied in the design of the magnetron illustrated in figure 2^{2b} using an iridium filament and no ion currents above background level were observed until a filament temperature of about 1500°K was reached, and above this temperature ratio plots gave a negative slope, the gradient of which was irreproducible.

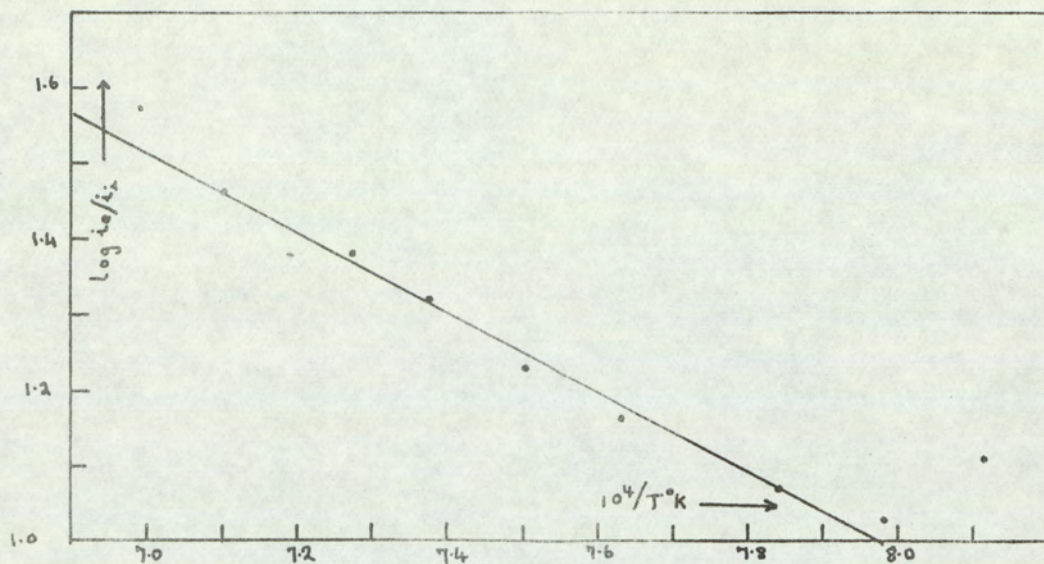


Fig. 3.5 Ratio plot for naphthalene on iridium

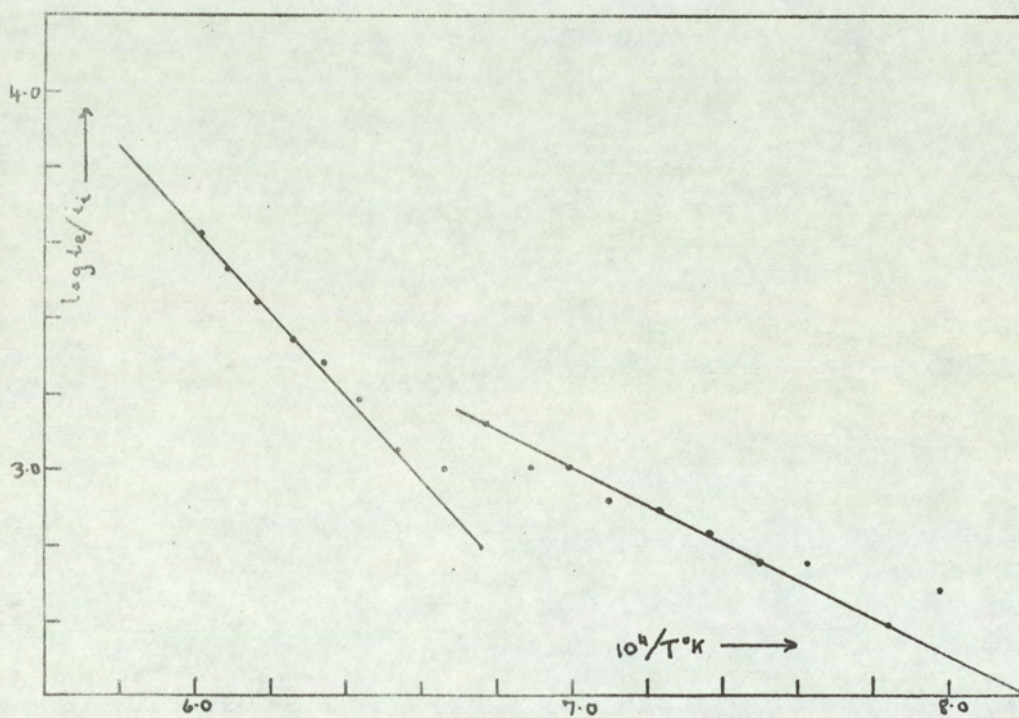


Fig. 3.6 Ratio plot for anthracene on iridium

3.2₄ - Azulene

A sample of azulene obtained from Koch-Light was sublimed onto a platinum filament keeping the sample holder in a dewar flask filled with boiling water. Electron and ion currents were measured at known intervals of filament temperature. Ratio plots gave a scatter of points. The purity of the sample was estimated by ultraviolet spectroscopic analysis. The spectrum obtained was compared with those obtained by Tilney, Barrett, and Walters⁽⁵¹⁾. No extra peaks were observed and the $\log \epsilon$ values agreed to within 0.03. More reproducible results were obtained on a carbided tungsten filament than on the platinum filament. Ratio plots gave two different slopes, the one at the lower mean temperature of 1350°K corresponding to an apparent electron affinity of 66.5 ± 1.1 kcal/mole and that at the higher mean temperature of 1600°K to an energy of -34.3 ± 0.9 kcal/mole. Figure 3.7 shows an example of such a plot.

3.2₅ - Other Hydrocarbons

Pyrene, chrysene, and tetracene were put into the electrically heated sample holder (figure 2.5) directly beneath the filament in an attempt to sublime some of the compound onto the filament, but the measured currents were of the same order as the background values of the ion current measured in the absence of any substrate. The anode connection was made directly to the amplifier, by-passing the switch S in figure 2.8, and the pumping rate was reduced but still no appreciable ion current was observed. Figure 3.8 shows the ion currents obtained in the presence of these hydrocarbons compared with those obtained when the magnetron was completely pumped out. The electron and ion currents which were measured were plotted on a ratio

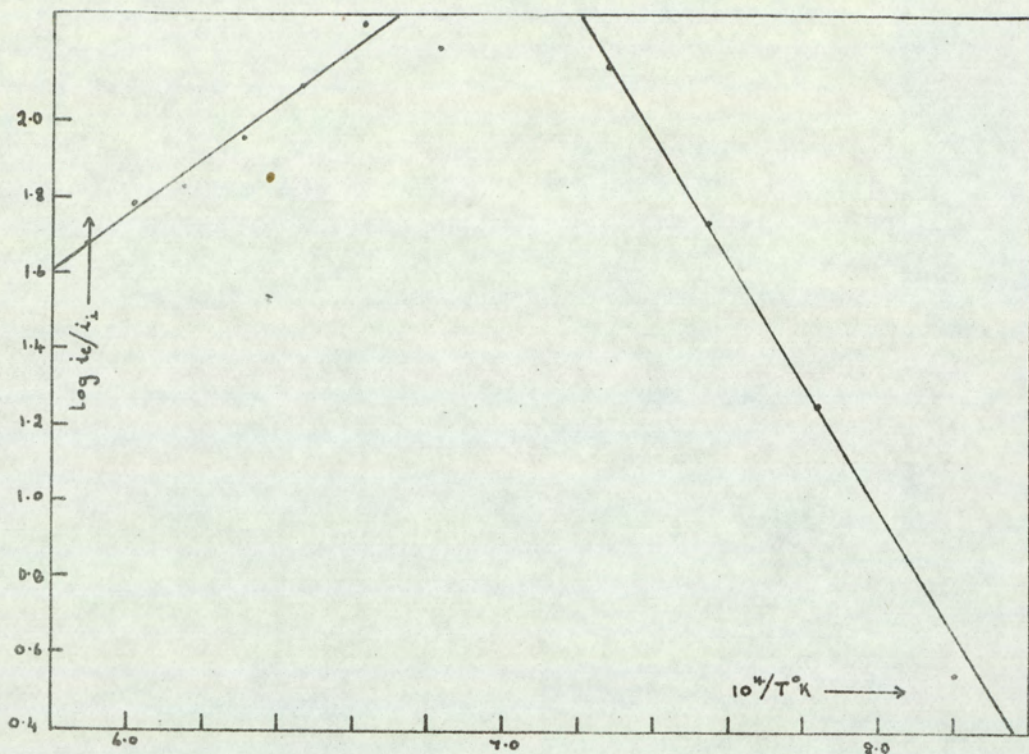


Fig. 3.7 Ratio plot for azulene on tungsten carbide

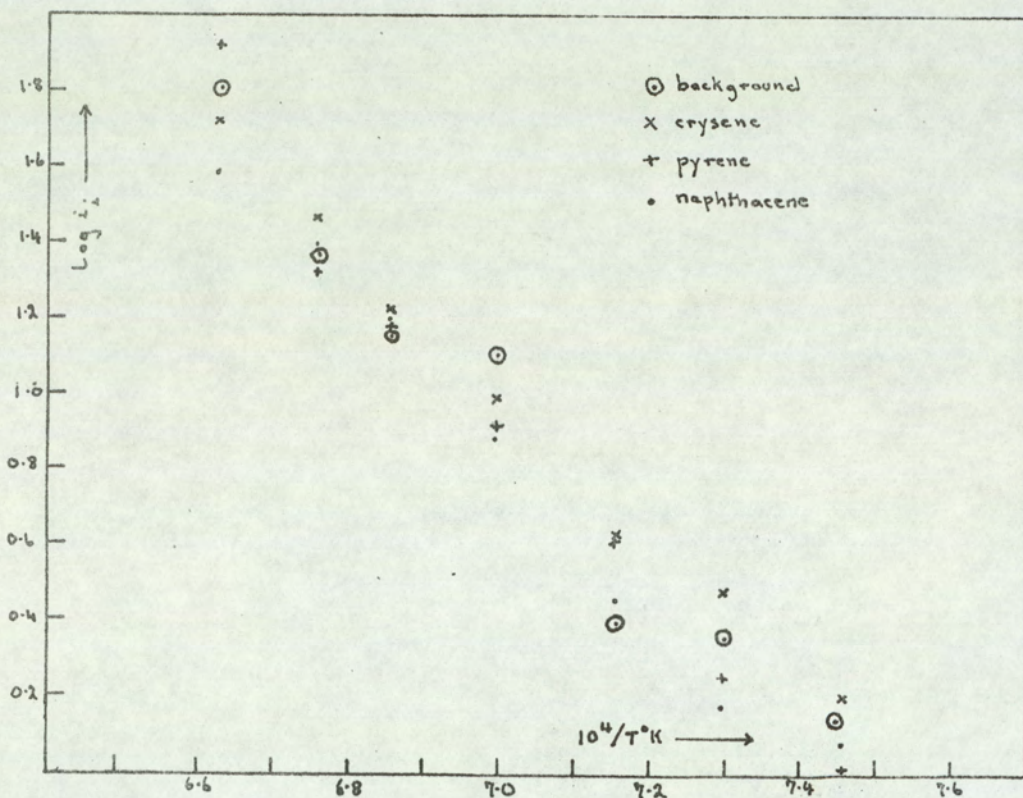


Fig. 3.8 $\log i_i$ against $10^4/T$ for some polycyclic hydrocarbons

plot and a complete scatter of points was obtained. Hence it was not possible to obtain an estimate of the electron affinities of any of these compounds.

TABLE 3.1 - Results of magnetron measurements on hydrocarbons

Compound	Filament	Process	Ion Formed	$E'(T)$	$(T)^\circ K$	E'_o	E_o	ΔS
Benzene	Ir	H loss	$C_6H_5^-$	28.5 ± 1.4	1300	20.7 ± 1.4	56.7 ± 1.4	85.9
Naphthalene	Ir	H loss	$C_{10}H_7^-$	23.0 ± 0.5	1330	15.0 ± 0.5	51.0 ± 0.5	90.0
	Pt	D.C. ?	$C_{10}H_8^-$	53.5 ± 7.3	1200	48.7 ± 7.3	48.7 ± 7.3	115
	Pt	H loss	$C_{10}H_7^-$	22.2 ± 0.2	1250	14.7 ± 0.2	50.7 ± 0.2	83.1
	WC	H loss	$C_{10}H_7^-$	32.5 ± 4.0	1400	24.1 ± 4.0	58.1 ± 4.0	91.7
Anthracene	Ir	H loss	$C_{14}H_9^-$	20.9 ± 0.4	1400	14.6 ± 0.4	48.6 ± 0.4	93.6
	Ir	?		50.4 ± 3.5	1600			106.0
Azulene	WC	D.C.	$C_{10}H_8^-$	66.5 ± 1.1	1350	61.1 ± 1.1	61.1 ± 1.1	118.7
	WC	H loss	$C_{10}H_7^-$	-34.3 ± 0.9	1600	-40.7 ± 0.9	61.3 ± 0.9	47.8

3.3 Discussion of observations on hydrocarbons

3.3₁ - Introduction

As will be shown in the final section of this dissertation there are very few molecules whose electron affinities have been experimentally determined. The few measurements that have been made are mainly for simple molecules such as the halogens. Molecular orbital calculations^(13,22-25) suggest that benzene should have a negative electron affinity, the value for naphthalene should be just positive and the stability of the anthracene negative ion should be about half an electron volt. It was shown earlier (section 2.9) that the magnetron technique is limited to the measurement of negative ion stabilities greater than 1 eV. If, therefore, the values of electron affinities calculated from molecular orbital theory are correct, one would not expect to observe direct capture by benzene or naphthalene but might reasonably expect to be able to measure the electron affinities of the higher polycyclic hydrocarbons such as pyrene and chrysene which have higher predicted values.

As was discussed in section 2.8, the apparent electron affinity of a molecule may be obtained from the slope of a graph of $\log i_e/i_i$ against $10^4/T$. It has also been shown that in order to calculate the actual electron affinity it is generally necessary to know the dissociation energy of any bond which is broken and the heat of adsorption of any residual fragment on the filament. In the case of hydrocarbons which form ions from radicals produced by loss of hydrogen to the filament, the particular parameters required are the C-H bond energy, and the heat of adsorption of hydrogen on the various filament materials. The heat of adsorption of hydrogen on

tungsten has been found by Page⁽²⁷⁾ using hydrogen chloride, hydrogen bromide and water as substrates. Since the electron affinities of chlorine, bromine⁽⁵²⁾, and oxygen⁽⁵³⁾ and the necessary bond energies are known⁽⁵⁴⁾, the heat of adsorption may be found from the equation

$$E' = E - D + q$$

Page gave the value of 73.0 ± 1.1 kcal/mole and Gaines and Page⁽³²⁾ suggested that the value on tungsten carbide was similar. By comparing results obtained using different filament materials the following heats of adsorption were found by Page⁽⁴⁰⁾ - the heat of adsorption of hydrogen on platinum : 70.0 kcal/mole; and, hydrogen on iridium : 67.0 kcal/mole. These values have been used for calculating the electron affinities in table 2.1.

Little data, either experimental or theoretical, exists on bond energies in aromatic hydrocarbons. Cottrell⁽⁵⁴⁾ quotes a value for $D(C_6H_5-H)$ of 101.8 kcal/mole. This was obtained by Szwarc and Williams⁽⁵⁵⁾ from the activation energy of the pyrolysis of bromobenzene, using the toluene carrier technique. This is near the value for the (C-H) bond energies in aliphatic hydrocarbons obtained by electron impact methods⁽⁵⁴⁾. $D(C_6H_5-H)$ has also been obtained from measurements on the rates of reaction of phenyl radicals (produced by the photolysis of acetophenone) with acetophenone, methane, cyclopropane and iso-butane. The value thus obtained was 102 kcal/mole⁽⁵⁶⁾. Skinner and Pilcher⁽⁵⁷⁾ consider some empirical methods of obtaining bond energies in hydrocarbons but their schemes are mainly restricted to paraffins. Bernstein⁽⁵⁸⁾ set out to calculate numerical values for the bond energies of hydrocarbons by attempting to find a

relationship between the bond energy and bond distance. He considered the bond energy to be primarily a function of bond order, modified by the interactions between neighbouring atoms. The heats of atomisation of condensed aromatic hydrocarbons were calculated assuming all C-H bonds to have the same energy as that found for $\text{C} \begin{smallmatrix} \text{H} \\ \text{H} \end{smallmatrix}$ from thermochemical data on ethylene. The values obtained agreed well with the observed heats of atomisation to within one kcal/mole. This suggests that $D(\text{C-H})$ does not vary very much in the different aromatic hydrocarbons.

The (C-Br) bond energies in bromobenzene (70.9 kcal/mole), 1 - bromonaphthalene (70.9 kcal/mole), 2 - bromonaphthalene (70.0 kcal/mole), and 9 - bromoanthracene (65.6 kcal/mole) have been determined by the same pyrolysis method as was used to measure $D(\text{C}_6\text{H}_5\text{-H})$ ⁽⁵⁹⁾. As these energies are very similar it is reasonable to suppose that $D(\text{C-H})$ will be similarly little affected by the numbers of aromatic rings in the molecule.

Since there is little interaction between the delocalised π system of electrons and the electrons of the $\sigma(\text{C-H})$ bond, it is not surprising that the bond energy should be very similar in all condensed aromatic hydrocarbons.

3.3₂ - Benzene

The experimental apparent electron affinity of benzene was found to be 28.5 ± 1.4 kcal/mole at a mean temperature of 1300°K. Using the bond dissociation energies and heats of adsorption discussed the electron affinity of the phenyl radical may be calculated to be

56.7 ± 1.4 kcal/mole at 0°K . A value of 85.9 e.u. for the entropy change suggests that the reaction is in fact dissociation with adsorption. Gaines and Page (32) measured the electron affinity of the phenyl radical using a carbided tungsten filament. At a mean filament temperature of 1563°K and benzene as substrate they obtained a value of 52.7 ± 1.2 kcal/mole at 0°K . With benzil as substrate they obtained a similar value of 50.9 ± 1.2 kcal/mole. If their value of E' obtained from benzene is corrected to 0°K using the specific heat corrections as used in the present work, a value of 55.1 ± 1.2 kcal/mole is obtained, in good agreement with the present value, obtained using an iridium filament.

Negative ion formation from several compounds has been studied in a mass spectrometer by Rosenstock et al (60). The gaseous species were passed over a tungsten filament at pressures of about 10^{-3} torr. The most abundant ions observed were, in the case of benzene, CH^- , C_2^- and CN^- , but not C_6H_5^- . A possible reason for C_6H_5^- forming in the magnetron while not being observed in the mass spectrometer is the lack of conditioning of the filament in the latter case. In order to obtain consistent results with the magnetron it is often necessary to allow the substrate to pass over the heated filament intermittently for several days. This process would assist the removal of nitrogen from the filament. Since the process of ion formation occurs on the surface, the crystal structure of the filament is important and with continued heating in the presence of benzene it is possible that the crystal sites will be altered so that the benzene molecules will fit in better.

3.3₃ - Naphthalene

The results for naphthalene using a platinum filament indicated that two processes occurred. At a mean temperature of 1200°K the experimental electron affinity obtained was 53.5 ± 7.3 kcals and at 1250°K the value was 22.2 ± 0.2 kcals/mole. Consideration of the energetics of the processes suggest that the former is direct capture by the naphthalene molecule to form the negative ion. Since the former measurement was made at the lower mean temperature and with the filament temperature ascending it is more likely to be direct capture than the latter case where measurements were made in order of descending temperature, and decomposition products were likely to build up. The experiments at a mean filament temperature of 1200°K involved the measurement of very small ion currents and, as indicated by the large standard deviation, the results for the apparent electron affinity showed a wide scatter. The value of 53.5 kcals/mole for the electron affinity of naphthalene should therefore be accepted with caution. With a tungsten carbide filament the value of 58.1 kcals/mole was obtained for the electron affinity of the naphthyl radical from the apparent electron affinity of 32.5 kcals/mole. This was greater than the values obtained using iridium and platinum filaments which gave similar results of 51.0 ± 0.5 and 50.7 ± 0.2 kcals/mole at 0°K respectively. A rather higher value of 56.5 ± 2.8 kcals/mole has been obtained⁽⁶¹⁾ from measurements taken using a platinum filament, when carbided tungsten filaments had been found to give irreproducible results.

As might be expected the electron affinity of the phenyl and

naphthyl radicals are very similar since it is σ capture onto an sp^2 hybridised carbon atom which occurs in both cases. The delocalised π system will not affect the value of σ capture electron affinities to any great extent. In the benzene molecule the self-polarisabilities for each (C-H) bond are the same and no particular carbon atom is preferentially attacked. In naphthalene however, the self polarisability is greater at the α position than at the β position and hence the former is more readily attacked by electrons⁽⁶²⁾. One would therefore expect that if hydrogen were abstracted from naphthalene it would be at the α position.

The self polarisabilities for anthracene decrease in the order of position $9 > 1 > 2$ ⁽⁶²⁾. Consequently position 9 will be the most reactive to electrons and the most likely position for hydrogen loss. There are, however, eight α and β position and only two γ . Statistically therefore one would expect more α and β than γ hydrogen atoms to be lost. The orientation of the molecules also affects which (C-H) bond is broken, since if it lies flat, all the carbon atoms are equally accessible to the electrons, which is not the case if the molecule lies perpendicular to the surface of the filament. The difference in the energy required to form negative ions from the various possible radicals, will however be very small and well within the experimental error of the present work. It is not therefore known which is the dominant ion produced.

3.3₄ - Anthracene

Anthracene did not appear to show direct capture but lost hydrogen even at the lowest temperature range of the apparatus.

Direct capture, if it occurs does so at a lower temperature than this and so is not observable. Since molecular orbital theory ⁽²⁴⁾ and studies in solution ⁽⁴⁴⁾ suggest that the electron affinity of anthracene should be greater than that of naphthalene, the value of 53.5 kcals/mole obtained for naphthalene probably does not represent its direct capture electron affinity, particularly as a ratio plot of electron and ion current measured in the absence of any gas gave a slope corresponding to about 60 kcals/mole.

The apparent electron affinity of anthracene was found to be 20.9 ± 0.4 kcals/mole at a mean temperature of 1400°K . It is reasonable to explain this energy in terms of a hydrogen loss reaction giving an electron affinity of the anthryl radical as 48.6 ± 0.4 kcals/mole at 0°K . The value of 94 e.u. for the entropy change lies at the lower limit expected for direct capture and so is not decisive in determining the mode of ion formation. Entropy calculations on the results obtained in the high temperature region suggest direct capture to be occurring but it is energetically very unlikely that direct capture occurs more efficiently at the high temperature of 1600°K and dissociation at a lower temperature of 1400°K . Probably fragmentation of the molecules leads to the formation of many ionic species all of which contribute to the ion current. This conclusion is supported by the different results obtained in the two different modifications of the apparatus. In design 2.2b with the faster pumping rate no ions were observed until a filament temperature of about 1540°K was reached and above this temperature ratio plots gave a positive slope indicating a fragmentation of the

molecule. The change-over from the smaller to the greater slope given by ratio plots, using the magnetron of the design shown in figure 2a occurred at about the same temperature. Presumably with the lower pumping rate fragmentation products build up from which ions may be formed efficiently to give a slope corresponding to an apparent electron affinity of 53.5 kcal/mole. The values of $D(C-Br)$ in the bromine derivatives of benzene, naphthalene and anthracene quoted in section 3.3₁ show that $D(C-Br)$ is lower in anthracene than in the other two. If $D(C-H)$ were lower in anthracene than in benzene and naphthalene, that is less than 102 kcal/mole, the electron affinity of the anthracyl radical would be less than 48.6 kcal/mole. If, however, the bond energy were greater, which is possible since the bromine and hydrogen atom have opposite inductive effects, then the electron affinity of the anthracyl radical would be greater than 48.6 kcal/mole.

3.3₅ - Azulene

Azulene showed two distinct temperature regions (fig. 3.4). At a mean temperature of 1350°K the apparent electron affinity was 66.5 ± 1.1 kcal/mole which may be reasonably interpreted as direct capture. An entropy change of 118.7 e.u., at the upper limit expected for direct capture reactions supports this conclusion. At a mean temperature of 1600°K the apparent electron affinity was -34.3 ± 0.9 kcal/mole. If this is a hydrogen loss reaction and the $(C-H)$ bond energy is 102 kcal/mole as in benzene the electron affinity of the azulyl radical may be found to be 61.3 ± 0.9 kcal/mole

at 0°K assuming the hydrogen molecule is not adsorbed onto the filament surface. If the hydrogen were adsorbed the electron affinity would be -5.7 kcal/mole which is unreasonably low. An entropy change of 47.8 e.u. is within the limits expected for dissociative reactions where no adsorption occurs. The value of 61.1 kcal/mole for the electron affinity of the azulyl radical is rather high compared with the electron affinity of the naphthyl radical as is shown in table 3.1. This could be because the energy of rearrangement of azulene to naphthalene is included in the apparent electron affinity. From the measurements made with naphthalene using a carbided tungsten filament the overall energy for the formation of a naphthyl radical was found to be 24.1 kcal/mole which was interpreted as a dissociative reaction with adsorption leading to an electron affinity of 58.1 kcal/mole for the naphthyl radical. If the reaction with azulene is azulene \longrightarrow naphthalene \longrightarrow naphthyl⁻ + H

the electron affinity of ^{azulene} ~~the azulyl radical~~ is $R + E'$ where R is the rearrangement energy of azulene to naphthalene and E' is the apparent electron affinity of naphthalene. Hence R may be found to be $61.1 - 24.1 = 37.0$ kcal/mole.

The rearrangement energy may also be found from the difference in the heats of formation of the two substances in their gaseous states. These are 34.3 ± 1.5 kcal/mole for naphthalene ⁽⁶³⁾ and 72.5 ± 2.5 kcal/mole ⁽⁶⁴⁾ for azulene. The difference of 38.2 kcal/mole agrees remarkably well with that obtained from the difference in the electron affinities of the radicals.

A value for the (C-H) bond energy in ~~the~~ cycloheptatriene has been estimated by Harrison, Honnen, Dauben and Lossing⁽⁶⁵⁾ to be 74 ± 7 kcal/mole. If this value is used for azulene, in view of the structural similarity with cycloheptatriene, and rearrangement does not occur, the electron affinity of the azulyl radical may be calculated to be 39.7 kcal/mole which is rather low.

The low temperature reaction gave an apparent electron affinity of 61.1 ± 1.1 kcal/mole. If this included the rearrangement energy of azulene to naphthalene the electron affinity of naphthalene would be 22.9 kcal/mole which is rather higher than the value of about half an electron volt obtained by semi-empirical methods discussed in the final section.

No positive conclusions could be drawn from experiments on the higher polycyclic hydrocarbons since the ion currents were very low and the lines obtained from ratio plots were irreproducible, probably due to the formation of a variety of ions by fragmentation of the molecules.

3.3₆ - Summary

As can be seen from table 3.1 direct capture was not observed except in the case of azulene and possibly naphthalene but the electron affinities of the radicals formed by hydrogen loss from benzene, naphthalene, anthracene and azulene have been found. As might be expected the stabilities of the negative ions formed are very similar. It is unfortunate that low volatility prevented the possible measurement of direct capture electron affinities for the

higher polycyclic hydrocarbons which have higher predicted electron affinities.

3.4 Experimental observations on fluorocarbons

The samples of fluorocarbons were supplied by the Imperial Smelting Corporation unless otherwise stated and were used without further purification. The liquids were frozen in the sample holder (figure 2.4) and the vapour was admitted through a vacuum tap in the side arm. An iridium filament was used for all the measurements since it has been found that in the previous work with the hydrocarbons, this type of filament gave the most reproducible results.

3.4₁ - Perfluorobenzene

Perfluorobenzene showed two different types of reaction at high and low filament temperatures, the change occurring at 1330°K. Ratio plots gave rather a scatter of points and the apparent electron affinity was obtained by averaging the values obtained from the slopes of the ratio plots of twenty sets of measurements, an example of which is shown in figure 3.9. Below a temperature of 1330°K the apparent electron affinity was 32.8 ± 1.6 kcal/mole and above this temperature the ratio of $\log i_e/i_i$ was constant within the limits of the experimental error indicating a thermoneutral reaction. As the gas pressure was the same throughout the series it was possible to obtain a mean value alternatively by plotting a graph of $\log i_e/i_i$ against $10^4/T$ where the ratio of the electron to ion currents at each temperature was the mean obtained from all the sets of measurements. The slope of such a graph corresponded to an apparent electron affinity of 29.5 kcal/mole at a mean filament temperature

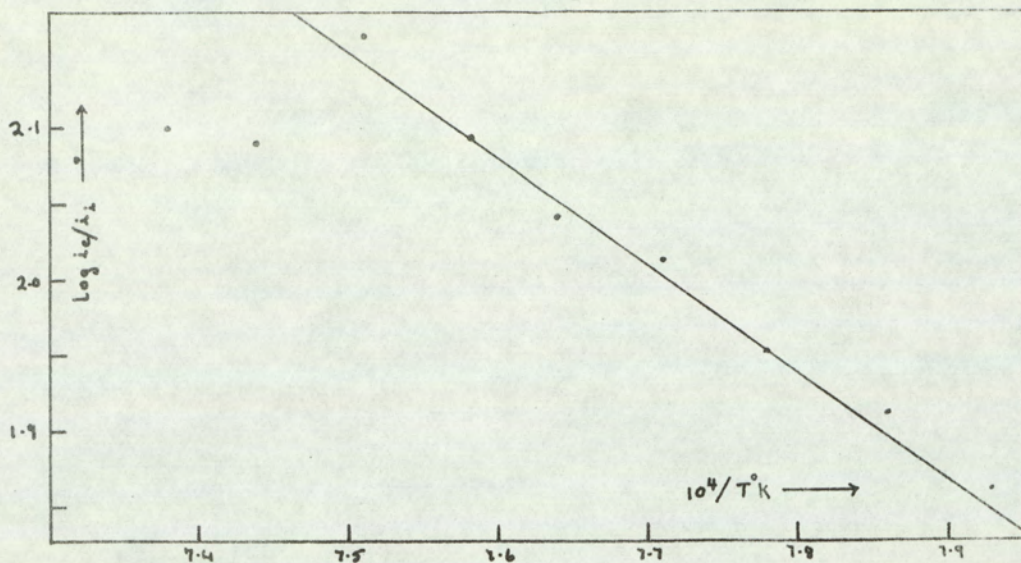


Fig. 3.9 Ratio plot for hexafluorobenzene on iridium

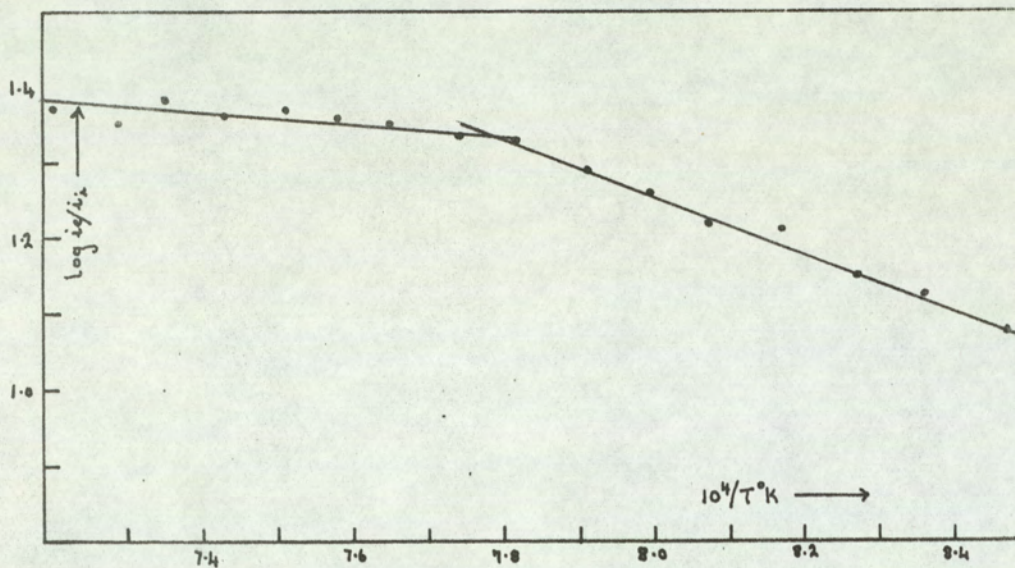


Fig 3.10 Ratio plot for pentafluorobromobenzene on iridium

of 1300°K. Above a temperature of 1330°K a thermoneutral reaction was again indicated.

3.4₂ - Pentafluorobromobenzene

This compound also showed two distinct types of behaviour, as is shown in figure 3.10. At filament temperatures in the narrow range of 1180°K to 1280°K the slope of a ratio plot corresponded to an apparent electron affinity of 17.2 ± 0.7 kcal/mole. The process changed above 1280°K to give a positive slope corresponding to an apparent electron affinity of about -2 kcal/mole.

3.4₃ - Pentafluorochlorobenzene

The ion currents observed for this compound were very small and reducing the pumping rate in an attempt to increase the values had no significant effect. With the pump valve fully open and pressures of 2.0×10^{-3} to 3.5×10^{-3} mm Hg indicated on the Pirani pressure gauge reasonably consistent results were obtained in spite of low currents. The mean value obtained for the apparent electron affinity was 17.5 ± 0.5 kcal/mole at a mean filament temperature of 1400°K. An example of the measurements made is shown in figure 3.11.

3.4₄ - Pentafluoroiodobenzene

The ratio of $\log i_e/i_i$ remained constant within the limits of experimental error for the temperature range of 1200°K to 1500°K through which this compound was studied. This indicates a thermoneutral reaction as was observed at the higher temperatures with perfluorobenzene and pentafluorobenzene.

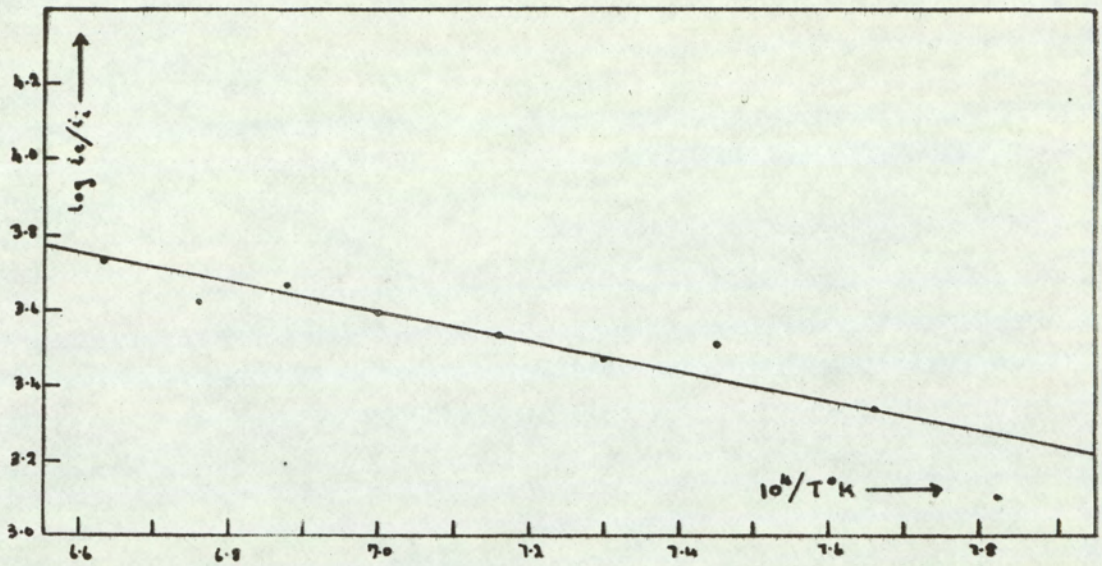


Fig. 3.11 Ratio plot for pentafluorochlorobenzene on iridium

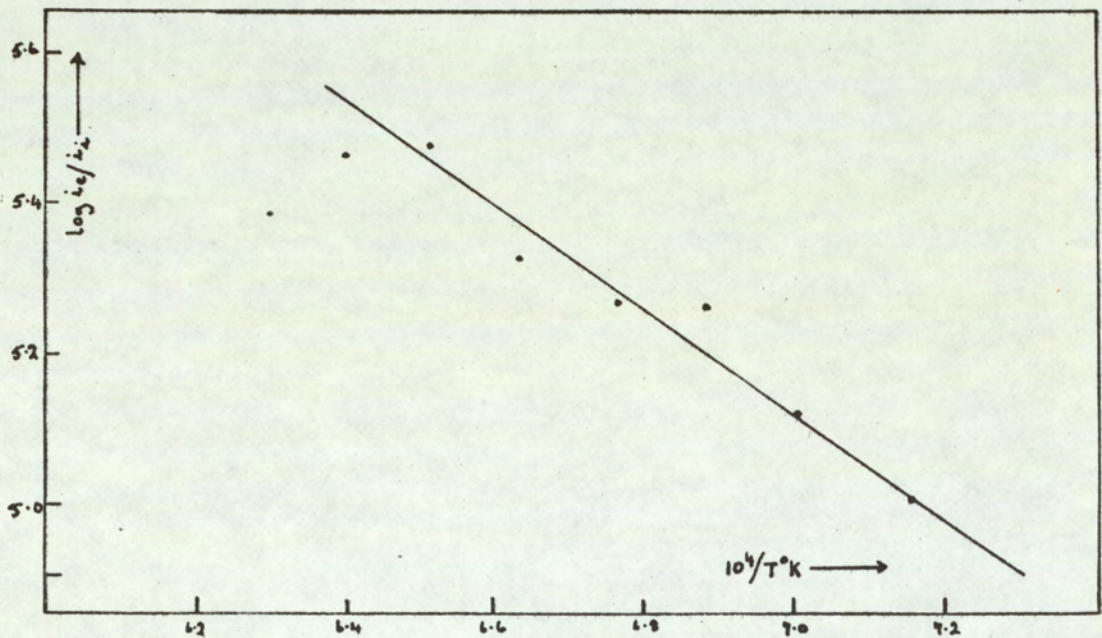


Fig. 3.12 Ratio plot for 1,2,3,4, tetrafluoronaphthalene on iridium

3.4₅ - Pentafluorobenzene

The ratio plots obtained from this compound gave a line of steep gradient for temperatures below 1400°K and a curve above. The steep slope corresponded to an apparent electron affinity of 30 to 40 kcal/mole. Since the magnitudes of the ion currents at these temperatures were of the same order as the background the result is probably not significant. The ion currents at higher temperatures were plotted as $\log i_i$ against $10^4/T$ and the slope of the line was the same as that of a graph of $\log i_e$ against $10^4/T$. This indicates an apparent electron affinity of zero.

3.4₆ - 1, 2, 3, 4 Tetrafluoronaphthalene

This compound was supplied by Dr. Patrick of Birmingham University. As there was a limited quantity available, only a few sets of measurements were possible. The values obtained for the apparent electron affinity from five ratio plots were 33.0, 42.9, 32.1, 40.0, and 29.3 kcal/mole. In the last of these measurements the pumping speed was reduced in order to increase the ion current. This probably resulted in fragment ions accumulating in the magnetron and a lower value for the electron affinity. The mean of the first four runs gave a value for the apparent electron affinity of 37.0 ± 4.4 kcal/mole at a mean filament temperature of 1450°K. At temperatures above 1500°K a ratio plot showed a steep positive gradient the slope of which corresponded to an apparent electron affinity of about 80 kcal/mole. One of the sets of measurements is illustrated in figure 3.12.

3.4₇ - Perfluoronaphthalene

This compound was obtained from the same source as the 1,2,3,4 tetrafluoronaphthalene. The ion currents were only about ten times greater than the background level even at the higher end of the temperature range of 1200°K to 1560°K for which measurements were made. Ratio plots were drawn but the slopes of the lines were not reproducible. The apparent electron affinity obtained from these graphs varied from 10 to -10 kcals/mole. The points on the graphs were fairly scattered and it was difficult to decide where the best straight line lay.

3.4₈ - Perfluorocyclohexane

This compound showed two different types of behaviour. In the temperature range 1220°K to 1400°K a graph of $\log i_1$ against $10^4/T$ indicated an apparent electron affinity of about 10 kcals/mole (figure 3.13). However, the ion currents in this temperature range were measured on the lowest scale of the D.C. amplifier and were therefore subject to variable zero error. Moreover an increase in the pressure of the gas in the magnetron did not appreciably increase the ion currents. Measurements were therefore taken with the anode lead connected directly to the amplifier by-passing the switch (S) in figure 2.8. Above a filament temperature of 1400°K the slope of the line was the same as a work function plot indicating a thermoneutral reaction.

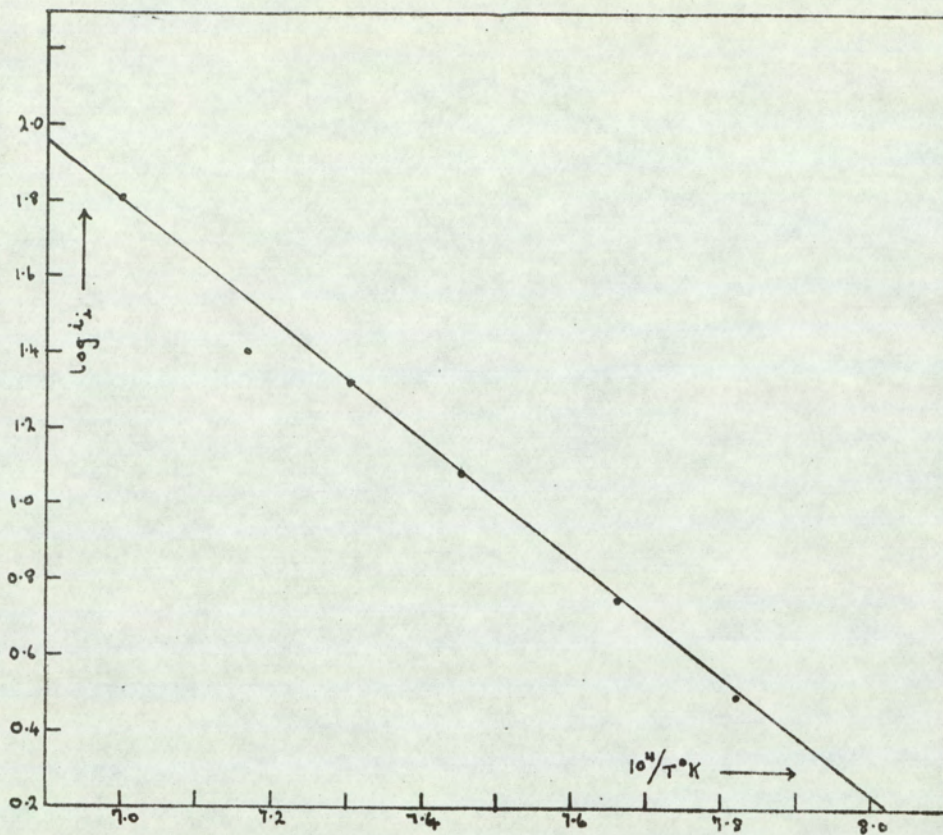


Fig. 3.13 $\log i_1$ against $10^4/T$ for perfluorocyclohexane on iridium.

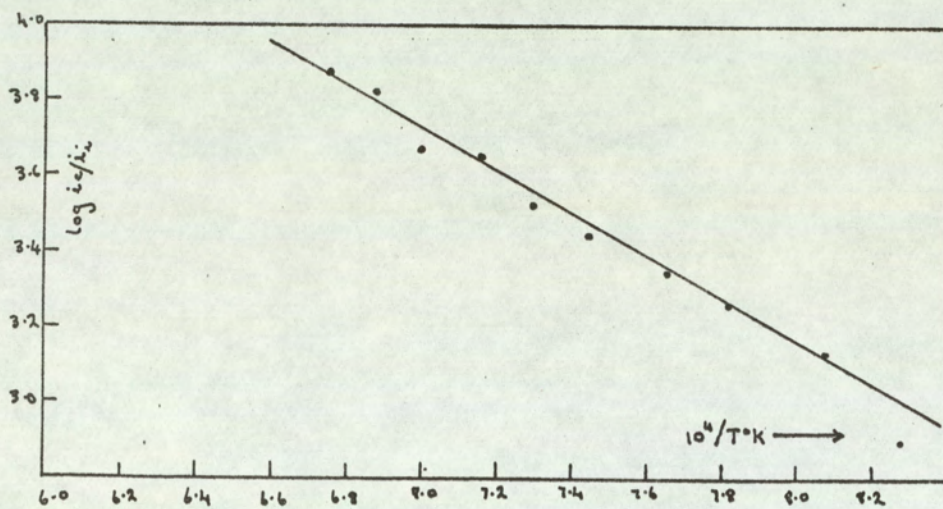


Fig. 3.14 Ratio plot for perfluorodecalin.

3.4₉ - Perfluorodecalin

The ion currents observed were ten times greater than the background level for the temperature range studied. Ratio plots gave good straight lines with a mean slope corresponding to an apparent electron affinity of 27.9 ± 1.9 kcal/mole at a mean temperature of 1370°K (figure 3.14).

3.4₁₀ - Octofluorocyclobutane

Over a temperature range of 1280°K to 1560°K the ratio of $\log i_e/i_i$ was constant within the limits of experimental error indicating a thermoneutral reaction. Ion currents were again very low.

Table 3.2 - Results of magnetron measurements on fluorocarbons

Compound	Process	Ion	E'_T kcal/mole	$T^\circ K$	E'_O kcal/mole	E_O kcal/mole	ΔS eu
Perfluorobenzene	i) Direct capture	$C_6F_6^-$	32.8 ± 1.6	1300	26.6 ± 1.6	26.6 ± 1.6	95.5
	ii) Double ion	$C_6F_5^-$ and F^-	0	1450	-8	57.2	70.5
Pentafluorobromobenzene	i) Br loss	$C_6F_5^-$	17.2 ± 0.7	1220	9.9 ± 0.7	57.9 ± 0.7	71.3
	ii) Double ion	$C_6F_4Br^- F^-$	0	1350	-8	57.2	70.7
Pentafluoroiodobenzene	Double ion	$C_6F_4I^-$ and F^-	0	1400	-8	57.2	63.5
Pentafluorochlorobenzene	Cl loss	$C_6F_5^-$	17.5 ± 0.5	1400	9.1 ± 0.5	65.9 ± 0.5	90.0
Pentafluorobenzene	Double ion	$C_6F_4H^-$ and F^-	0	1400	-8	57.2	77.7
1,2,3,4, tetrafluoronaphthalene	Direct capture	$C_{10}H_4F_4^-$	37.0 ± 4.4	1450	31.2 ± 4.4	30.7 ± 4.4	103.8
	or H loss	$C_{10}H_3F_4^-$			or 28.3 ± 4.4	or 64.7 ± 4.4	
Perfluoronaphthalene	Double ion?	$C_{10}F_7^-$ and F^-	0	1470	-8	57.2	72.5
Perfluorocyclohexane	Double ion?	$C_6F_{11}^-$ and F^-	0	1450	-8	57.2	84.5
Perfluorodecalin	Direct capture	$C_{10}F_{18}^-$	27.9 ± 1.9	1370	22.4 ± 1.9	22.4 ± 1.9	95.2

3.5 Discussion of observations on fluorocarbons

Substitution of fluorine into organic molecules will affect the ionisation potential in two ways, by inductive effects which act mainly by changing the binding of the electrons in the ground state and by resonance effects which stabilise the molecular ion when formed. These two effects oppose each other in affecting the ionisation potential. It has been shown experimentally⁽⁶⁶⁾ that on substituting fluorine into benzene the inductive effect is the larger, except in the mono- and para-disubstituted compounds, and a theoretical explanation for this effect has also been offered⁽⁶⁶⁾. Since the electrons of the system are, by the inductive drawn toward the fluorine atoms, the electron density in the carbon ring will be reduced and it will therefore be easier to add an extra electron. Hence one would expect the fluorocarbons to have a higher electron affinity than the corresponding hydrocarbons.

3.5₁ - The dissociation energy of the carbon fluorine bond

In order to find the electron affinity of the radicals formed by dissociation of substrate molecules, it is necessary to know the dissociation energy of any bond which is broken, such as the carbon fluorine bond.

Farmer et al⁽⁶⁷⁾ have found the bond energy $D(\text{CF}_3\text{-F})$ to be 123 ± 2 kcal/mole. They obtained this by measuring the ionisation potential of CF_3 by electron impact using $\text{CF}_3\text{N:NCF}_3$ as substrate and found a value of 10.10 ± 0.05 eV. Using Warren and Craggs data⁽⁶⁸⁾ for the appearance potential of CF_3^+ from CF_4 ($15.4 \pm .05$ eV) they calculated the bond energy from the difference in the appearance

potential $A(\text{CF}_3^+)$ and the ionisation potential $I(\text{CF}_3)$. This is valid providing there is no interference by negative ion formation.

Dibeler et al ⁽⁶⁹⁾ quote the bond energy $D(\text{CF}_3\text{-F})$ as 143 ± 5 kcal/mole. They used thermochemical measurements of the bond dissociation energies, (64.5 kcal/mole for $D(\text{CF}_3\text{-Br})$ ⁽⁷⁰⁾ (and 79.5 kcal/mole for $D(\text{CF}_3\text{-Cl})$ ⁽⁷¹⁾) and their own measured appearance potentials of the respective CF_3^+ ions to obtain an average value of 9.3 ± 0.2 eV for $I(\text{CF}_3)$. Calculations of $D(\text{CF}_3\text{-F})$ from this ionisation potential and the measured appearance potential of CF_3^+ from CF_4 gives 143.5 ± 5 kcal/mole for the bond energy $D(\text{CF}_3\text{-F})$.

Dibeler et al ⁽⁷²⁾ studied perfluorobenzene and found the appearance potential of C_6F_5^- to be 16.9 eV. In the absence of thermochemical data for hexafluorobenzene they suggested that one might expect a difference between the ionisation potentials, $I(\text{C}_6\text{F}_6)$ and $I(\text{C}_6\text{F}_5)$ similar to that between $I(\text{C}_6\text{H}_6)$ and $I(\text{C}_6\text{H}_5)$. Using this analogy they estimated the ionisation potential of C_6F_6 to be 10.6 eV., and from the appearance potential of C_6F_5^+ calculated $D(\text{C}_6\text{F}_5 - \text{F})$ to be 6.3 eV or 145 kcal/mole. This is equal, within experimental error, to the value of 143 kcal/mole for $D(\text{CF}_3 - \text{F})$ obtained from the study of the trifluoromethyl halides by the same group of workers, but differs from that of 123 kcal/mole obtained by Farmer et al ⁽⁶⁷⁾. The equality of the two bond dissociation energies is analagous to that observed for $D(\text{C}_6\text{H}_5 - \text{H})$ and $D(\text{CH}_3 - \text{H})$ ^(section 3.3.1). Although a value of 145 kcal/mole seems uncommonly high there appears to be more evidence to support this value rather than the lower value of 123 kcal/mole. The fact that

C_6F_6 is much more stable to heat than C_6H_6 is suggested by the large abundance of the positive molecular ion and the formation of a negative molecular ion at low energies in a mass spectrometric studies⁽⁷²⁾. This contrasts to the break up of the benzene molecules. Bibby and Carter⁽⁷³⁾ studied the negative ion spectrum of hexafluorobenzene and obtained spectra similar to those obtained by Dibeler et al⁽⁷²⁾, but their calibration of the electron energy scale differed markedly. Bibby and Carter considered the earlier work to be in error because the negative ion $C_6F_6^-$ is quoted as appearing at an incident electron energy of 4.0 e.V. At this high energy the negative molecular ion would decompose with the elimination of a fluoride ion since the combined incident electron energy and electron affinity of fluorine would exceed 7.3 eV or 168 kcal/mole, a value which is in excess of all known chemical bond energies. Hence it is seen that there is considerable doubt about the magnitude of the carbon fluorine bond dissociation energy. The electron affinities derived from experimental data on fluorocarbons were therefore calculated using each of the proposed values of 121 and 145 kcal/mole to see which gave the more reasonable energies for the stabilities of the negative ions.

3.5₂ - Perfluorobenzene

The apparent electron affinity of 32.8 ± 1.6 kcal/mole at 1300°K (table 3.2) obtained for perfluorobenzene may be interpreted as the direct capture of an electron leading to the formation of $C_6F_6^-$. The entropy change of 96 e.u. is within the range of 110 ± 17 e.u. expected for direct capture reactions. It

was shown (section 2.9) that it is not possible to measure in the magnetron ion stabilities below a minimum value of about 25 kcal/mole. Since the measured electron affinity of C_6F_6 is not much greater than this value, poor reproducibility and large scatter of results is to be expected as was observed. However, by making many measurements of the electron affinity it was possible to obtain a mean value and, neglecting values which differed from the mean by more than twice the standard deviation, to recalculate a mean value for the electron affinity of C_6F_6 as 26.6 ± 1.6 kcal/mole at $0^\circ K$.

The thermoneutral reaction which occurred at higher temperatures is likely to be one of dissociative capture. If the bond dissociation energy $D(C_6F_5 - F)$ is 145 kcal/mole a possible process giving a thermoneutral reaction would be the simultaneous formation of the two ions $C_6F_5^-$ and F^- when the bond breaks. Since the electron affinity of fluorine is 79.4 kcal/mole⁽⁵²⁾ the electron affinity of $C_6F_5^*$ may be found, by subtraction, to be 65.6 kcal/mole at $1400^\circ K$. If this value is corrected to $0^\circ K$ by making the same specific heat corrections as for the other compounds the stability of $C_6F_5^-$ may be found to be 57.2 kcal/mole at $0^\circ K$. Since, however, the slopes of the different ratio plots corresponded to electron affinities between -5 and +5 kcal/mole there is a possible error of at least 5 kcal/mole in this figure, which is only slightly greater than the value of 56.7 kcal/mole obtained for the electron affinity of $C_6H_5^*$. Although the capture of two electrons by one molecule, leading to the formation of two ions simultaneously would seem unlikely, the appearance potentials of $C_6F_5^-$ and F^- were indeed found by Dibeler

and Rees⁽⁷²⁾ to be the same, suggesting that the formation of two ions could occur. If the bond energy is 123 kcal/mole, as found by Farmer et al⁽⁶⁷⁾ for $D(CF_3 - F)$, the thermoneutral reaction could be explained by a dissociative reaction with the adsorption of a fluorine atom. The heat of adsorption of fluorine on platinum has been found to be 50.2 kcal/mole⁽⁷⁴⁾. The heat of adsorption of fluorine on iridium may be approximately estimated by plotting a graph of heat of adsorption of the halogens on platinum against heat of adsorption on iridium since the other energies have been estimated⁽⁴⁰⁾. The value for the heat of adsorption of fluorine on iridium found by this method was 50.0 kcal/mole (fig. 3.15). Hence for the thermoneutral reaction, and a bond energy of 123 kcal/mole, the stability of $C_6F_5^-$ may be calculated to be 73 kcal/mole which is rather high but 145 kcal/mole for the energy of the carbon fluorine bond would imply an electron affinity of 90 kcal/mole which is unreasonably high compared with values obtained for other species.

3.5₃ - Pentafluorobromobenzene

Pentafluorobromobenzene showed two different types of behaviour, one above and the other below a temperature of 1250°K (table 3.2). At a mean temperature of 1220°K an apparent electron affinity of 17.2 kcal/mole was obtained. This value is rather low to represent direct capture and since it was observed over a narrow temperature range possibly has no significance. It could, however, be interpreted as a dissociative reaction as suggested by the change in entropy of 70.7 e.u. leading to the formation of $C_6F_5^-$ by the breaking of a carbon-bromine bond. It has been found thermochemically that the C-Br bond

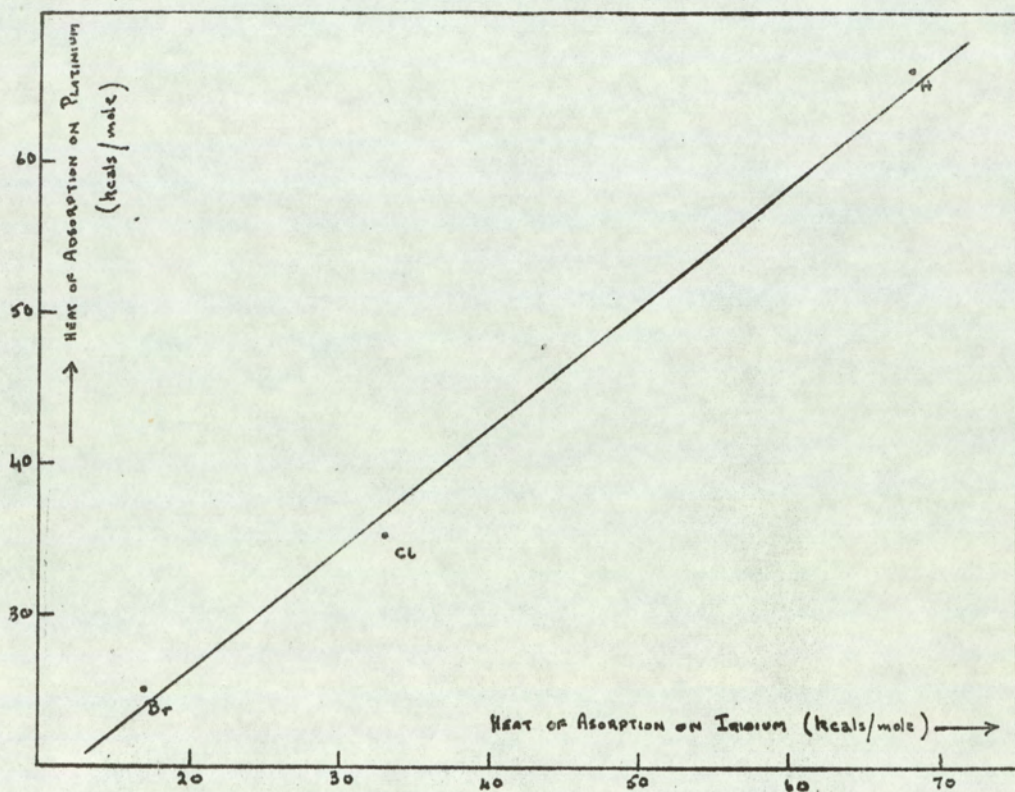


Fig. 3.15 Heats of adsorption on platinum and iridium.

in CF_3Br has a dissociation energy of 65 kcal/mole⁽⁷⁰⁾. In the absence of measurements of $D(\text{C}_6\text{F}_5 - \text{Br})$ it may be taken to be the same since $D(\text{C}_6\text{H}_5 - \text{H})$ is about the same as $D(\text{CH}_3 - \text{H})$ and $D(\text{C}_6\text{F}_5 - \text{F})$ is the same as $D(\text{CF}_3 - \text{F})$ according to Dibeler et al⁽⁷²⁾. Using this value of 65 kcal/mole for the bond dissociation energy and 17 kcal/mole for the heat of adsorption of bromine on iridium⁽⁴⁰⁾ the stability of the negative ion C_6F_5^- may be calculated to be 57.9 kcal/mole at 0°K which is only slightly higher than the 56.7 kcal/mole obtained (section 3.3₂) for the stability of C_6H_5^- , and agrees with the value of 57.2 kcal/mole for the stability C_6F_5^- obtained from the study of perfluorobenzene (section 3.5₂).

If the bromine, instead of being adsorbed, had captured an electron to form a bromide ion the $(\text{C}_6\text{F}_5 - \text{Br})$ bond energy may be found from the measured apparent electron affinity and the known electron affinity of bromine which is 77.6 kcal/mole at 0°K ⁽⁵²⁾. The value thus obtained for $D(\text{C}_6\text{F}_5 - \text{Br})$ is 67.7 kcal/mole at 0°K and is slightly less than the carbon-bromine bond dissociation energy measured in bromobenzene which is 71 kcal/mole⁽⁵⁴⁾. This is consistent with the order of the values obtained for methyl bromide and its fluorine analogue trifluoro-methyl bromide which are 67 kcal/mole and 65 kcal/mole respectively⁽⁵⁴⁾.

At temperatures above about 1280°K the reaction observed was thermoneutral. If it was in this temperature region that the dissociative reaction of bromine loss occurred with adsorption then the stability of the C_6F_5^- ion may be calculated to be 48 kcal/mole which is rather low. It is possible that a similar reaction occurs

as with C_6F_6 , that is two ions, $C_6F_4Br^-$ and F^- , or, $C_6F_5^-$ and Br^- , are formed simultaneously. Although the C-F bond energy is greater than $D(C - Br)$ there are more of the former type of bond so that one of these could break in preference to a C - Br bond, particularly if the molecule sits flat on the surface of the filament. If this is the case the low temperature region cannot be explained by bromine loss and is probably not significant.

3.5₄ - Pentafluorochlorobenzene

Only one process was observed for the temperature range studied which gave an apparent electron affinity of 17.5 kcal/mole at a mean temperature of 1400°K (table 3.2). This is rather low to be direct capture (section 2.9) and the entropy change of 90 e.u. lies between the limits for direct capture and dissociation with adsorption. If this is a dissociative reaction where the carbon-chlorine bond is broken and chlorine is adsorbed onto the filament with a heat of adsorption of 33 kcal/mole⁽⁷⁵⁾ and $D(C_6F_5 - Cl)$ is 89.9 kcal/mole⁽⁷⁵⁾, the stability of $C_6F_5^-$ may be calculated to be 65.9 kcal/mole at 0°K, which is rather higher than the value obtained from the study of hexafluorobenzene. The breaking of a fluorine bond using either 145 kcal/mole or 123 kcal/mole for $D(C_6F_4Cl - F)$ leads to an unreasonably large value for the stability of $C_6F_4Cl^-$, and such a reaction is not therefore likely to occur.

3.5₅ - Pentafluoriodobenzene and pentafluorobenzene

Both of these compounds gave a thermoneutral reaction between 1300°K and 1500°K, which was the temperature range studied (table 3.2). The only reaction which would give reasonable energies is again the formation of two ions after the breaking of a C-F bond with a

dissociation energy of 145 kcal/mole. This leads to a value of 65.6 kcal/mole (or 57.2 kcal/mole when corrected to 0°K) for the stability of $C_6F_4I^-$ and $C_6F_4H^-$ as for $C_6F_5^-$ derived above.

3.5₆ - Perfluoronaphthalene

The ratio plots obtained for this compound were not reproducible, the apparent electron affinity varying between +10 and -10 kcal/mole. If this represents a thermoneutral reaction it could be accounted for by the formation of two ions, $C_{10}F_7^-$ and F^- , after the breaking of a carbon fluorine bond. Using the same values for the electron affinity of fluorine and bond dissociation energy as above, the stability of $C_{10}F_7^-$ is found to be the same as that of $C_6F_5^-$, $C_6F_4I^-$, and $C_6F_4H^-$ discussed above. One might reasonably expect the stabilities of $C_{10}F_7^-$ and $C_6F_5^-$ to be very similar as was indeed found for their hydrocarbon analogues but the apparent electron affinities in these thermoneutral reactions have errors of between 5 and 10 kcal/mole so it is not possible from the present results to observe differences between the stabilities of these ions.

3.5₇ - 1,2,3,4 - Tetrafluoronaphthalene

It is seen from Table 3.2 that this compound gave an apparent electron affinity of 37.0 ± 4.4 kcal/mole which could be accounted for by direct capture. It is, however, difficult to understand why this compound should capture an electron when perfluoronaphthalene did not. Since the latter symmetrical compound has C-F dipoles at every carbon atom withdrawing electrons from the π system one would

have expected that to capture an electron rather than the less symmetrical compound. An alternative explanation for the apparent electron affinity of 31.2 kcal/mole at 0°K is that of a dissociative reaction where a C-H bond is broken and hydrogen is adsorbed by the filament. Assuming $D(\text{C-H})$ to be 102 kcal/mole and the heat of adsorption of hydrogen on iridium to be 68 kcal/mole (section 3.3₁), the electron affinity of $\text{C}_{10}\text{F}_4\text{H}_3^{\bullet}$ may be calculated to be 64.7 kcal/mole at 0°K. This is rather larger than the value of 59.2 kcal/mole obtained for the naphthyl radical. The difference could be accounted for by the C-F dipoles present in the fluorocarbons which would be expected to have a second order effect on σ capture electron affinities.

3.5₈ - Perfluorocyclohexane

At temperatures below 1350°K ratio plots showed slopes indicating an apparent electron affinity of about 10 kcal/mole and at higher temperatures a thermoneutral reaction occurred (Table 3.2). Since the value of 10 kcal/mole was obtained over a narrow temperature range and the ion currents were of the same order as the background level it is of dubious significance. It is unlikely to be direct capture (section 2.9) and the reaction occurred at rather a low temperature to represent the breaking of a C-F bond. The thermoneutral reaction at the higher temperatures is probably one of dissociation similar to those already discussed.

3.5₉ - Perfluorodecalin

An apparent electron affinity of 27.9 ± 1.9 kcal/mole at a mean temperature of 1370°K was obtained for this compound (Table 3.2).

The entropy change lies within the limits expected for direct capture. If in fact such a reaction did occur it is reasonable to suppose that the electron could be 'held' at the centre of the molecule by the field created by the C-F dipoles. Alternatively, it could be interpreted as a dissociative reaction but this would lead to abnormally high energies of over 80 kcals/mole for ion stabilities assuming the bond dissociation energies and heat of adsorption discussed earlier.

3.5₁₀ - Octofluorocyclobutane

A thermoneutral reaction was observed for the whole of the temperature range studied and probably represented a dissociative reaction.

3.5₁₁ - Summary

The results which were obtained for the fluorocarbons are summarised in Table 3.2. From this it is seen that direct capture was observed for perfluorobenzene, perfluorodecalin and, possibly 1,2,3,4 tetrafluoronaphthalene. Most of the other compounds gave thermoneutral reactions and these have been interpreted as the breaking of a C-F bond with a dissociation energy of 145 kcals/mole, and the formation of two ions, F^- , and the negative ion formed from the radical. Since the electron affinity of fluorine is 79.4 kcals/mole the stability of the radical negative ion is $E' + (145.0 - 79.4)$ kcals/mole. For the thermoneutral reaction E' is near zero but it is not possible to decide on the apparent electron affinity E' to within ± 5 kcals/mole for these small

gradients. Therefore, the electron affinities of the radicals formed from the various compounds are in the region of 57.2 ± 5 kcal/mole at 0°K . By comparison with the stability of the hydrocarbon negative ions (Table 3.1) it is seen that the values, between 50 and 60 kcal/mole, lie within the same range as the fluorocarbon radical negative ions. Since the electron is captured into a σ orbital rather than into the π system one would expect the fluorine to exert only a second order effect and the two types of negative ions to have very similar stabilities.

3.6 Experimental Observations on quinones

The substituted benzoquinones, naphthaquinones and anthraquinones were obtained from Imperial Chemical Industries unless otherwise stated and were used without further purification. When the compounds were placed in the sample holder directly under the filament the ion currents observed at low filament temperatures were comparable with the background level measured with no sample in the magnetron. Even with the pumping rate reduced the number of ions produced was very low, and in many cases the ion current was measured on the lowest scale of the D.C. amplifier. It was therefore necessary to heat the holder electrically to sublime the compound directly onto the iridium filament. The vapour pressure of some of the quinones was great enough to produce sufficient ion precursors at the filament to obtain a reasonable ion current but it was not possible to estimate the actual pressure with the Pirani pressure gauge.

3.6₁ - Benzoquinone

Commercially obtained benzoquinone was recrystallised from

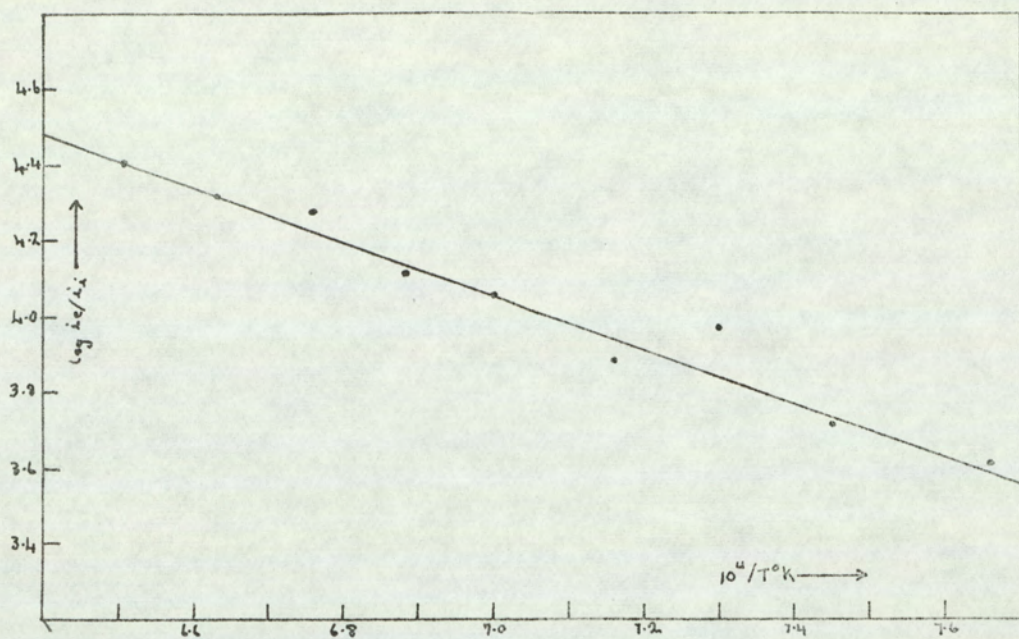


Fig. 3.16 Ratio plot for benzoquinone on iridium

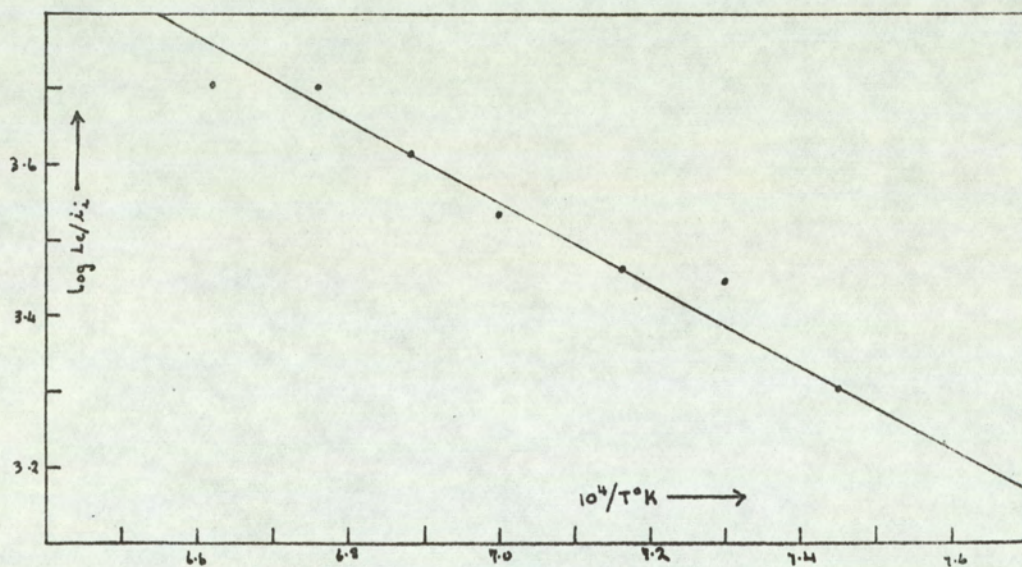


Fig. 3.17 Ratio plot for naphthaquinone on iridium

petroleum ether. The vapour pressure of this compound was great enough to be measured on the Pirani pressure gauge without heating the sample holder. With a relatively high pressure of 5×10^{-3} torr consistent results were obtained and an apparent electron affinity of 31.4 ± 2.4 kcal/mole at 1400°K was found from the slope of graphs of $\log i_e/i_i$ against $10^4/T$.

3.6₂ - Naphthaquinone

It was necessary to sublime the naphthaquinone onto the filament. Ion and electron currents were measured but initial ratio plots gave a scatter of points. When the filament had become conditioned, the results were more consistent and an apparent electron affinity of 23.1 ± 1.4 kcal/mole in the temperature range $1350 - 1560^\circ\text{K}$ was obtained. When $\log i_i$ was plotted against $10^4/T$ a similar value was obtained using the measured value of 89.6 kcal/mole for the work function of iridium. Above a temperature of 1560°K the slope of the ratio plot became positive and erratic.

3.6₃ - Anthraquinone

Anthraquinone was sublimed onto the iridium filament and electron and ion currents measured. The slopes of the ratio plots however varied over a range of 10 kcal/mole. In order to calculate a mean value, a comparatively large number of runs were required. Individual measurements which differed from this mean by more than twice the standard deviation were neglected in calculating a new mean for the apparent electron affinity as 32.1 ± 2.1 kcal/mole at a mean filament

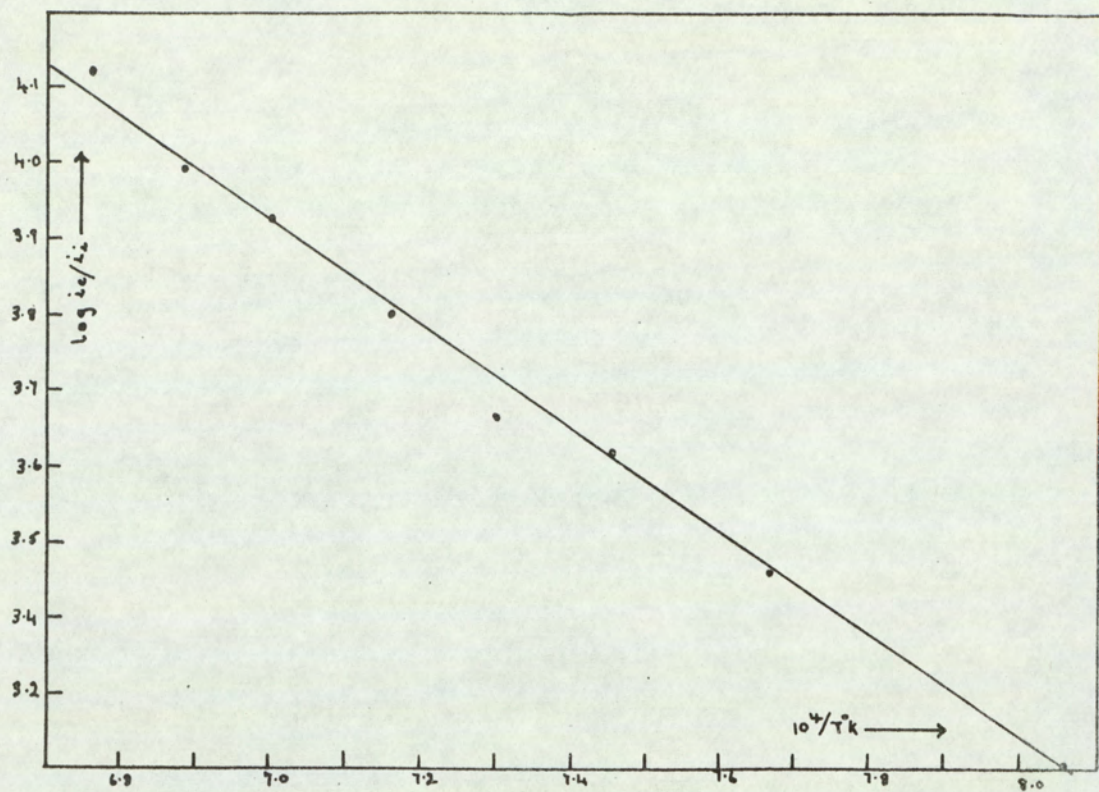


Fig. 3.18 Ratio plot for anthraquinone on iridium

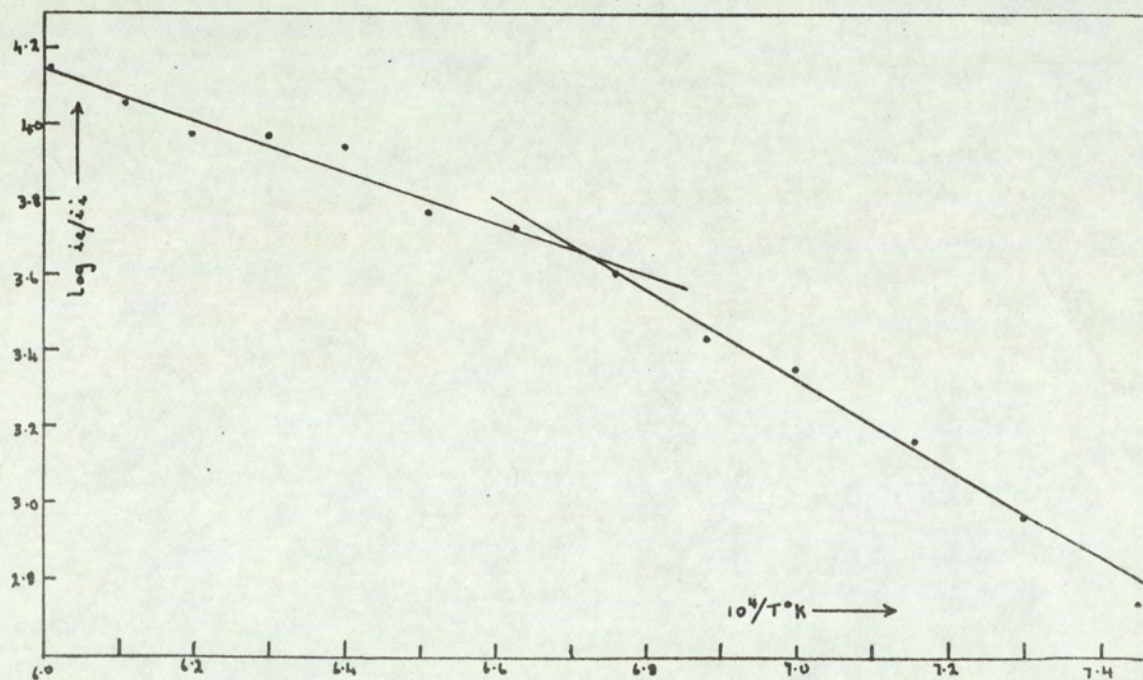


Fig. 3.19 Ratio plot for chloranil on iridium

temperature of 1450°K . Above a temperature of about 1500°K the slope of the ratio plot indicated a negative electron affinity, but the value of this was not reproducible.

3.6₄ - Chloranil

In order to obtain a mean value for the apparent electron affinity it was necessary to make many measurements since the individual values obtained from the ratio plots varied greatly from each other. Rejecting values deviating from the mean of the measured values by more than twice the standard deviation the recalculated mean of 34 measurements gave an apparent electron affinity of 49.8 ± 1.9 kcal/mole at a mean temperature of 1430°K . There was a change of process at a filament temperature of 1500°K and the apparent electron affinity above this temperature was 32.4 ± 1.4 kcal/mole.

3.6₅ - Fluoranil

The sample was held in the side arm sample holder and admitted through a vacuum tap. Even at a filament temperature of 1200°K the ion current was 100 times greater than the background level. Exceptionally good straight lines were obtained of consistent slope for every set of measurements. The value obtained for the apparent electron affinity was 57.7 ± 0.5 kcal/mole at a mean filament temperature of 1370°K .

3.6₆ - 2,6-Dichlorobenzoquinone

The compound was sublimed directly on to the filament and electron and ion currents measured at various filament currents. Over a temperature range of 1200°K and 1300°K the slope of the ratio plots

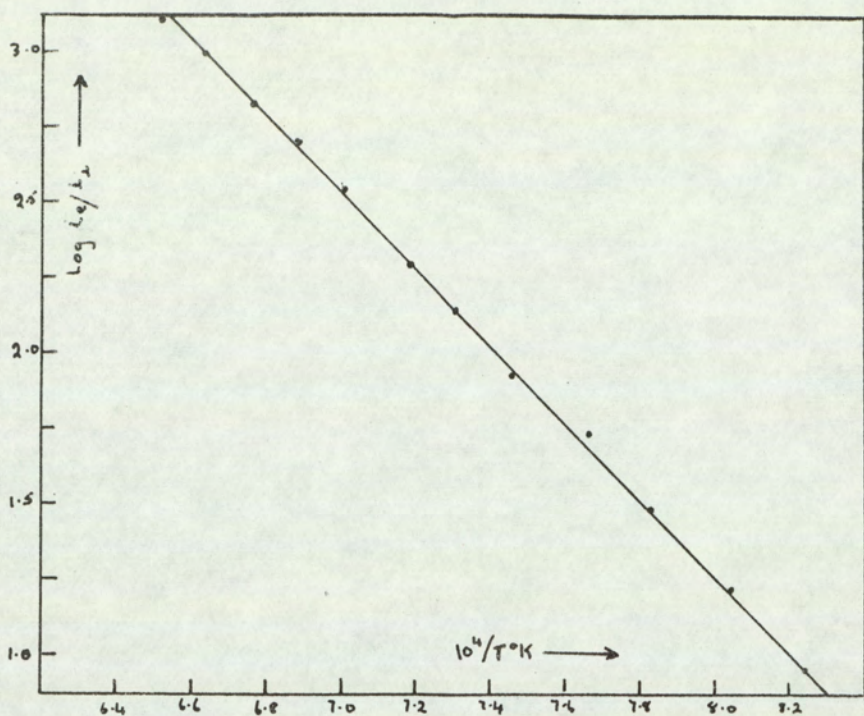


Fig. 3.20 Ratio plot for fluoranil on iridium

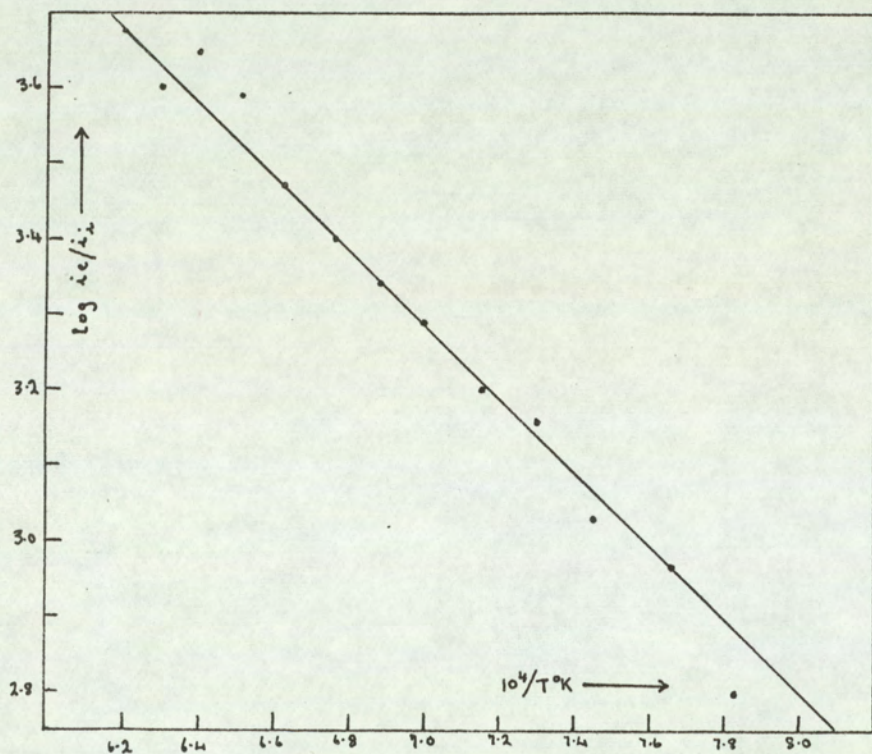


Fig. 3.21 Ratio plot for chloroquinone on iridium

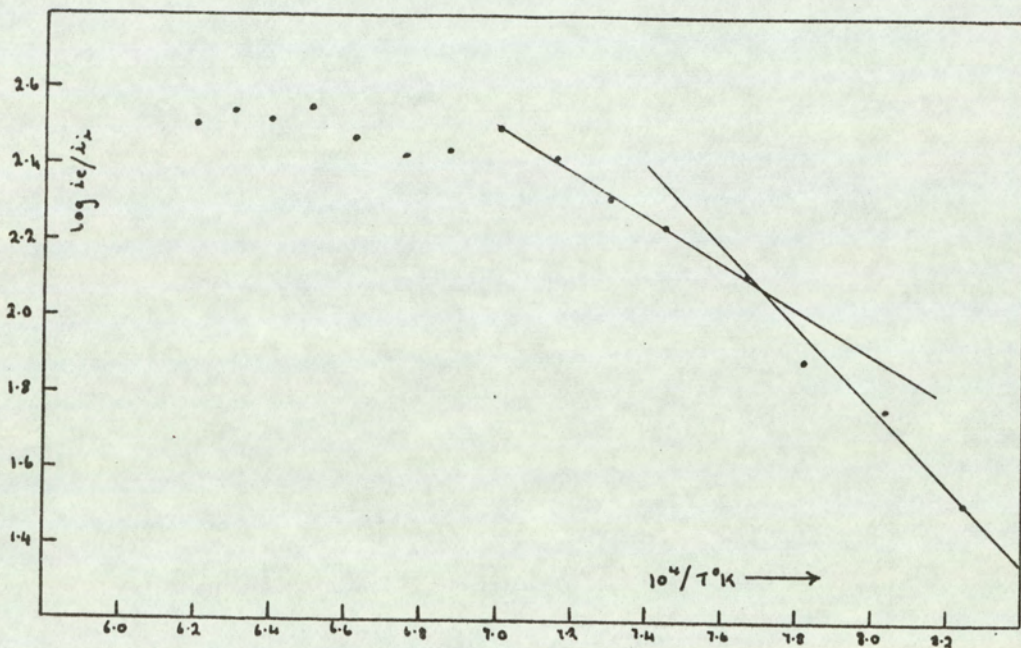


Fig. 3.22 Ratio plot for 2,6, dichlorobenzoquinone on iridium

indicated an apparent electron affinity of 51.2 ± 2.7 kcal/mole. Between 1300°K and 1400°K the slope of the graph corresponded to an apparent electron affinity of 30.0 ± 4.7 kcal/mole. Above this temperature range the ratio of electron to ion currents remained constant indicating a thermoneutral reaction. Since the temperature range was so small for each reaction, electron and ion currents were measured at filament currents between the usual values and the corresponding values of $10^4/T$ interpolated from the graph of $\log i_e$ against $10^4/T$.

3.6₇ - Chloroquinone

Chloroquinone was made by oxidation of the hydroquinone as described by Gillman and Blatt⁽⁷⁶⁾. With the sample held in the sample holder pressures of about 2×10^{-3} Torr were indicated on the pressure gauge. The apparent electron affinity obtained from ratio plots was 19.0 ± 1.0 kcal/mole, at a mean temperature of 1450°K .

3.6₈ - Other Quinones

An attempt was made to measure the apparent electron affinities of chloro- and bromo- substituted naphthaquinones and anthraquinones but their vapour pressures were so low that the ion currents produced were no greater than the background level, even when the compounds were sublimed directly onto the filament. The apparent electron affinities obtained were about 60 kcal/mole which is the value obtained without any substrate in the magnetron.

Compound	Process	Ion	E'_T kcal/mole	$T^{\circ}K$	E'_0 kcal/mole	E_0 kcal/mole	ΔS eu
Benzoquinone	Direct Capture	$C_6H_4O_2^-$	31.4 ± 2.4	1400	25.8 ± 2.4	25.8 ± 2.4	95.6
Naphthaquinone	H. loss	$C_{10}H_5O_2^-$	23.1 ± 1.4	1450	14.4 ± 1.4	48.4 ± 1.4	90.0
Anthraquinone	Direct Capture	$C_{14}H_8O_2^-$	32.2 ± 2.1	1450	26.3 ± 2.1	26.3 ± 2.1	94.1
Chloranil	i) Direct Capture	$C_6Cl_4O_2^-$	49.8 ± 1.9	1430	44.1 ± 1.9	44.1 ± 1.9	110
	ii) Cl loss	$C_6Cl_3O_2^-$	32.4 ± 1.4	1620	22.4 ± 1.4	78.3 ± 1.4	96.2
Fluoranil	Direct Capture	$C_6F_4O_2^-$	57.7 ± 0.5	1370	52.2 ± 0.5	52.2 ± 0.5	117.8
2,6 Dichloro- benzoquinone	i) Direct Capture ?	$C_6Cl_2H_2O_2^-$	51.2 ± 2.7	1230	46.2 ± 2.7	46.2 ± 2.7	112.0
	Cl loss ii) or H loss	$C_6ClH_2O_2^-$ or $C_6Cl_2HO_2^-$	30.0 ± 4.7	1350	22.2 ± 4.7	78.8 ± 4.7 or 55.9 ± 4.7	95.6
Chloroquinone	Cl loss or H loss	$C_6H_3O_2^-$ or $C_6H_2ClO_2^-$	19.0 ± 1.0	1450	10.4 ± 1.0	67.3 ± 1.0 or 44.4 ± 1.0	91.6

Table 2.3 - Results of magnetron measurements on Quinones

3.7 Discussion of observations on quinones

Relative electron affinities have been estimated for a number of quinones using techniques such as charge transfer spectroscopy and polarography. In the final chapter of this dissertation these will be discussed and compared with the results in this section. The carbon-oxygen dipoles may be expected to lead to an increase in the electron affinity of a quinone compared to the corresponding hydrocarbon. Farragher⁽⁵⁰⁾ found that the electron affinity of a molecule could be approximately predicted by summation of the contributions due to each substituent. He found that the contribution due to a C = O dipole in a molecule was about 20 kcal/mole. Therefore it was likely that the magnetron method could be used to measure the larger electron affinity of the quinones where it had not been possible to obtain values for the corresponding hydrocarbons whose electron affinities lay below the limit of measurement by the magnetron method.

3.7₁ - Benzoquinone

The apparent electron affinity of benzoquinone was 31.4 ± 2.4 kcal/mole at a mean temperature of 1400°K . This is most reasonably interpreted as a direct capture reaction although the change in entropy lies near the lower limit expected for this type of behaviour. The value of 37.1 kcal/mole obtained by Farragher⁽⁵⁰⁾ using a carbided tungsten filament is rather higher than the present value. His measurements were made over a higher temperature range and in drawing the best straight lines for the ratio plots, the points at the lower temperatures were ignored. If these had been taken into

account a lower value would have been obtained. The mean temperature of 1470°K at which his measurements were made is rather high for direct capture to occur.

If the present value of 31.4 kcal/mole represents a hydrogen loss and adsorption reaction the stability of the $\text{C}_6\text{H}_3\text{O}_2^-$ ion may be calculated to be 57.6 kcal/mole at 0°K , a figure not much higher than the value of 56.7 kcal/mole obtained for the phenyl ion (Table 3.1)

3.7₂ - Naphthaquinone

The apparent electron affinity of naphthaquinone was found to be 23.1 ± 1.4 kcal/mole at a mean temperature of 1450°K . This could be direct capture but is significantly lower than the result for benzoquinone and anthraquinone (Table 3.3). Possibly electron capture is hindered by assymetry and a carbon-hydrogen bond is broken. If the bond dissociation energy is 102 kcal/mole as in benzene (section 3.3), the stability of the negative ion formed is 48.4 kcal/mole which is rather lower than the electron affinity of the phenyl and naphthyl radicals listed in Table 3.1. The entropy change of 90 eu for the reaction lies between the limits for direct capture and dissociation with adsorption reactions and so can not be used to decide on reaction type.

3.7₃ - Anthraquinone

The apparent electron affinity of anthraquinone was found to be 32.2 ± 2.1 kcal/mole at a mean temperature of 1450°K . This is probably a direct capture reaction. The entropy change lies just within the limit expected for this type of reaction. One would expect

the electron affinity of anthracene to be below this value owing to the inductive effect of the oxygen atoms in the quinone leaving the ring system more positively charged than in the hydrocarbon. The electron affinity of anthracene as well as benzene and naphthalene was probably therefore below the limit of measurement using the magnetron and was therefore not susceptible to measurement by the experiments described in Section 3.2.

3.7₄ - Chloranil

Chloranil showed two different types of process above and below a temperature of 1500°K (Table 3.3). At a mean filament temperature of 1430°K the apparent electron affinity was 49.8 ± 1.9 kcals/mole. This probably represents direct capture, and the change in entropy is in agreement with this interpretation. Farragher⁽⁵⁰⁾ using the magnetron technique, found the electron affinity of chloranil to be 55.3 kcals/mole at 0°K, a value slightly greater than the present one for fluoranil whereas one would expect fluoranil to have the greater electron affinity. The mean temperature of his experiments was 1514°K, higher than in the present work, and the magnetron was heated to about 70°C to prevent condensation of the chloranil. The higher value obtained could therefore have been due to fragment molecules, formed by chlorine loss, capturing the electrons rather than to direct capture by the chloranil molecules.

The value of 32.4 ± 1.4 kcals/mole obtained in the present work for temperatures above 1500°K is probably due to chlorine loss. From a bond dissociation energy $D(C - Cl)$ of 89.9 kcals/mole⁽⁷⁵⁾ and a heat of adsorption of chlorine on iridium of 33 kcals/mole (75) the

stability of $C_6Cl_3O_2^-$ is calculated to be 78.3 kcal/mole at $0^\circ K$, a value considerably higher than that obtained for the phenyl ion (section 3.3). The difference in the slopes of the two lines in the different temperature regions on a ratio plot was not very great, and a single line could be drawn through all the points giving a single reaction throughout the temperature range with an apparent electron affinity of 40 kcal/mole. The change in entropy for this reaction lies within the limits expected for direct capture so this could well be interpreted as the formation of the ion $C_6Cl_4O_2^-$ with a stability of 33.9 kcal/mole at $0^\circ K$.

3.7₅ - Fluoranil

The apparent electron affinity of fluoranil was 57.7 kcal/mole at $1370^\circ K$ (Table 3.3). The reaction occurring appears to be direct capture and the entropy change is well within the expected limits for this process. Moreover the apparent electron affinity is too high to represent a dissociative reaction and the formation of ions even at low filament temperatures of $1200^\circ K$ also suggests direct capture rather than dissociation. The stability of the fluoranil negative ion is greater than that of the chloranil negative ion which is reasonable since the C-F dipoles create a stronger field at the centre of the molecule than do the C-Cl dipoles, since the C-F bond length is shorter than the C-Cl bond.

3.7₆ - 2,6 - Dichlorobenzoquinone

The apparent electron affinity of 46.2 kcal/mole at $0^\circ K$ would be most reasonably interpreted as direct capture particularly with the entropy change being within the expected limits, but is rather

high compared with the result of 45.8 kcal/mole at 0°K obtained for chloranil which one would expect to be higher. If, in fact, the electron affinity of chloranil is 55.3 kcal/mole as found by Farragher, the present value for 2,6 dichlorobenzoquinone is more reasonable by comparison but both are rather nearer to the measured electron affinity of fluoranil than would be expected. Since the ion currents were not very great and the temperature range small, this value possibly has no significance.

The value of 30 kcal/mole obtained at the higher temperatures is probably one of dissociation. If a carbon-chlorine bond were broken the stability of the $C_6H_2ClO_2^-$ ion would be 78.8 kcal/mole at 0°K using the value of 89.9 kcal/mole for $D(C-Cl)^{(75)}$ and 33.0 kcal/mole for the heat of adsorption of chlorine on iridium⁽⁷⁵⁾. This is rather high and a more reasonable value is obtained from the hypothesis of a hydrogen-loss reaction. This gives the stability of $C_6H Cl_2O_2^-$ as 55.9 kcal/mole at 0°K if the same values are used for the bond dissociation and heat of adsorption energies as were used in section 3.3. The entropy change of 95.6 e.u. lies within the range for direct capture and the apparent electron affinity of 30 kcal/mole could well be this type of reaction in which case the low temperature value of 51.2 kcal/mole would not be significant.

3.7₇ - Chloroquinone

The value of 19.0 ± 1.0 kcal/mole for the apparent electron affinity is rather low to be direct capture (Section 2.9), and the entropy change is below the limit expected for such a reaction. The weakest bond in the molecule is the carbon-chlorine bond. If this

breaks and $D(\text{C-Cl})$ is 89.9 kcal/mole⁽⁷⁵⁾ the stability of $\text{C}_6\text{H}_3\text{O}_2^-$ may be calculated to be 67.3 kcal/mole at 0°K . The reaction could, however, well be hydrogen loss for there are more carbon hydrogen bonds and $D(\text{C-H})$ is only about 12 kcal/mole greater than $D(\text{C-Cl})$ and, moreover, the heat of adsorption of hydrogen is twice that of chlorine. This process leads to a value of 44.4 kcal/mole at 0°K for the stability of $\text{C}_6\text{H}_2\text{ClO}_2^-$ which is however rather low compared with values obtained for other σ capture electron affinities.

3.78 - Summary

It has been possible to obtain direct capture electron affinities for several quinones and these are shown in Table 3.3. Naphthaquinone did not appear to capture an electron, but the apparent electron affinity is interpreted in terms of a hydrogen loss reaction. In other cases dissociation occurred though it is not possible to say whether a carbon-hydrogen or carbon-chlorine bond broke. In the mono- and di- substituted chlorobenzoquinones the stability of the ions formed from both these reactions have been calculated from the apparent electron affinity and the values are included in Table 3.3., with the rest of the results obtained from studies on quinones.

Chapter 4 - The electron capture cell

4.1 Introduction

The electron capture detector was developed by Lovelock and Lipsky⁽⁴²⁾ for use in gas chromatography. Its action depends on the fact that neutral molecules can capture thermal electrons and form negative ions. The work done by bringing an electron from infinity to the lowest unoccupied orbital of the molecule is its electron affinity. The energy varies from about four eV to almost zero for gases which show electron attachment, and is negative for those which do not. The cell detects the attenuation in electron concentration produced by a known number of acceptor molecules. Since the electron affinity of different molecules varies, the attenuation produced by the same concentration of different compounds will also vary and the detector may be used qualitatively. Usually, however, it is used quantitatively particularly in the measurement of very low concentrations of halogen containing compounds which capture electrons very readily, and to which the detector is therefore highly sensitive⁽⁷⁷⁾. Although the detector is a valuable and widely used tool in gas chromatography, the physical processes occurring within the cell are not well understood. In an attempt to elucidate the mode of action of the detector various compounds which had been previously examined in the magnetron were introduced into the cell. The concentration of the compound, and temperature of the cell, were varied in order to study the kinetics of the reactions involved in the formation of the negative ions, with a view to obtaining values for the electron affinity of the molecules to compare with values obtained by other methods.

The cell used (figure 4.1) was essentially the same as that described originally by Lovelock and Lipsky with plane parallel geometry of the electrodes.

The carrier gas, argon with 5% methane, was allowed to flow through the detector cell and was ionised by the β -particles emitted from the foil containing adsorbed tritium. This foil formed one electrode and the other, separated from it by a 1cm thick spacer, was a wire gauze. The electrons were drawn across the cell by a pulsed voltage applied across the two electrodes, and the resulting mean current was measured. In the presence of an acceptor gas some of the electrons were captured, with a resulting decrease in the number of electrons reaching the anode. The decrease in current was therefore a measure of the number of electrons lost by the formation of negative ions, and by other reactions that occurred within the cell.

First attempts to relate the capture coefficients measured by Lovelock^(78, 7) to the physical parameters of the capturing molecules were made by Wentworth and Becker^(43, 79). Their interpretation of the capturing process was based on the establishment of an equilibrium between the neutral gaseous molecules, the free thermal electrons and gaseous negative ions derived from the molecules. In earlier work⁽⁸⁰⁾ the capture coefficient had been defined by an exponential law analogous to Beer's Law for light adsorption of the form

$$[e^-] = [e_0] \exp(-\lambda[A]) \quad \dots \quad (4.1)$$

where $[e^-]$ is the concentration of electrons in the presence of the organic molecules of concentration $[A]$, and $[e_0]$ is the electron concentration in the absence of any acceptor molecules.

Equation 4.1 may be rewritten to a first approximation as

$$[e^-] = [e_0] (1 - \chi[A]) \quad \dots \quad (4.2)$$

Under conditions where the electron concentration is much greater than the concentration of the A equation 4.2 becomes

$$\chi = \frac{[A^-]}{[e^-][A]} \quad \dots \quad (4.3)$$

where $[A^-]$ is the concentration of the negative ions and is equal to $[e_0] - [e^-]$

This is identical with the equilibrium constant K_A for the reaction



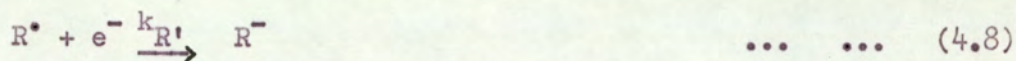
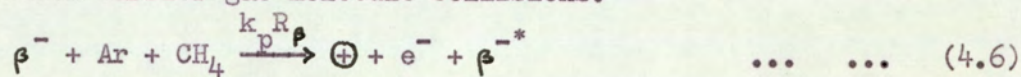
given by

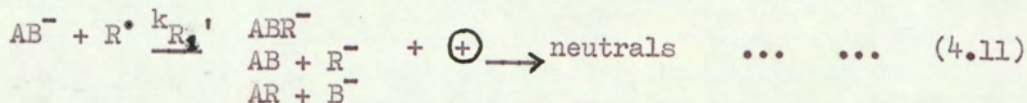
$$K_A = \frac{[A^-]}{[A][e^-]} = \frac{f_{A^-}}{f_A \cdot f_e} \exp - E/kT \quad \dots \quad (4.5)$$

where f_{A^-} , f_A and f_e are the partition functions for the negative ion, molecule and electron respectively. E is the enthalpy change of the reaction of equation 4.4 and is equal to the electron affinity of A.

Lovelock^(78,7) determined several electron absorption coefficients which he referred to chlorobenzene as standard. Wentworth and Becker⁽⁴³⁾ determined the absolute equilibrium constant for electron capture by anthracene, and hence the electron affinity from equation 4.5 by assuming that f_{A^-}/f_A remained constant and equal to 2 because of the electron spin degeneracy of the ion. By using the previously measured relative adsorption coefficients they plotted a graph of $\ln K$ against electron affinities of hydrocarbons calculated by Hoyland and Goodman⁽¹³⁾ from polarographic half-wave reduction potentials and showed that a reasonably linear relationship existed.

Later (81) a kinetic model for the mechanism leading to stable negative ion formation was developed by Wentworth, Chen and Lovelock. This was applied to the processes occurring within the electron capture detector operated in the pulse sampling mode. They assumed that the rate of production of thermal electrons was not affected by the presence of a capturing species; that the reaction zone included a cloud of positive and negative ions, electrons, and radicals, in addition to the argon-methane mixture and electron capturing species; that owing to their lower mobility there was an excess of the positive ions present; that losses by diffusion were minor; and, that the amount of material which effected electron capture was small in comparison to the total amount of material present. The processes occurring in the reaction zone were described by the following equations in which \oplus represents the positive ions, e^- the electrons, β^- the β particles emitted from the foil, R^* any radicals formed, and AB the capturing species. $k_p R_\beta$ is the rate constant used to represent a composite process for the thermal electron production. This process includes ionisation of the carrier gas by β particles followed by numerous electron-carrier gas molecule collisions.





If the positive ion concentration were much greater than the electron concentration, the rate of change of electron concentration in the absence of a capturing species would be

$$\frac{d[e^-]}{dt} = k_p R_p - k_{N_1} [\oplus][e^-] - k_{R_1} [R^*][e^-] \dots \dots (4.12)$$

and this may be solved to give the concentration b of the electrons in the absence of a capturing species if R^* the radical concentration is constant

$$b = \frac{k_p R_p}{k_{R_1} [R^*] + k_{N_1} [\oplus]} \left(1 - \exp^{-[k_{N_1} [\oplus] + k_{R_1} [R^*]]t} \right) (4.13)$$

In the presence of a capturing species AB of concentration a , which did not dissociate and providing $[\oplus] \gg [e^-]$ and $[AB] = a - [AB^-] \approx a$ as previously assumed then

$$\frac{d[e^-]}{dt} = k_p R_p - k_{N_1} [\oplus][e^-] - k_1 a [e^-] + k_{-1} [AB^-] - k_{R_1} [R^*][e^-] \dots \dots (4.14)$$

and the equation for the formation of AB^- is

$$\frac{d[AB^-]}{dt} = k_1 a [e^-] - k_{-1} [AB^-] - k_{N_1} [\oplus][AB^-] - k_{R_1} [R^*][AB^-] \dots \dots (4.15)$$

These equations were solved simultaneously to give the concentration of electrons at time infinity when AB was present as

$$[e^-]^\infty = k_p R_p / k_D \left[\frac{k_L k_1 a}{k_D (k_L + k_{-1})} + 1 \right] \dots \dots (4.16)$$

where $k_L = k_{N_1} [\oplus] + k_{R_1} [R^*]$

$$\text{and } k_D = k_{N^+} [\oplus] + k_{R^+} [R^+]$$

Since from equation 4.13 the electron concentration in the absence of AB and at time infinity was given by

$$b^\infty = \frac{k_p R \beta}{k_{R^+} [R^+] + k_{N^+} [\oplus]} \quad \text{or} \quad \frac{k_p R \beta}{k_D} \quad \dots \quad \dots \quad (4.17)$$

$$\frac{b^\infty - [e^-]}{[e^-]} = \frac{k_L k_1 a}{k_D (k_L + k_{-1})} \quad \dots \quad \dots \quad (4.18)$$

= Ka where K is the capture coefficient

It was suggested that since the capture coefficient K contains the term $(k_L + k_{-1})$ it was convenient to consider the case where $k_L \gg k_{-1}$ and $k_{-1} \gg k_L$ in order to examine the type of temperature dependence to be expected. If the temperature variation for the forward reaction were small, corresponding to no energy of activation for the addition of an electron, and if the electron affinity of the molecule were appreciable then the backward rate constant k_{-1} must have a significant temperature variation. Hence it was suggested that there were two temperature regions, termed α and β . At low temperatures k_L which is the rate constant for negative ion re-combination and relatively temperature independent would be greater than k_{-1} , and at higher temperatures the opposite would be true. These were termed the β and α region respectively. For $k_{-1} \gg k_L$ equation 4.18 becomes

$$\frac{b - [e^-]}{[e^-]} = Ka = \frac{k_L}{k_D} \frac{k_{-1}}{k_{-1}} a = \frac{k_L}{k_D} K_{eq} a \quad \dots \quad (4.19)$$

and since

$$K = \frac{k_L}{k_D} K_{eq} = \frac{k_L}{k_D} AT^{-3/2} \exp E/kT \quad \dots \quad (4.20)$$

$$\ln KT^{3/2} = \ln \frac{k_L}{k_D} + \ln A + E/kT \quad \dots \quad (4.21)$$

By plotting $\ln KT^{3/2}$ against $1/T$ Wentworth et al⁽⁸¹⁾ calculated the electron affinities of several aromatic hydrocarbons from the slope of the graphs in the α region. The values obtained for phenanthrene anthracene and pyrene differed from values calculated by Hoyland and Goodman⁽¹³⁾ by only about 5%, but the agreement for naphthalene and azulene was not so good.

For $k_{-1} \ll k_L$ equation 4.19 becomes

$$\frac{b - [e^-]}{[e^-]} = Ka = \frac{k_{-1}}{k_D} a \quad \dots \quad (4.22)$$

and since there was no barrier to the addition of an electron, K should have been relatively insensitive to temperature in this region.

Wentworth et al have found an abrupt change from the α to the β region to occur at a temperature of about 130°C. If there were an abrupt change over from one type of behaviour to the other, the ratio of the rate constants k_{-1} for electron attachment and k_L for ion recombination must change rapidly over a small temperature range. The rate constants may be written

$$k_{-1} = A \exp (- E/RT) \quad \dots \quad (4.23)$$

where E is the electron affinity of the molecule

$$k_L = B \exp(-H/RT) \quad \dots \quad (4.24)$$

where H is the effective activation energy for reactions leading to negative ion recombination, and hence to the loss of these ions.

Defining k_{-1}/k_L as J and the energy difference $E - H = Z$

$$J = A/B \exp -Z/RT \quad \dots \quad (4.25)$$

therefore

$$\frac{d \ln J}{d 1/T} = -Z/R \quad \dots \quad (4.26)$$

If the ratio J of the rate constants increased by e , about half an order of magnitude then

$$\Delta 1/T = -4/Z \quad \dots \quad (4.27)$$

From the results of experiments by Wentworth et al ⁽⁸¹⁾ the sudden change in the variation of the equilibrium constant occurred at about 400°K , so that if Z is 400 kcal/mole $\Delta 1/T$ is 10^{-5} and the change occurs fairly abruptly over about four degrees. If, however, Z is only about 40 kcal/mole the same change in J occurs over a 40 degree range. As will be shown later (section 4.4₁) there is an upper limit, of about 20 kcal/mole, on the value of electron affinities which can be measured using the electron capture cell. This is because equilibrium for molecules of higher electron affinities cannot be set up under the conditions existing in the detector. Since the electron affinity must be less than 20 kcal/mole the maximum value for Z is about 10 kcal/mole. Hence the ratio of the rate constants k_{-1}/k_L increase by half an order of magnitude over a temperature range of about 60°C , and one would not therefore expect an abrupt change of slope in the graph of $\ln K$ against $1/T$ but rather a smooth curve for the transition. The kinetic model

has been further developed by Wentworth and Chen⁽⁸²⁾ to lead to a model for the mechanism of ion formation where the molecules undergo dissociation upon electron attachment. This again led to the conclusion that compounds which undergo electron attachment without dissociation should give graphs of $\ln K_T$ against $1/T$ of a positive slope at high temperatures with a near zero slope at lower temperatures. For dissociative reactions K should be independent of temperature.

In this section an attempt has been made to discuss some of the reactions which have been postulated to explain the mode of action of the detector. The purpose of the present work is to elucidate this further by observing the effect of varying the concentration of the acceptor molecule in the carrier gas stream and of altering the temperature of the cell. If indeed electron affinities may be measured by this method they may be compared with values obtained by other methods, in particular by the magnetron method described in earlier sections.

4.2 The electron capture cell and ancillary apparatus

The electron capture detector (figure 4.1) was supplied by W.G.Pye and Co. Limited. The β particle source was a piece of copper sheet 1cm square with titanium evaporated onto one side, in which tritium had been occluded to give the foil an activity of 150 millicuries. The electrodes were separated from each other by a hollow cylinder of polytetrafluoroethylene (PTFE). For most of the compounds studied, the cell was used with the electrodes 1cm apart but for some

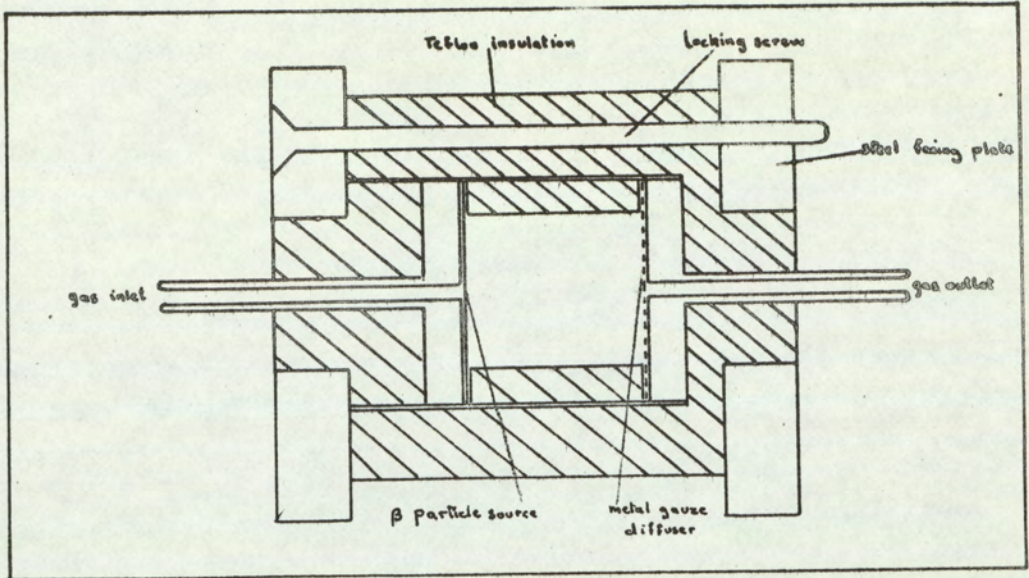


Fig. 4.1 The electron capture detector.

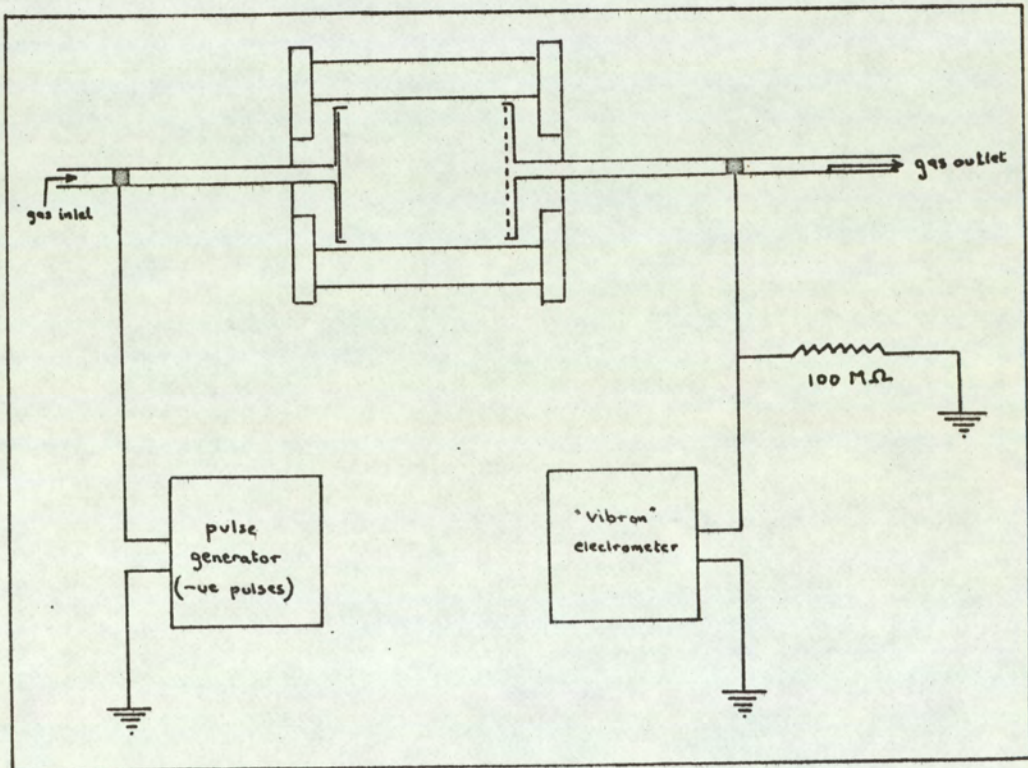


Fig. 4.2 Electrical circuit for electron capture detector.

of the work a cell with 0.7 cm separation between the electrodes was used. The β source was in electrical contact with the gas outlet tube and acted as the cathode, and a piece of gauze in contact with the inlet tube formed the anode. Electrical connections to the inlet and outlet tubes were made by soldering wires to fine copper wire wound tightly in several layers around the tubes. The gauze acted as a diffuser to ensure a uniform distribution of the gas which could escape from the cell around the edges of the foil.

The cell as a whole was insulated by inserting a section of PTFE tubing between the cell and external copper tubing. It was shielded against stray electrical fields by enclosure in a metal box. The electrical circuit used is shown in figure 4.2. The voltage source was a 'Labgear' square wave double pulse generator supplied by W.G. Pye & Co.Ltd. The amplitude of the pulse was continuously variable from 0 to 20 volts, and the duration of the pulse from 0.2 to $10^4 \mu$ seconds, and the interval between pulses from 1 to $10^5 \mu$ seconds. The current flowing in the cell was measured as the voltage drop across the high input resistance of a vibrating reed electrometer. The instrument used was an E.I.L Vibron model 33C with two additional resistances of 10^7 and 10^8 ohms fitted in the convertor unit. The full scale deflection of the meter was 1000 mV and the input resistance was variable from 10^7 to 10^{12} ohms in powers of 10.

The gases were supplied by the British Oxygen Company unless otherwise stated and the flow of gas through the system was measured by flowmeters supplied by the Rotameter Manufacturing Company. These were calibrated by means of a bubble flow meter. 1/4" O.D. copper

tubing with "Ehots" connections was used where possible for carrying the gas, but where glass components were necessary polythene tubing was used for the connections. All the joints were tested for leaks with soap solution. The gas line used is shown in figure 4.3. The argon/5% methane mixture, used as a carrier gas, was passed through a molecular sieve supplied by Kenmor Incorporated in order to remove any moisture. The gas was then fed into a wide glass tube containing reduced catalyst supplied by Badische Anilin & Soda - Fabrik, in order to remove any oxygen that was present, and then into an "Ehots" T junction fitting, one side of which was connected directly to the detector oven and the other to the saturator in a second oven. The two ovens were connected by 1/8" O.D. copper tubing. The saturator (figure 4.4) was a U-shaped glass tube with a sintered glass disc in the wider, gas inlet side to support the compound and effect better mixing of the carrier gas with the vapour of the compound.

There were two methods of altering the concentration of the capturing species in the gas stream entering the cell. For solids of low vapour pressure all of the carrier gas was passed through the compound before entering the cell, and by altering the temperature of the saturator the vapour pressure of the solid was altered and hence the concentration of capturing species in the gas stream could be varied. For liquids with high vapour pressures the concentrations obtained by this method were so great that all the electrons in the cell were absorbed so an alternative method was used. The saturator was kept at a constant temperature and the proportion of the total flow through it was varied. These flow rates were measured either

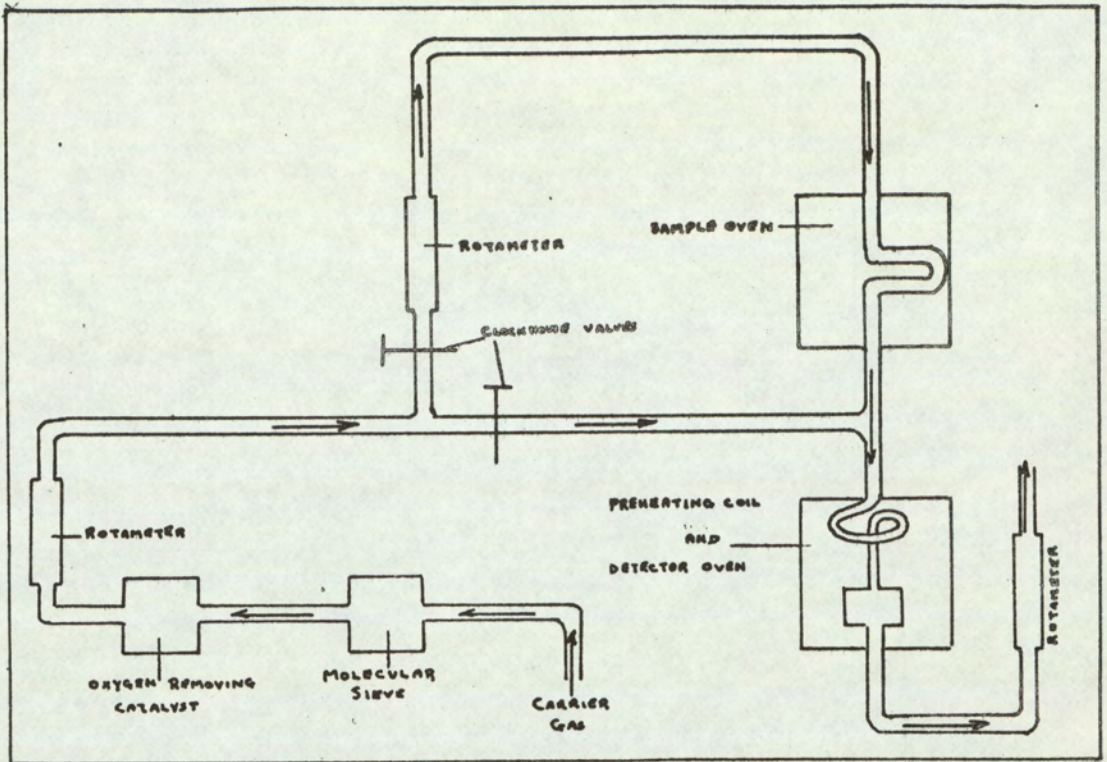


Fig. 4.3 Gas line for electron capture detector.

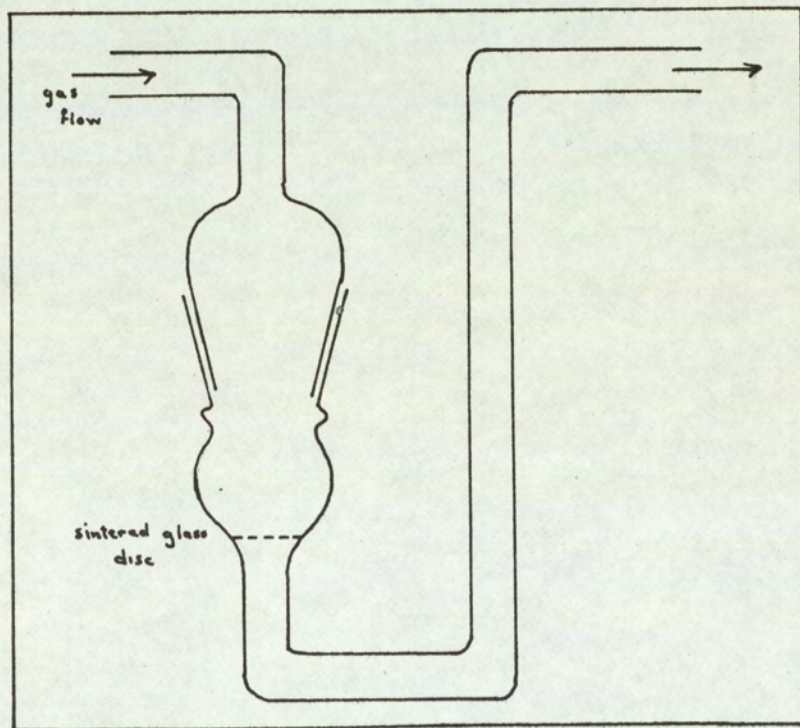


Fig. 4.4 Saturator.

by a 'Rotameter' or, for very low flow rates, by a capillary flow meter filled with tertiary butyl phthalate. It was assumed that when the carrier gas had passed through the saturator the partial pressure of the compound in the gas was equal to the saturation vapour pressure of the compound, and the concentration of the acceptor molecules in the detector was calculated on this basis. Measurements described in section 4.4₄ were made of the reduction in electron concentration due to the presence of anthracene vapour. The experiments were done at two different total flow rates with similar results, indicating that near saturation probably occurred. If, however, the temperature of the saturator were lower than the measured temperature of the oven, owing to surface cooling by the loss of latent heat by evaporation, the calculated vapour pressure would be higher than the actual vapour pressure of the compound in the gas stream. This effect would become smaller at higher oven temperatures and would only be likely to occur at high flow rates of gas through the saturator, and when the temperature of the oven was much lower than the boiling point of the solid. The carrier gas containing a known concentration of electron capturing species was passed into a preheating coil made from about 10 feet of 1/4" O.D. copper tubing inside the detector oven and thence into the cell itself. The total flow, which for most experiments was kept at 4 ml per second, was measured by a 'Rotameter' at the outlet of the cell.

The two ovens were built from six asbestos sheets, 12" x 12" x 1/4", bolted together through aluminium angle strip. The cell was

suspended in the centre of one oven by the 1/8" O.D. copper tubing through which the carrier gas was introduced into the cell. The saturator was in a separate oven so that its temperature could be altered independently from that of the cell. The temperature of each oven was measured and controlled by the same method. A nickel resistance thermometer was made by winding 0.005" diameter nickel wire onto a "Tufnol" former. This was connected across CD in the bridge network of figure 4.5. The helical potentiometers R_1 and R_2 were set such that there was a voltage drop across AB. This voltage drop was applied across a three-stage amplifier, built using the circuit diagram in figure 4.6. The amplified voltage actuated a relay which switched on a heating coil screwed to the side of the oven opposite to the nickel resistance thermometer. The temperature of the oven could be altered by changing the values of resistances R_1 and R_2 which were the coarse and fine controls respectively. The temperature of the oven was measured by a mercury in glass thermometer in the lid of the oven and the reading on this remained constant to within 0.2°C when the equilibrium temperature had been reached.

4.3 Preliminary experiments with the electron capture cell

Before introducing electron acceptor gasses into the detector it was necessary to discover how the current flowing through the cell depended on the operating conditions. The various parameters such as applied voltage characteristics, flow rate of the gas, and temperature of the cell were varied and the effect on the detector current was observed.

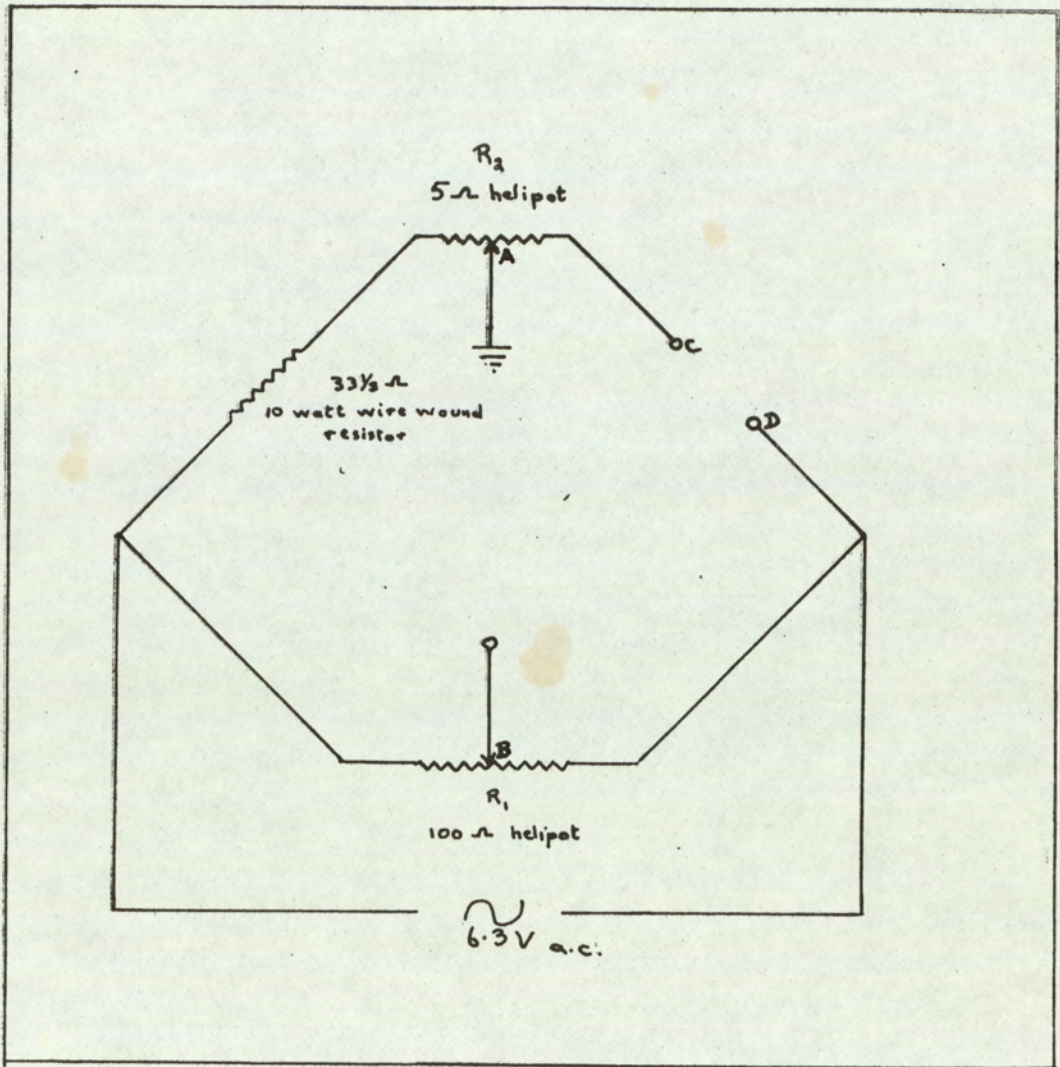
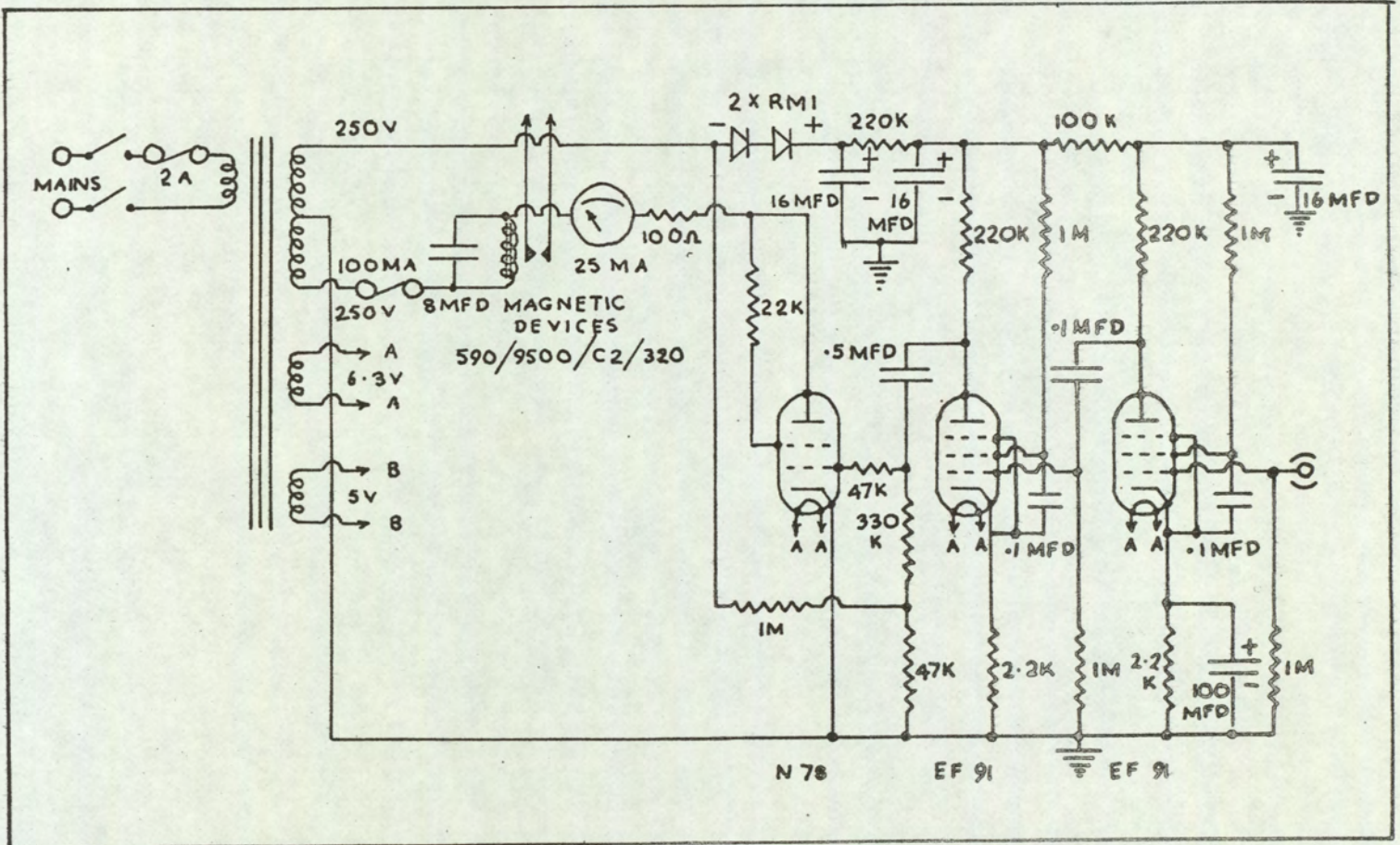


Fig. 4.5 Bridge network for oven thermostat.

Fig. 4.6 Amplifier circuit diagram.



4.3₁ - Applied voltage

The original electron capture cell described by Lovelock and Lipsky⁽⁴²⁾ was operated using a constant applied voltage but since then it has been found that the pulsed mode has several advantages over the original D.C. system, particularly when used for analysis^(80&77). A comparison of the two types of applied voltage has been made by Schmit and Peters⁽⁷⁷⁾ who found that in the D.C. system the sensitivity was a function of the voltage and therefore a sample containing several compounds could not be analysed at maximum sensitivity for each component. In the pulsed system, however, the sensitivity is a function of pulse interval and it was found that for the compounds which were studied the maximum sensitivity occurred at the same pulse interval which enabled several compounds to be determined quantitatively on the basis of a single chromatographic analysis. A further advantage of the pulsed system is that space charge effects are unlikely to occur since the external voltage is only applied for a small fraction, about 1%, of the total time. When a constant voltage is applied however the electrons are collected at the anode very soon after they are formed whilst the positive ions with lower drift velocities move much more slowly and tend to accumulate as a space charge at the cathode. Thus a potential gradient is set up in opposition to the externally applied voltage and the collection of electrons may be hindered. In the presence of an electron absorbing gas the mobility of the electrons will be different, and hence the extent of the space charge and observed current flow will be altered and will depend on the concentration of these molecules⁽⁸⁰⁾. At high applied potentials Lovelock⁽⁸⁰⁾ found that the detector did not show a linear response to varying concentrations, and explained this

by suggesting that charge separation did not allow the plasma to equilibrate by recombination of the ions. At lower applied potentials, where one might expect better linearity in response, other factors such as contact potentials affected the electron currents. Most of these objections were overcome by using the pulsed mode of operation where, because of the low frequency of the intermittently applied voltage, space charges are unlikely to build up and the electrons can reach thermal equilibrium before being collected at the anode and kinetic equilibrium is more likely to occur.

In the present work a pulsed voltage was used generally. However initial experiments were performed with a D.C. voltage to measure the saturation level of the current through the cell which could then be compared with the maximum current obtained using a pulsed voltage. The direct voltage was supplied by an Exide 1007 dry battery connected to the cell through a potential divider, and the voltage across the cell was measured on an "Avo" meter. With the carrier gas glowing through the cell, the voltage was gradually increased and the resulting current observed. As is seen from figure 4.7 the current gradually increased with increasing voltage as more of the electrons were drawn across before recombining with the positive ions but above a certain voltage any further increase, up to 120 volts, had no further effect on the current flowing through the cell. The voltage required to obtain this saturation level of the current depended on the polarity of the cell. When the tritiated foil was positive with respect to the metal gauze which formed the other electrode, saturation was not reached until about

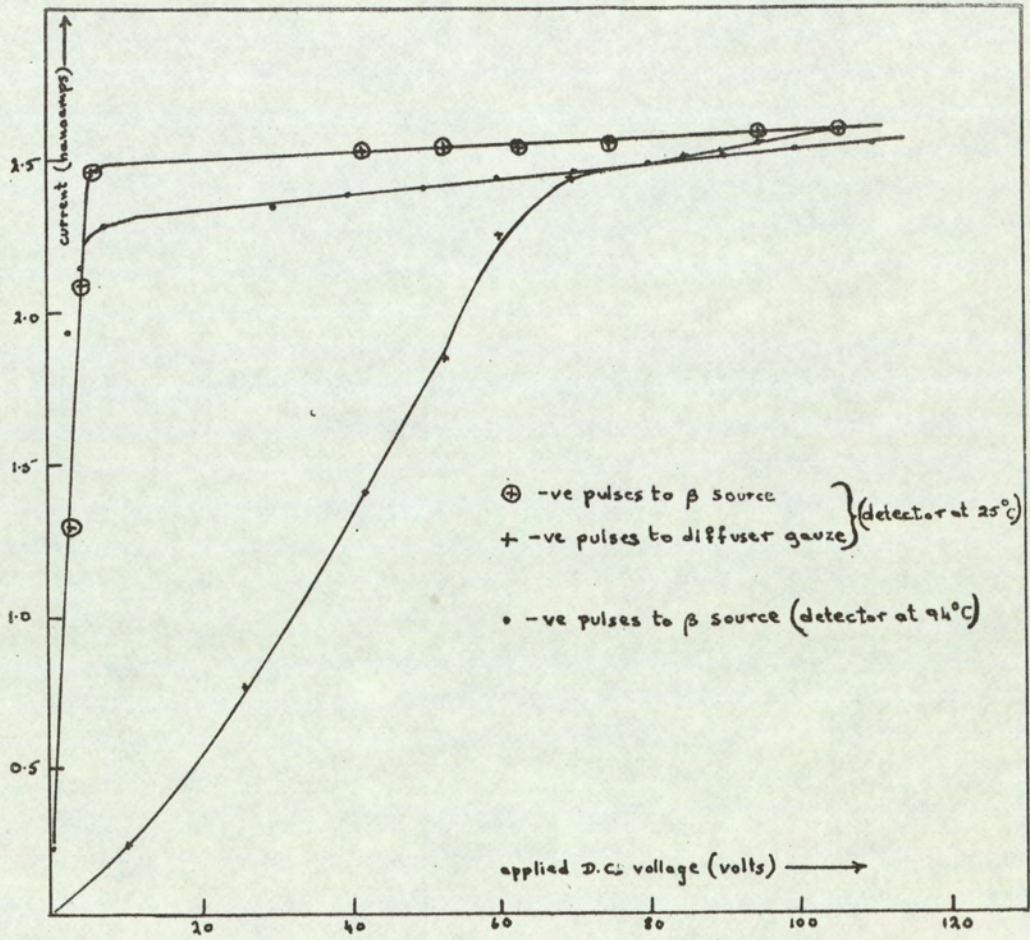


Fig. 4.7 Graph of detector current against applied D.C. voltage.

90 volts but with the polarity reversed it only required 10 volts to reach the maximum current. This effect occurred because of the relative mobilities of the positive ions and electrons. When the foil was positive the heavier argon positive ions had to be drawn across the cell from the plasma where they were produced. However, when the potential gradient was reversed the much lighter electrons had to be drawn across the cell and the positive ions with a mobility about 200 times less than the electrons only had to travel a relatively short distance to the cathode. Figure 4.7 also shows that increasing the temperature of the cell to 94°C had little effect on the saturation current or the voltage required to attain it under D.C. conditions.

The maximum saturation level reading on the "Vibron" electrometer was of the order of 300 mV across an input resistance of 10^8 ohms, which corresponds to a current of 3.0×10^{-9} amps. The number of electrons produced by the particles can be estimated by making some very rough calculations⁽⁸³⁾. The activity of the foil was 0.15 curies/cm², and its "thickness", assuming one atom of titanium per atom of tritium, is 250 mg/cm². The maximum energy of the particles emitted is 18 KeV⁽⁸⁴⁾ and it may be assumed that they are all emitted with an average energy of 9 KeV since the energy distribution is Maxwellian. In this energy region the range is approximately proportional to the square of the energy, hence only those particles emitted from, say, the top 125 mg/cm² of the foil will escape. Those emitted in a backward direction will be lost and of those emitted in a forward direction some, say half, will be emitted at too

great an angle to the normal to escape. Hence the effective source may be calculated to be $0.15 \times 3(1/2)$, or approximately 0.02 curies/cm² and so the number of β particles emitted from the surface of the foil is about 7×10^8 β particles cm⁻² sec⁻¹. Although the average energy of the β particles when emitted from the tritium is about 9 KeV, most of this energy is lost by collisions within the foil and the particles therefore leave the surface with a much lower energy of about 1 KeV. The particles then collide with, and ionise, the gas molecules losing their energy until it is less than that required to form an ion pair. This has been determined to be 25.8 eV for α particles in argon/5% methane and the value for β particles emitted from tritium should be somewhat similar⁽⁸¹⁾. Hence the number of electrons produced may be calculated to be 10^{10} electrons per second which corresponds to a current of 10^{-9} amps and is of the same order as the measured value of 3.0×10^{-9} amps indicating that all the electrons formed by ionisation are drawn across and collected at the anode.

The same saturation current was observed when a pulsed voltage was applied across the cell. Figure 4.8 shows the effect of increasing the amplitude of the voltage at 5.0μ sec duration and at various pulse intervals. From this it is seen that an amplitude of at least 10 volts was necessary to obtain the saturation current. When the measurements described in section 4.4 were made the voltage was kept at 20 volts, sufficiently high to take all of the electrons out at each pulse.

4.3₂ - Pulse duration

It is desirable to have the pulse duration as short as possible

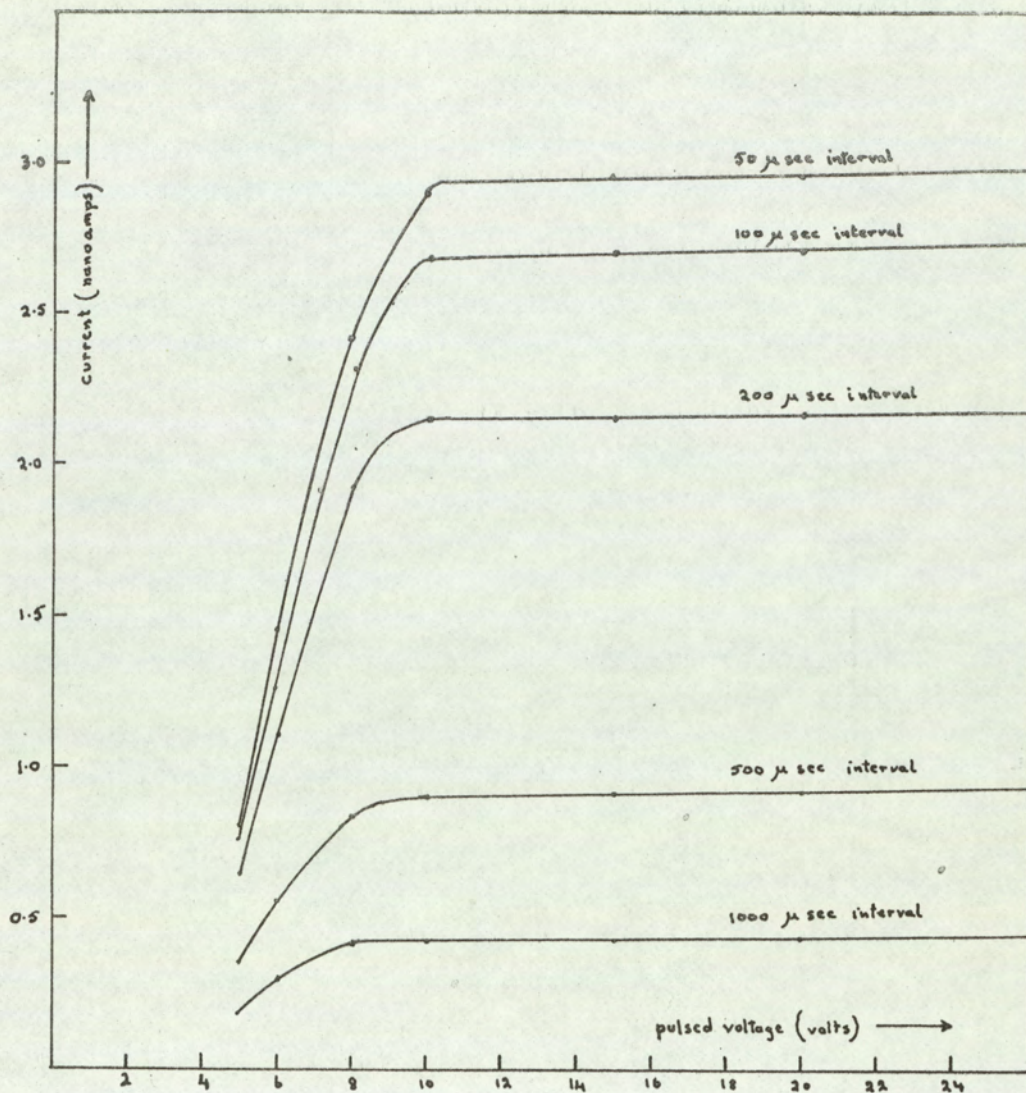


Fig. 4.8 Graph of detector current against applied pulsed voltage.

so that the number of electrons formed during the pulse is not appreciable, and the electrons have the maximum possible time to reach thermal equilibrium. If the duration is too short however there is not sufficient time for all the electrons to be removed, the saturation current is not reached, and the square wave shape of the voltage pulse is likely to be distorted. From figure 4.9 it is seen that for pulse intervals from 50μ sec to 1000μ sec a duration of 5μ sec is sufficient to withdraw all the electrons in the cell. An oscilloscope trace of the voltage output of the pulse generator at 5.0μ sec pulse duration showed that a square wave form was in fact being applied to the cell. In the experiments described in section 4.4 a duration of 5.0μ sec was used. This was small compared with the pulse intervals of the order of $10^2 \mu$ sec which were used.

4.3₃ - Pulse interval

As well as the amplitude of the voltage and the length of time for which it was applied, the interval between pulses also affected the current flowing through the cell. At short intervals of the same order of magnitude as the pulse duration, the electrons were withdrawn as they were formed and not lost by recombination with the positive ions. With increasing time between the pulses, however, some of the electrons produced could recombine with the positive ions and so fewer were collected at the anode and the current through the cell decreased. If the reactions within the cell were kinetically controlled, it was important that time should be allowed for the

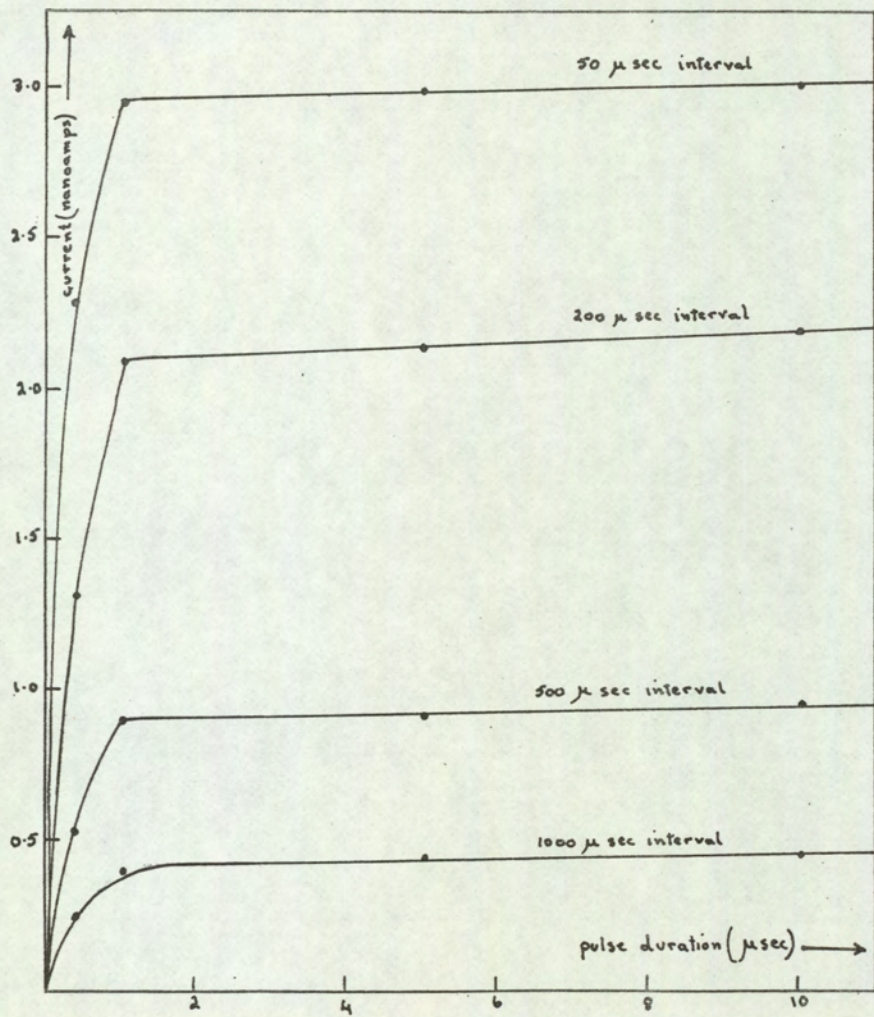


Fig. 4.9 Graph of detector current against pulse duration.

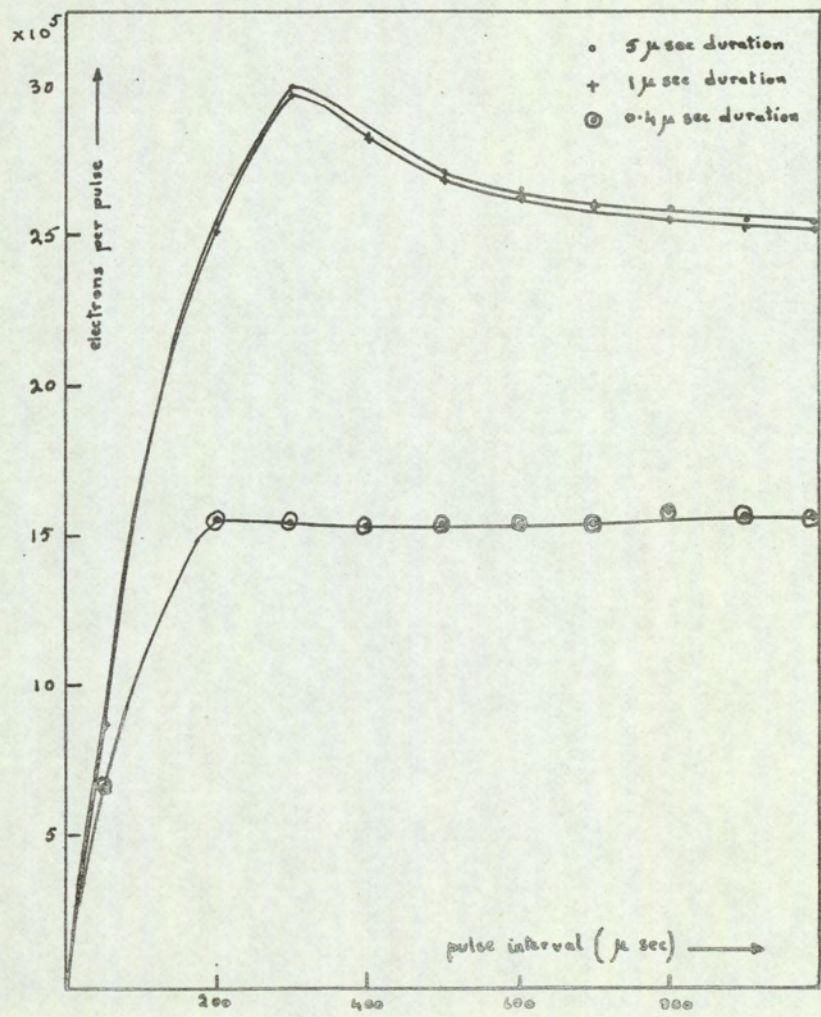


Fig. 4.10 Graph of electrons per pulse against pulse interval.

system to reach a steady state between pulses and it was necessary to know what pulse interval was required to achieve this.

If the pulse interval is τ seconds, then there are $1/\tau$ pulses per second and if the measured current is I electrons per second, the number of electrons per pulse is $I\tau$. From a graph of $I\tau$ against τ it should therefore be possible to find the smallest pulse interval at which a steady state is achieved, when the number of electrons per pulse becomes independent of pulse interval. Figure 4.10 shows $I\tau$ plotted against τ with an amplitude of 20 volts and various pulse durations for argon/5% methane. This curve has a slight maximum at $300\mu\text{sec}$ for which there is no obvious explanation. At pulse intervals above this value however the number of electrons withdrawn per pulse is nearly constant and the experiments in section 4.4 were therefore carried out at pulse intervals of 500μ to $1000\mu\text{sec}$.

4.3₄ - Carrier gas

Throughout these experiments a mixture of 95% argon and 5% methane was used as a carrier gas since this gave slightly higher standing currents than argon/10% methane. In pure argon it is more difficult for the electrons to reach thermal energies. The β particles emitted from the foil lose their energy by ionisation of the gas molecules until their energy is less than that required to form an ion pair. They still, however, have some excess energy. In pure argon only elastic collisions can occur but, in the presence of a polyatomic non-electron absorbing gas such as methane, there are other possible ways of absorbing the energy such as by the vibrational and rotational excitation of the molecules. These non-elastic collisions

reduce the energy of the free electrons so that thermal equilibrium with the carrier gas is achieved. In addition any metastable ionic species of the argon which may be formed are removed by deactivating collisions. These effects are apparent in the large differences in the drift velocities of electrons in argon and argon/methane mixtures⁽⁸¹⁾.

4.3₅ - Effect of flow rate

During a pulse interval the electrons are formed by ionisation and removed by recombination and by the carrier gas flowing through the cell. It is therefore necessary to study the effect on the current of variation in the flow rate of the carrier gas. The flow rate of the argon/5% methane was varied between 0 and 5 ml/sec and the standing current measured at various pulse intervals. Initially the current rose, but above about 3 ml/sec there was little further increase. A similar effect was observed when the detector was heated to 125°C. Using argon/10% methane again similar curves were obtained. Studies have been made over a range of flow rates from 0 to 30 ml/sec⁽⁸⁵⁾ and it was found that the current increased with increasing flow rate to about 15 ml/sec after which it levelled off. The explanation offered for this was the possible increase in plasma volume with increasing flow rate. In the present work, however, no appreciable increase in current was observed above about 3 ml/sec up to 5 ml/sec.

In equation 4.7, section 4.1, it was shown that

$$b = k_p R \rho / k_D$$

and it was assumed that the flow did not affect the electron current.

If a term $u [e]$, where u is the flow rate of the gas, and $[e]$ is the concentration of electrons, is included in the expression for b and the equation is integrated then

$$b = \frac{k_p R \rho}{k_N [\oplus] + k_R [R] + u} \quad \dots \quad \dots \quad (4.29)$$

If it is now assumed that the radical concentration is negligible and that the positive ion concentration is given by b/μ (since there must be b positive ions in a volume μ if equal numbers of each of the positive and negative species are pulled out with each pulse)

$$b = \frac{k_p R \rho}{k_N b/\mu + u} \quad \dots \quad \dots \quad (4.30)$$

Therefore

$$bu = k_p R \rho - k_N b^2/\mu \quad \dots \quad \dots \quad (4.31)$$

Figure 4.11 shows bu plotted against b^2 and the curve rises initially and levels out at about 3.5 ml/sec which suggests that after this point the current is no longer dependent on flow rate.

4.36 - Effect of temperature on standing current

In order to investigate the effect of the temperature of the cell on the standing current the temperature of the detector oven

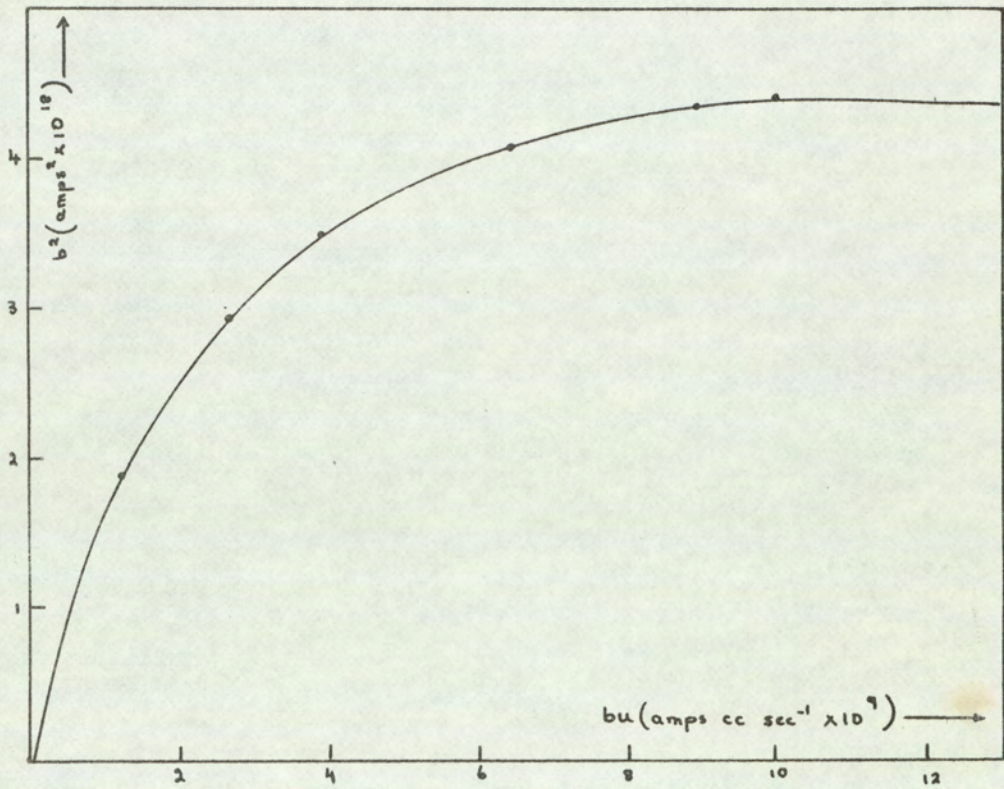


Fig. 4.11 Graph showing effect of rate of gas flow on detector current.

was varied and the current flowing through the cell was measured on the "Vibron" electrometer. It was found that the current fell with increasing detector temperature. This phenomenon has not been reported in previous work where it was not specified whether the standing current was measured at one temperature only, or at each temperature where experiments involved the measurement of reduction in electron concentration at different temperatures.

The rate of production of electrons will be constant below the temperature at which tritium begins to boil off of the foil. As was described above, the critical voltage required for the saturation current to be achieved does not alter with temperature which implies that the amplitude of the voltage is great enough to draw all the electrons across at the higher temperature. It was thought that the effect could have been due to the fact that the plasma was filling the whole volume of the cell and extending beyond when the cell was heated.

Since the range of the β particles depends on the number of molecules in their path they would have a shorter range at higher pressures and so the plasma volume would decrease. The effect of increasing the pressure of the gas in the cell was therefore investigated. The outlet of the cell was connected to a mercury manometer with a screw type needle valve on the other side. Graphs of current flowing through the cell against the excess pressure in cm of Hg were drawn for various temperatures from 46°C to 95°C. These are shown in figure 4.12, where it is seen that the electron current

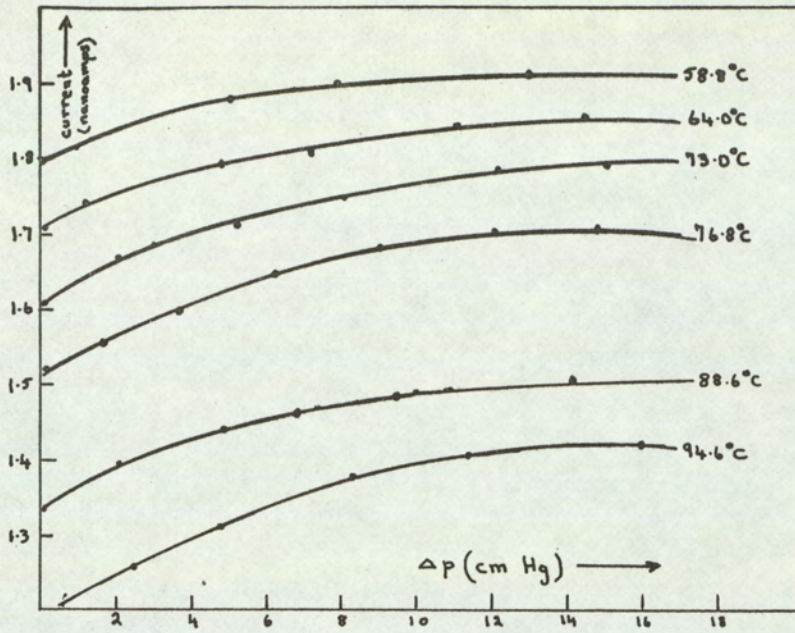


Fig. 4.12 Graph of detector current against excess pressure.

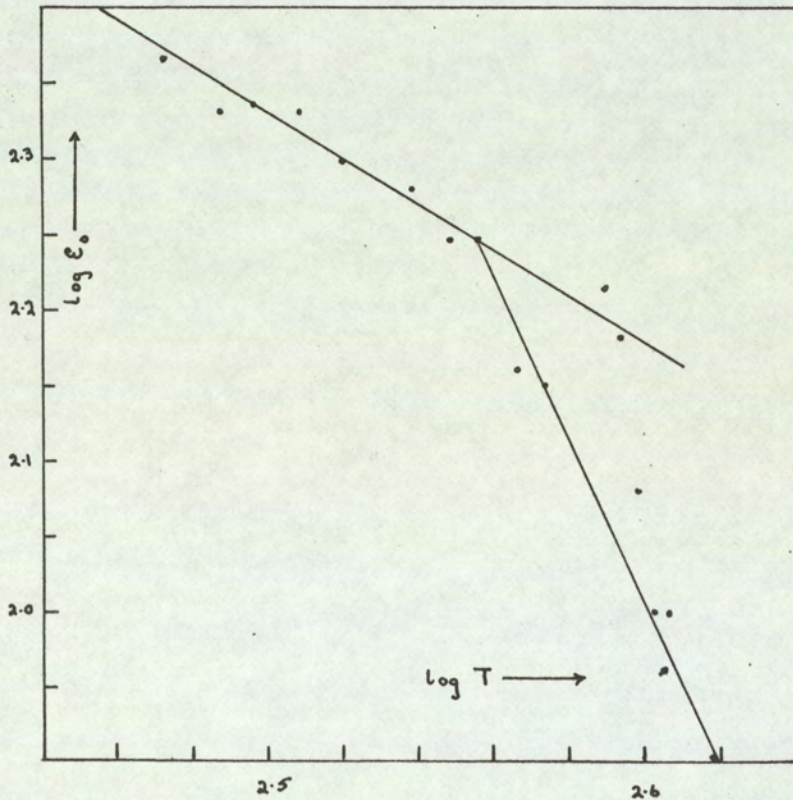


Fig. 4.13 Graph showing effect of temperature on detector current.

rose gradually with increasing pressure in all cases. It was therefore concluded that at atmospheric pressure the plasma was well confined within the cell.

In figure 4.13 $\log \xi_0$, the concentration of electrons in the cell through which only carrier gas was flowing, is plotted against $\log T$. The slope of this graph at low temperatures, below about 90°C has a slope of -1.5 , which indicates that the current is proportional to $T^{-3/2}$. At higher temperatures there appeared to be a greater dependence on T but the experimental points in this region were not so reproducible, possibly because of traces of capturing species previously adsorbed onto the "Teflon" wall of the cell desorbing into the gas stream. A possible explanation for the fall of the standing current with temperature is the increase in the recombination coefficient. Massey and Burhop⁽⁸⁶⁾ have extended J.J. Thompson's theoretical treatment of a three body collision for the recombination of positive and negative ions to apply to positive ion electron recombination. This theory predicts a $T^{-3/2}$ dependence of the recombination coefficient.

Fox and Hobson⁽⁸⁷⁾ have used a shock tube technique to measure recombination coefficients in argon over a temperature range of 1000°K to 3000°K , and have found that the recombination coefficient is proportional to $T^{-3/2}$. This data extrapolated back to 300°K gives recombination coefficients which agree well with values obtained by other methods. It is therefore to be expected that the observed current will show some temperature dependence due to the recombination

coefficient of the positive ions and electrons being temperature dependent. When a direct voltage was applied to the cell with carrier gas flowing through it the maximum standing current was not dependent on temperature (section 4.3₁). This is presumably due to the fact that the electrons are drawn across the cell as soon as they are formed and do not therefore have time to recombine with the positive ions. Since the current flowing through the cell was dependent on the temperature under the pulsed voltage conditions used, the standing current was measured at each temperature before measuring the reduced current in the presence of the electron adsorbing gas. The attenuation in electron concentration due to the formation of negative ions was then obtained from the difference.

The operating conditions of the electron capture cell have been investigated in order to determine how the standing current varies with the characteristics of the applied voltage, flow rate of the gas, and temperature of the cell in order to find the best set of conditions to use in studying the effect of adding an electron capturing species in known concentration into the gas stream.

4.4 Experimental studies on various compounds using the electron capture cell

4.4₁ - Introduction

In a previous section the magnetron method for measuring electron affinities has been described and direct capture electron affinities of several compounds have been obtained. The electron capture cell offered an alternative method for measuring the stability

of negative ions, and the possible opportunity of comparing the electron affinity of a compound determined directly by two different methods. Various compounds were therefore studied by passing a known concentration through the detector and measuring the reduction in electron concentration within the cell. When a capturing species is in collision with an electron a negative ion will be formed providing the liberated energy can be absorbed by a third body or by excitation of the negative ion A^- . This may be represented by the reaction



The rate of the backward reaction will depend on the collision frequency of A^- and its stability. For negative ions of low stability the reverse reaction is more likely to occur since the kinetic energy of a collision will be more likely to exceed the necessary activation energy. The collision frequency Z_{AB} of molecules A and B at number concentration n_A and n_B is given by kinetic theory as

$$Z_{AB} = n_A n_B d_{AB}^2 \left[8 \pi kT \frac{m_A + m_B}{m_A \cdot m_B} \right]^{1/2} \quad \dots \quad \dots \quad (4.33)$$

where m_A and m_B are the masses of A and B, d is the average diameter of the two molecules, and T is the absolute temperature.

For a 1% by volume mixture of oxygen in argon at 300°K the collision frequency may be calculated to be 1.7×10^{26} molecules/cc/sec. Since each cc contains 2.68×10^{17} oxygen molecules the collision frequency of one oxygen molecule is $6.3 \times 10^8 \text{ sec}^{-1}$.

Collision frequencies for the capturing molecules will therefore be of the order of 10^8 sec, the exact value depending on their masses and diameters. If equilibrium is to be achieved there must be at least one chance of a negative ion colliding with another molecule while in the cell. Hence the rate of the back reaction of equation 4.32 must be such that at least one collision occurs while the gas molecule is in the cell. The rate of the reaction v is given by

$$v = Z_{AB} \exp -(E/RT) \quad \dots \quad (4.34)$$

where E is the activation energy of the reaction, in this case the electron affinity of the capturing species. Since the molecules are in the cell for about 0.25 sec. the rate of the reaction should be at least 4 molecules per second. Therefore in equation 4.34 by putting $v = 4$ and $Z_{AB} = 6.8 \times 10^8$, E may be calculated to be 12.7 kcal/mole at 300°K . This implies that negative ions with a stability of less than 12.7 kcal/mole will have a probability of colliding with sufficient energy with other gas molecules at least once during their passage through the cell, to dissociate into the neutral molecule and electron. If the temperature of the cell is raised to 400°K the maximum stability may be calculated to be 17 kcal/mole. Ions of greater stability than this will not dissociate since the mean kinetic energy of a collision will be less than the activation energy E necessary for dissociation. Hence electron affinities, if they can be found by this technique, may only be measured if they are below about 20 kcal/mole.

If the conditions of equilibrium are satisfied the equilibrium constant for the reaction represented by equation 4.32 may be

written as

$$K = \frac{[A^-]}{[A][e]} \quad \dots \quad \dots \quad (4.35)$$

providing $[A]$ is much greater than $[A^-]$ so that $[A] - [A^-]$ may be taken as equal to $[A]$. The concentration of the negative ions will be proportional to the difference between the electron current, ϵ_0 , in the absence of a capturing species and the electron current, ϵ , in the presence of a capturing species. Therefore

$$K = \frac{\epsilon_0 - \epsilon}{[A]\epsilon} \quad \dots \quad \dots \quad (4.36)$$

This is identical to the expression obtained by Wentworth, Chen and Lovelock discussed in section 4.1. If, therefore, the concentration of the capturing species is plotted against $(\epsilon_0/\epsilon - 1)$, the equilibrium constant may be obtained from the slope of the graph. The variation of equilibrium constant with temperature is given by

$$\frac{d \ln K}{dT} = E/RT^2 \quad \dots \quad \dots \quad (4.37)$$

where E is the electron affinity of the capturing species. Therefore since from equation 4.37

$$\frac{d \ln K}{d(1/T)} = -E/R \quad \dots \quad \dots \quad (4.38)$$

a graph of $\ln K$ against $1/T$ will have a slope of $-E/R$ and, hence, it should be possible to find the electron affinity E .

Alternatively, a third law method may be used to find E from

the measured equilibrium constant at a single temperature by applying the Saha equation for thermal ionisation, as follows

The thermal ionisation of a monatomic species may be represented by



The equilibrium constant for the reaction is given⁽⁴⁵⁾ by

$$K = \frac{[M^+][e]}{[M]} = \frac{q_{M^+} \cdot q_e}{q_M} \cdot \exp - \Delta \epsilon_0 / kT \quad \dots \quad \dots \quad (4.40)$$

where the q terms are the appropriate partition functions and $\Delta \epsilon_0$ is the difference between the energy of the free ion and electron on the one hand and the energy of the atom in the ground electronic state on the other hand, and is equal to the ionisation potential V of the atom M . Due to the absence of rotations and vibrations the sole partition function to be considered is the translational one, hence

$$K = \frac{g_{M^+} g_e}{g_M} \frac{\left[(2\pi m_{M^+} kT)^{3/2} / h^3 \right] \left[(2\pi m_e kT)^{3/2} / h^3 \right]}{\left[(2\pi m_M kT)^{3/2} / h^3 \right]} \exp - Ve/kT \quad \dots \quad \dots \quad (4.41)$$

Equation 4.41 will, to a first approximation, be valid for polyatomic molecules since the vibrations and rotational entropies of the molecule and ion will largely cancel. Hence

$$\log K = \frac{-5040V}{T} + \frac{5}{2} \log T - 6.4 \quad \dots \quad \dots \quad (4.42)$$

where K is the equilibrium constant for the reaction in equation 4.39 V is the ionisation potential of A , and T is the absolute temperature. The term 6.4 represents the ratio of the statistical weights of the atom to the ion and electron and, in general, will depend on the

species ionised but will not vary a great deal from 6.4⁽⁸⁸⁾. At the temperatures used, about 300°K, the term $(5/2)\log T$ is approximately equal to 6.4, hence to a first approximation

$$\log K = -5040V/T \quad \dots \quad (4.43)$$

Since the ionisation potential of an atom may be taken to be the same as the electron affinity of its positive ion, if electron interaction and rearrangement effects are ignored, equation 4.43 may be applied to the calculation of electron affinities. Therefore, using the equilibrium constant found by plotting $(\epsilon_0/\epsilon - 1)$ against the concentration of A introduced into the gas stream, it should be possible to obtain the electron affinities of the acceptor molecules. The values obtained should agree with the results obtained by the Second Law method of plotting $\log K$ against $1/T$ at a given concentration.

Various compounds were therefore studied by measuring the reduction in electron concentration in the cell due to a known amount of the substance in the carrier gas. The effect of raising the temperature of the detector was also investigated. The results of these experiments are discussed in the remainder of this section and the equilibrium constants found are summarized in Table 4.1

Unless otherwise stated the amplitude of the voltage was 20 volts and the pulse duration 5μ sec. Pulse intervals of 300μ sec to $1,000 \mu$ sec were used, since the number of electrons collected per pulse was independent of pulse interval above about 300μ sec. In plotting graphs of $(\epsilon_0/\epsilon - 1)$, against the concentration of capturing species, the value for ϵ_0/ϵ taken was the mean of the

values measured for pulse intervals from 300 μ sec to 1,000 μ sec. The total flow rate of the gas through the cell was maintained at 4 ml/sec and the concentration of the acceptor molecules was calculated by assuming that the partial pressure, after passing through the saturator, was equal to the saturation vapour pressure at the temperature of the saturator oven.

This vapour pressure was calculated from interpolation, or linear extrapolation, on a graph of the logarithm of the vapour pressure against the reciprocal of temperature, drawn using literature data. Extrapolation, particularly through a change of phase, could lead to inaccurate, absolute values for the vapour pressure at the different temperatures. However, in calculating equilibrium constants from graphs of $(\epsilon_0/\epsilon - 1)$ against concentration it is the rate of change of vapour pressure with temperature which is important, and this is likely to be subject to less error than the absolute values.

It was found necessary to keep some of the compounds at a low temperature of -78.5°C and vary their concentration in the cell by altering the percentage of the total carrier stream flowing through the saturator. Even at these low temperatures, very low flow rates, of the order of 10^{-2} ml/sec through the saturator, were required in order to avoid complete electron adsorption. Therefore, before making any measurements the carrier gas was allowed to flow for at least 48 hours through the capillary flowmeter and saturator (with a total volume of about 200 ml) to ensure that all the oxygen had been removed.

4.4₂ - Benzene

A sample of Analar benzene, dried over sodium was put in the saturator, held in an ice bath, and all of the carrier gas passed through it at 4 ml/sec. The vapour pressure of benzene at 0°C has been measured and was found to be 26.3 mm Hg⁽⁸⁹⁾.

The detector temperature was altered to study the effect of variation of the equilibrium constant with temperature. When $\log (\epsilon_0/\epsilon - 1)$ was plotted against $1/T$ (figure 4.22), the slope of the line was 2.5×10^2 degrees. An attempt was made to study the effect of different benzene concentrations in the cell by injecting microliter samples into a capillary column in the gas line. This column, situated just upstream of the detector was a stainless steel tube, 300 ft long and 0.03" in diameter. Squalane was used as the stationary phase. The signal from the "Vibron" electrometer was fed into a potentiometric recorder but neither the height of the peaks nor their area was proportional to the volume of benzene injected.

4.4₃ - Naphthalene

Microanalytical reagent naphthalene was put into the saturator in the oven and all of the carrier gas was allowed to flow through it at 4 ml/sec. The concentration of the naphthalene was varied by altering the temperature of the saturator oven over the range of 20°C to 35°C. The vapour pressure of the naphthalene at a particular temperature was estimated by interpolation of data obtained between 20°C and 70°C⁽⁹⁰⁾. A graph of $(\epsilon_0/\epsilon - 1)$ against vapour pressure was plotted for a range of 0.06 to 0.24 mm Hg and this

is shown in figure 4.14. The slope of the line was 60 (mm Hg)^{-1} with the detector at 80°C . The detector temperature was varied, keeping the saturator oven at a constant temperature of 31°C , which gave a vapour pressure of 0.123 mm Hg of naphthalene in the carrier gas stream. The slope of a line (figure 4.22) of $\log (\epsilon_0/\epsilon - 1)$ against $1/T$ was approximately 5×10^2 degrees. It was not possible to obtain a more accurate estimate of the slope since the points did not lie on a very good straight line.

4.4₄ - Anthracene

Microanalytical reagent anthracene was put into the saturator and all of the carrier gas was passed through it at 4 ml/sec . The concentration of anthracene in the carrier gas was varied from $0.1 \times 10^{-4} \text{ mm Hg}$ to $55 \times 10^{-4} \text{ mm Hg}$ by varying the temperature of the saturator oven between 32°C and 74°C . The vapour pressure was estimated by extrapolation of data measured between 100°C and 190°C ⁽⁹¹⁾. The slope of the line of the line of $(\epsilon_0/\epsilon - 1)$ plotted against concentration was $2.1 \times 10^3 \text{ (mm Hg)}^{-1}$. This graph is shown in figure 4.15. The dependence of equilibrium constant on temperature was studied at two different anthracene concentrations, and the slopes of the lines obtained by plotting $\log (\epsilon_0/\epsilon - 1)$ against $1/T$ were 1.2×10^3 at $1 \times 10^{-3} \text{ mm Hg}$., and 1.3×10^3 at $1.5 \times 10^{-4} \text{ mm Hg}$. The points on the graphs (figure 4.22) were rather scattered particularly at higher temperature owing to the very small changes of ϵ_0/ϵ with detector temperature. The experiment was repeated at the lower flow rate of 2 ml/sec of the carrier gas through the anthracene saturator and the detector, and the points on a graph

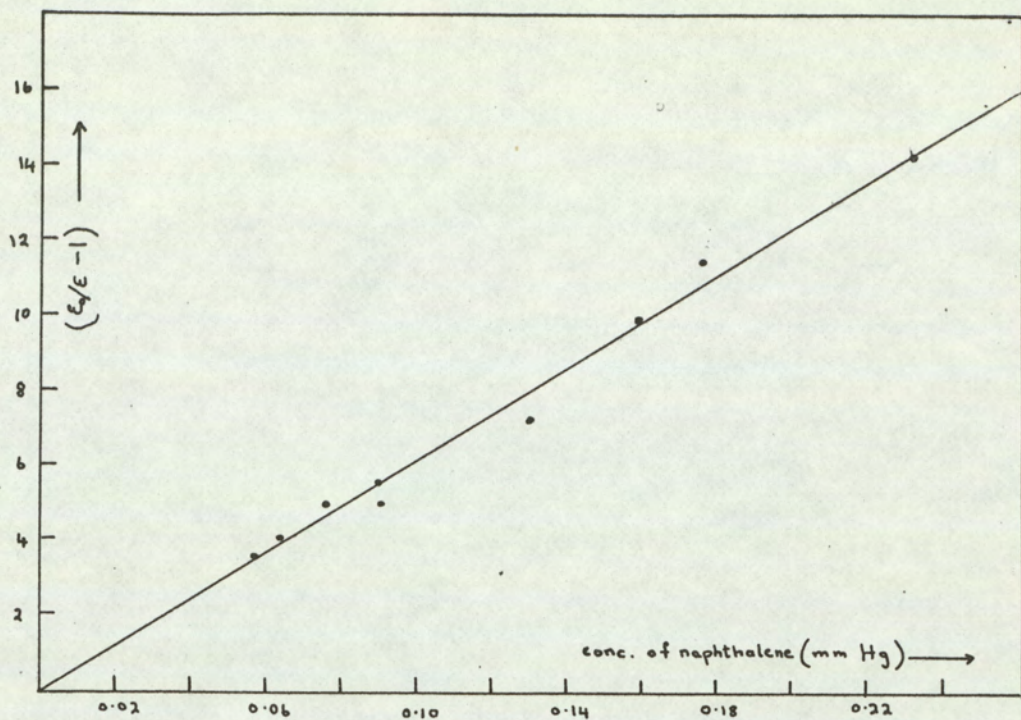


Fig. 4.14 $(\frac{\epsilon_y}{\epsilon} - 1)$ against concentration of naphthalene.

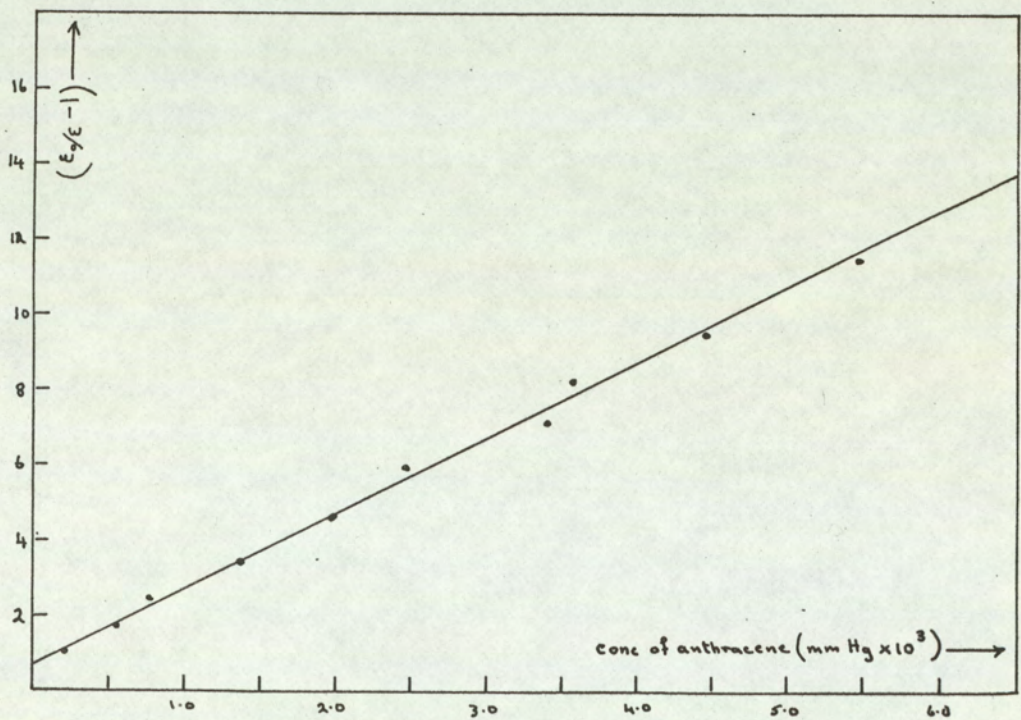


Fig. 4.15 $(\frac{\epsilon_y}{\epsilon} - 1)$ against concentration of anthracene.

of $\log (\epsilon_0/\epsilon - 1)$ against $1/T$ were scattered about the same straight line as that for the higher flow rate of 4 ml/sec although the absolute values of the current were less for the lower flow rate.

4.4₅ - Perfluorodecalin

The perfluorodecalin obtained from The Imperial Smelting Company was solidified by immersing the saturator in a slurry of solid carbon dioxide and acetone. The vapour pressure at this temperature was obtained by extrapolation from vapour pressure data measured between 0°C and 50°C⁽⁹²⁾. The extrapolated value found for the vapour pressure of perfluorodecalin at -78.5°C was 2.51×10^{-5} mm Hg. The total flow through the cell was kept constant at 4 ml/sec and the flow through the saturator varied from 0.002 ml/sec to 0.019 ml/sec. The "Vibron" reading in mV was noted at pulse intervals from 200 μ sec to 1000 μ sec and a mean value of the ratio (ϵ_0/ϵ) was obtained for each flow rate. The experiment was done with the cell at a temperature of 22°C and repeated at 86°C. Graphs of $(\epsilon_0/\epsilon - 1)$ against flow rate through the saturator were plotted (figure 4.16). With the detector at 22.0°C there were two lines, the one at lower flow rates going through the origin. The equilibrium constants found from the slopes of these lines are 2.1×10^3 and 1.1×10^3 per ml of saturated gas. With the detector at 86.0°C only the lower flow rates were studied and the equilibrium constant obtained from the slope of the graph of $(\epsilon_0/\epsilon - 1)$ against concentration was 9.4×10^2 per ml of saturated gas.

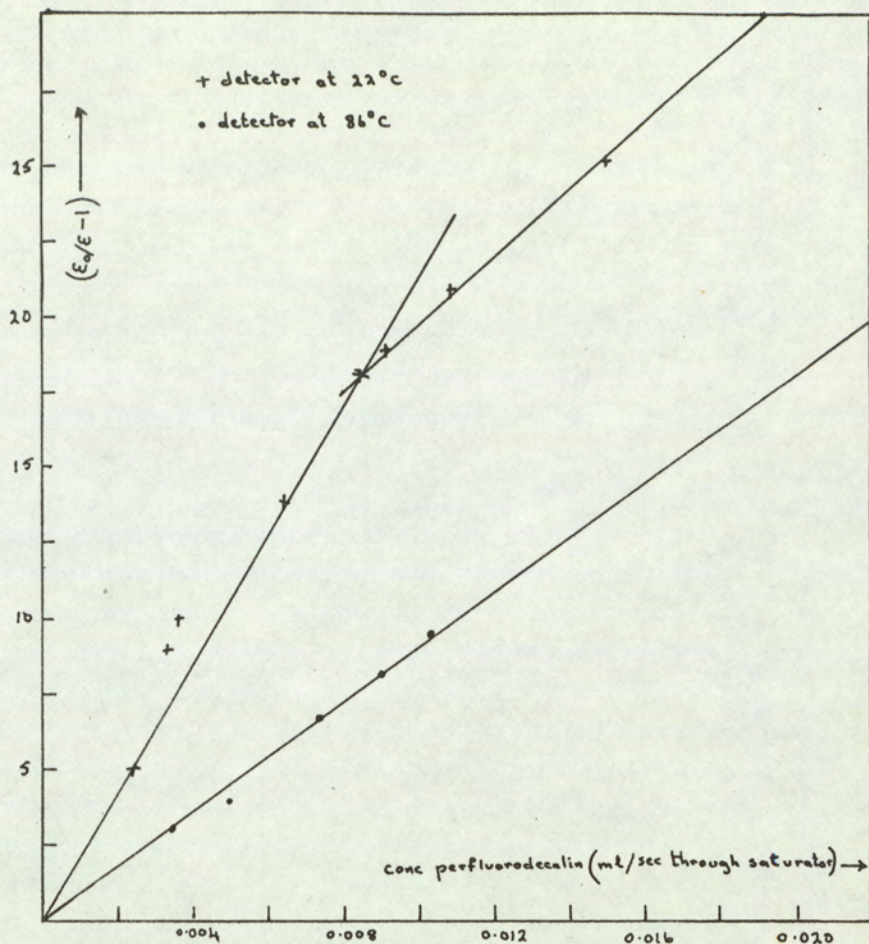


Fig. 4.16 $(\epsilon_g/\epsilon - 1)$ against concentration of perfluorodecalin

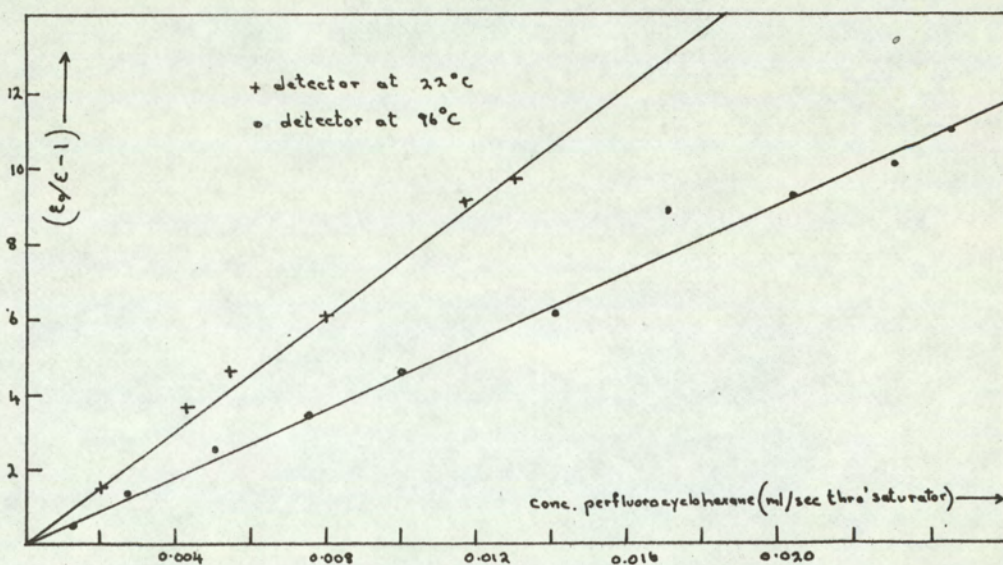


Fig. 4.17 $(\epsilon_g/\epsilon - 1)$ against concentration of perfluorocyclohexane

4.4₆ - Perfluorocyclohexane

The solid was sublimed out of the glass sample tube of the compound supplied by the Imperial Smelting Company into the saturator immersed in a slurry of solid carbon dioxide and acetone. The vapour pressure of perfluorocyclohexane at this temperature was obtained by extrapolation of vapour pressures measured between 19.8°C and 50.0°C⁽⁹³⁾ and was thus calculated to be 9.7×10^{-2} mm Hg at -78.5°C. The total flow through the cell was kept constant at 4 ml/sec and the flow through the saturator was varied from 0.002 ml/sec to 0.024 ml/sec as measured by a capillary flow meter. (ϵ_0/ϵ) was measured for each particular flow rate through the saturator and a graph of ($\epsilon_0/\epsilon - 1$) against flow rate was plotted (figure 4.17). With the detector at 22°C the slope of the line through origin had a slope corresponding to an equilibrium constant of 7.5×10^2 per ml of saturated gas. At 96.5°C the equilibrium constant was found to be 4.5×10^2 per ml of saturated gas.

4.4₇ - Benzoquinone

Commercial benzoquinone was recrystallised from petroleum ether and put in the saturator suspended in the oven. All of the carrier gas was passed through the benzoquinone and its concentration altered by varying the temperature of the saturator oven between 0°C and 30°C. The vapour pressure was estimated by extrapolation of data obtained between -13.3°C and 5.3°C⁽⁹⁴⁾. With the detector at a temperature of 122°C the equilibrium constant was $8.61 \text{ (mm Hg)}^{-1}$ (figure 4.18). The effect of varying the detector temperature was

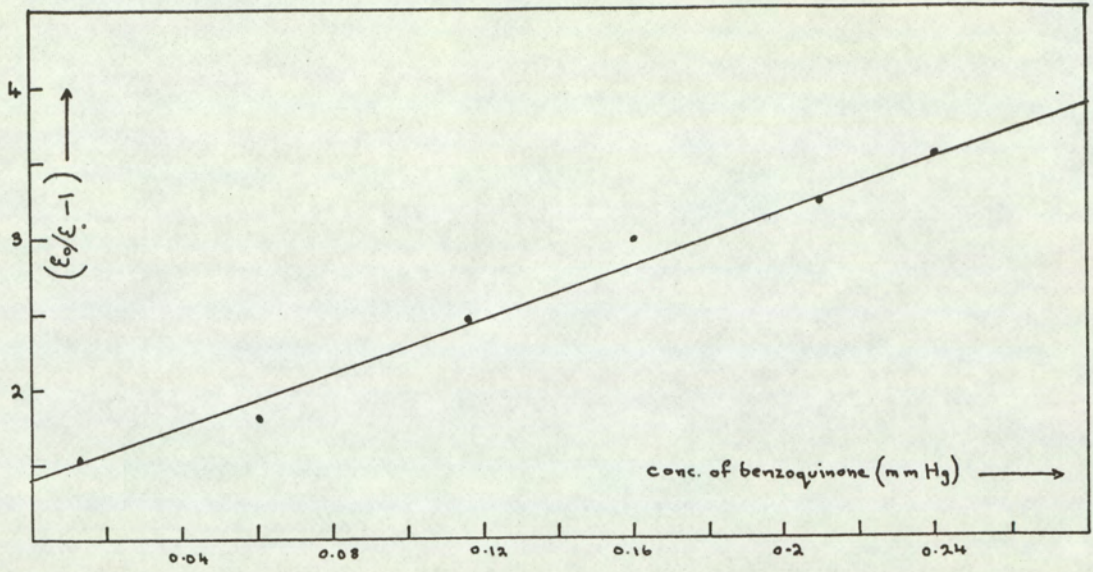


Fig. 4.18 $(\epsilon_0/\epsilon - 1)$ against concentration of benzoquinone.

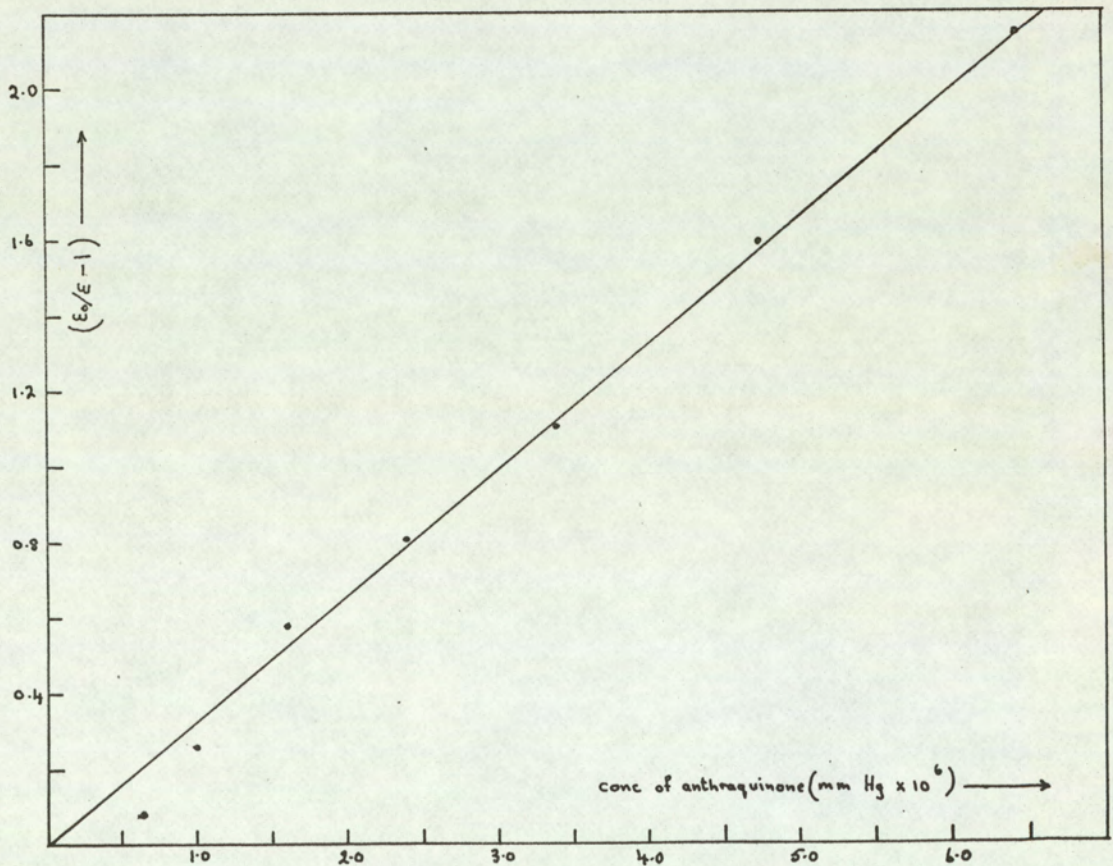


Fig. 4.19 $(\epsilon_0/\epsilon - 1)$ against concentration of anthraquinone.

studied and a graph of $\log (\epsilon_0/\epsilon - 1)$ against $1/T$ was plotted. The slope of the line obtained was 2.8×10^2 at a partial pressure of 0.174 mm Hg.

4.4₈ - Anthraquinone

The sample of anthraquinone was obtained from Imperial Chemical Industries and used without further purification. It was placed in the saturator in the second oven and all of the carrier gas was allowed to flow through it. The concentration of the anthraquinone was varied by varying the temperature of the oven between 30°C and 60°C with the detector at 95.0°C . The vapour pressure was estimated by extrapolation of data obtained at temperatures between 190°C and 285°C ⁽⁹⁴⁾. Graphs of $(\epsilon_0/\epsilon - 1)$ against vapour pressure in mm Hg were drawn. At partial pressures between 0.6×10^{-6} mm Hg and 7.0×10^{-6} mm Hg the slope of the line was 3.9×10^5 (mm Hg)⁻¹ (figure 4.19). The effect of varying the detector temperature between 50.0°C and 122.0°C was studied, and the slope of a graph of $\log (\epsilon_0/\epsilon - 1)$ against $1/T$ was 3.6×10^2 degrees at a concentration of 0.3×10^{-6} mm Hg.

4.4₉ - Chloranil

The carrier gas was passed through the chloranil in the saturator and then through the detector at 4 ml sec with the detector at 80.0°C . The concentration of the chloranil in the carrier gas was varied by altering the temperature of the saturator. Vapour pressure data measured over a range of 60.0°C to 82.7°C ⁽⁹⁴⁾ were extrapolated to estimate the vapour pressure of chloranil between 24°C and 36°C , the range of saturator temperatures used.

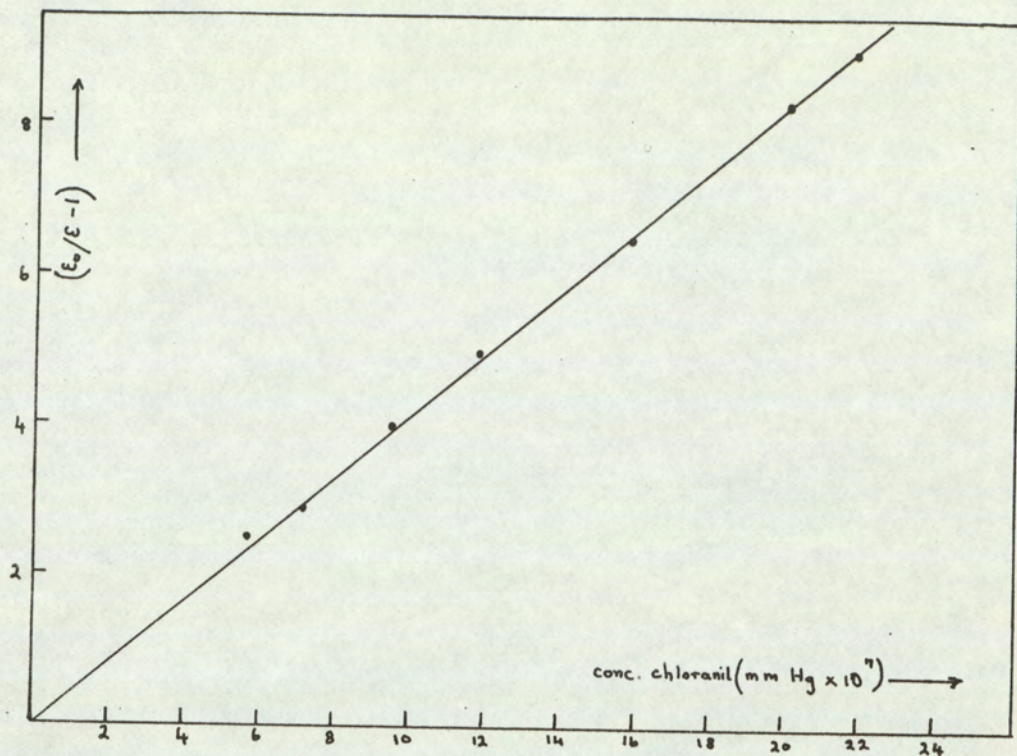


Fig. 4.20 $(\epsilon_0/\epsilon - 1)$ against concentration of chloranil.

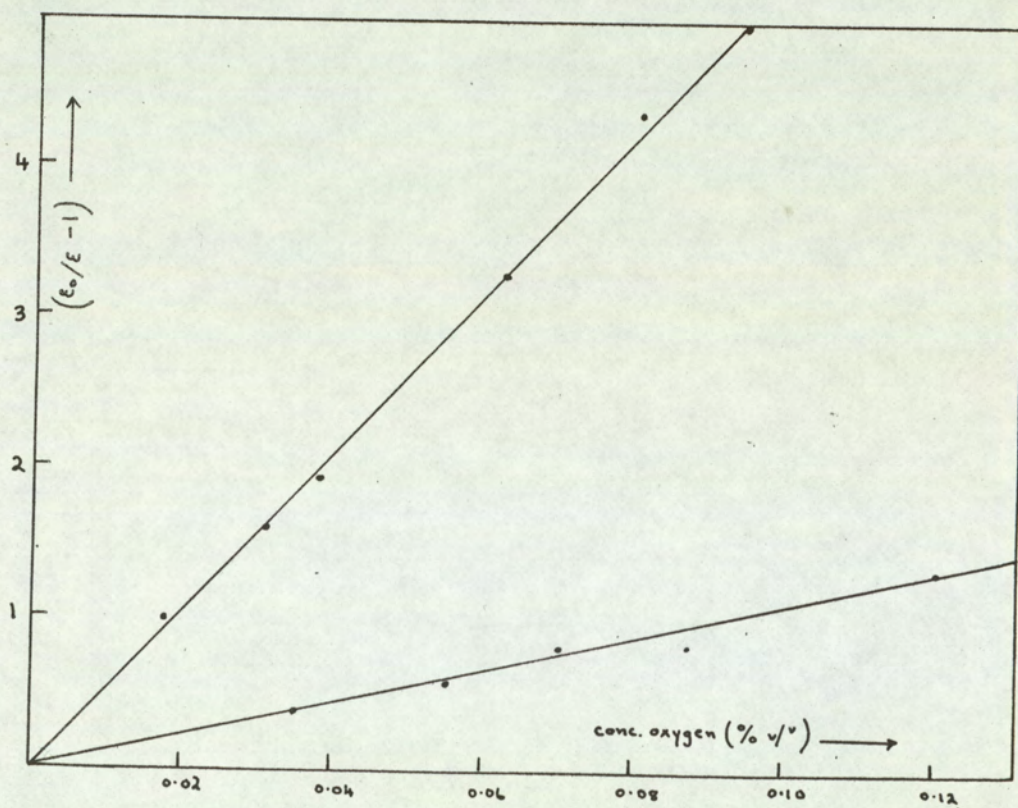


Fig. 4.21 $(\epsilon_0/\epsilon - 1)$ against concentration of oxygen.

A graph of $(\sigma / -1)$ against concentration (figure 4.20) had a slope of $4.12 \times 10^6 \text{ (mm Hg)}^{-1}$ with the detector at 80°C .

4.4₁₀ - Perfluorobenzene

The sample, provided by the Imperial Smelting Company, was used without further purification and put into the saturator, held in a slurry of solid carbon dioxide and acetone in a dewar flask. The carrier gas was split into two streams, most of it by-passing the saturator. Very low flow rates, of the order of 0.002 ml/sec measured on a pre-calibrated capillary flow meter, were put through the saturator after which the gas was fed into the main stream and then into the detector which was at a temperature of 22°C . Even at the lowest flow rates through the saturator the electron concentration in the cell dropped to zero. In case all the oxygen had not been removed from the capillary flow meter and saturator the argon methane mixture was left flowing for 48 hours. When the experiment was repeated the same effect occurred. When the temperature of the cell was raised to 0°C , again complete electron adsorption was observed. The vapour pressure of perfluorobenzene at -78.5°C was estimated by extrapolation of data obtained in the temperature range 20°C to 60°C (92) and has the value of $3.62 \times 10 \text{ mm Hg}$. With a flow rate through the saturator of 0.002 ml/sec and total flow rate of 4 ml/sec the partial pressure in the cell was $1.8 \times 10^{-5} \text{ mm Hg}$. Thus the minimum value for the equilibrium constant K is $5.5 \times 10^4 \text{ (mm Hg)}^{-1}$.

4.4₁₁ - Sulphur Hexafluoride

The electron affinity of sulphur hexafluoride has been measured in the magnetron by Kay and Page and a value of 34.3 kcal/mole (34)

obtained. The gas was therefore studied in the detector cell so that the results obtained by the two methods could be compared. The gas supplied by Imperial Chemical Industries was passed through a capillary flow meter at rates of the order of 0.002 ml/sec. This was then fed into the main stream of the gas before entering the detector. At the lowest flow rates of the sulphur hexafluoride through the capillary flow meter corresponding to a partial pressure of 3.8 mm Hg in the cell, all the electrons in the detector cell were absorbed. An attempt was made to dilute the sulphur hexafluoride with argon-methane mixture before introducing it into the system. This was done by collecting nine volumes of argon-methane mixture and one volume of sulphur hexafluoride over mercury. However, it was found that the argon-methane mixture collected over mercury caused a reduction in electron concentration in the cell, presumably due to the presence of mercury vapour. A diluted sample of sulphur hexafluoride was therefore ordered from Cambrian Chemicals Limited but was not delivered before practical work ended.

4.4₁₂ - Oxygen

Oxygen, supplied by the British Oxygen Company was introduced into the carrier gas at concentrations up to 0.1%. A capillary flow meter was used to measure the flow rate of the oxygen which was then fed into the main stream of the gas. The total flow rate was 4 ml/sec. Graphs of $(\epsilon_0/\epsilon - 1)$ against oxygen concentration were drawn (figure 4.21) and the equilibrium constant calculated to be 5.4×10^3 atmospheres⁻¹, with the detector at 31°C. When the experiment was repeated with the cell at 90°C the equilibrium constant was found to

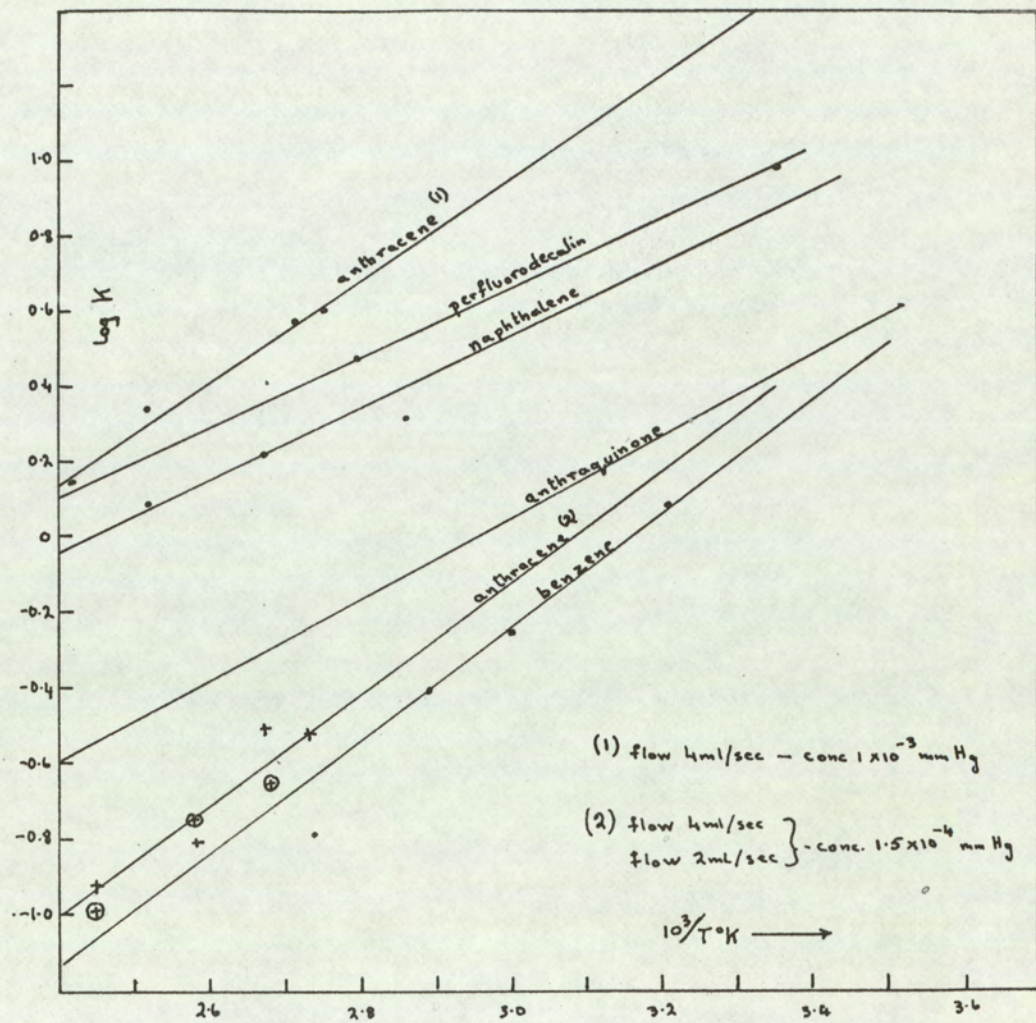


Fig. 4.22 Log K against $1/T^\circ K$ for several compounds.

be 3.3×10^3 atmospheres⁻¹.

4.4₁₃ - Summary

Experiments have been described showing the effect of introducing the compounds previously studied in the magnetron into the carrier gas stream through an electron capture detector. The reduction in electron concentration due to the presence of a known number of acceptor molecules has been measured and the effect of raising the temperature of the cell has been investigated. The results of these experiments are summarised in table 4.1 and are discussed in the following section.

For several compounds the equilibrium constant has been measured at different detector temperatures and slightly different values obtained. Since there was, however, so little variation with temperature the values obtained for a particular compound have been averaged to obtain the figure in column 1 of table 4.1.

4.5 Discussion of results obtained in the electron capture cell

In section 4.4 it was shown that the introduction of various compounds into the carrier gas stream of the electron capture detector affected the concentration of the electrons within the cell. There are several possible mechanisms which could be postulated to explain the mode of action of the detector and some of these will now be discussed and applied to the results obtained in section 4.4 with a view to obtaining a theoretical explanation for the observed effects.

Firstly using a model similar to that suggested by Wentworth

and Becker⁽⁷⁹⁾ and described in section 4.1 it may be assumed that kinetic equilibrium occurs in the cell, represented by the reaction



Negative ions are formed when neutral molecules collide with thermal electrons, and dissociate back to their original state, when the total kinetic energy of a subsequent collision is greater than the activation energy required. The equilibrium constant K for the reaction may be written

$$K = \frac{[A^-]}{[A][e]} = \frac{\epsilon_0 - \epsilon}{[A]\epsilon} \quad \dots \quad \dots \quad (4.45)$$

providing $[A] \gg [A^-]$ where ϵ_0 is the current through the cell with the carrier gas only flowing through it and ϵ is the corresponding current when a concentration $[A]$ of the electron absorbing molecules is introduced into the gas stream. K may therefore be calculated from the slope of graphs of $(\epsilon_0/\epsilon - 1)$ against the concentration $[A]$, and the values of the equilibrium constant for the compounds studied are shown in column 1 of table 4.1. As was shown earlier, if equilibrium conditions as represented by equation 4.44 do exist within the cell, the electron affinity may be calculated from the equilibrium constant by applying equation 4.43. The energies E_0 thus obtained are listed in column 2 of table 4.1. If, in fact, these do represent the electron affinities of the molecules it should be possible to obtain the same values from an Arrhenius type analysis.

The variation of the equilibrium constant K with temperature is given by

$$\frac{d \ln K}{dT} = \frac{\Delta U}{RT^2} \quad \dots \quad (4.46)$$

where T is the absolute temperature and ΔU is the enthalpy of the reaction. In this case ΔU may be equated with the electron affinity of A , since the forward direction of the reaction of equation 4.42 requires no activation energy. The equilibrium constants were therefore measured at several temperatures and the electron affinities calculated from the slopes of graphs of $\log (\epsilon_0/\epsilon - 1)$ against $1/T$ (figure 4.22). These energies E_T are listed in column 4 of table 4.1 from which it is seen that the equilibrium constant varies very little with temperature and the electron affinities of the different compounds all lie between 0.5 kcal/mole and 2.5 kcal/mole. These values do not agree with those in column 2 obtained by third law methods and neither of these agree with the electron affinities obtained by the magnetron technique and discussed in chapter 3 which are listed in column 5 of table 4.1. (The value quoted for oxygen is due to Phelps and Pack⁽⁹⁶⁾ who studied attachment and detachment coefficients and equilibrium constants for the reaction $2O_2 + e \rightleftharpoons O_2^- + O_2$ in pure argon and found the electron affinity of the oxygen molecule to be 0.44 eV or 10.15 kcal/mole). Since there is lack of agreement between the second and third law methods for calculating the electron affinities from the results summarised in table 4.1 it would seem that the electron affinity of the molecules is not the dominant factor involved in

electron capture under conditions existing in the detector.

An alternative mechanism, that of two balanced reactions, rather than actual kinetic equilibrium could be postulated to account for the observed results. If negative ions are formed according to the reaction



and are lost by a variety of reactions which have an effective rate constant k_2 and may be represented by the reaction



where X is a gas molecule which is excited by the collision to X^* .

When these two reactions are balanced the rates of the two reactions v_1 and v_2 are equal. The rate of a reaction between two molecules is given by

$$v = Z \exp - E/RT \quad \dots \quad \dots \quad (4.49)$$

where Z is the number of collisions per second between two molecules in 1 cm^3 of gas. Hence

$$Z_1 \exp - E_1/RT = Z_2 \exp - E_2/RT \quad \dots \quad \dots \quad (4.50)$$

where Z_1 and Z_2 are the collision frequencies, and E_1 and E_2 the activation energies for the reactions in equations 4.49 and 4.50 respectively. Since the activation energy E_1 is zero and E_2 equals E the electron affinity of A

$$\frac{Z_1}{Z_2} \exp E/RT = 1 \quad \dots \quad \dots \quad (4.51)$$

The collision frequency of two molecules A and B is given by the kinetic theory of gasses as

$$Z_{AB} = n_A n_B \sigma_{AB}^2 \left[8 \pi kT \frac{m_A + m_B}{m_A m_B} \right]^{1/2} \dots \dots (4.52)$$

where n_A and n_B are the number concentration of the molecules A and B and m_A and m_B are their masses. σ_{AB} is the average of the diameters of the two molecules and T is the absolute temperature.

Therefore

$$Z_1 = n_A \cdot n_e \sigma_{Ae}^2 \left[8 \pi kT \frac{m_A + m_e}{m_A \cdot m_e} \right]^{1/2} \dots \dots (4.53)$$

and

$$Z_2 = n_{A^-} \cdot n_X \sigma_{A^-X}^2 \left[8 \pi kT \frac{m_{A^-} + m_X}{m_{A^-} \cdot m_X} \right]^{1/2} \dots \dots (4.54)$$

where A, e, A^- , and X refer to the neutral capturing molecules, the electrons, the negative ions and the carrier gas molecules respectively.

If one considers the particular case of benzoquinone in a carrier gas of argon equation 4.51 may be re-written

$$\frac{n_{BQ} \cdot n_e \sigma_{BQe}^2}{n_{BQ^-} \cdot n_A \sigma_{BQ^-A}^2} \frac{\left[8 \pi kT \frac{m_{BQ} + m_e}{m_{BQ} \cdot m_e} \right]^{1/2}}{\left[8 \pi kT \frac{m_{BQ^-} + m_A}{m_{BQ^-} \cdot m_A} \right]^{1/2}} \exp E/RT = 1 \dots \dots (4.55)$$

where BQ refers to benzoquinone.

Compound	K (atmosphere) ⁻¹	E _c kcal/mole	slope of graph of log ($\epsilon_0/\epsilon - 1$) vs. 1/T ^o K (degrees)	E _T kcal/mole	E kcal/mole from magnetron (Chapter 3)
Benzene	22.2	1.83	2.5 x 10 ²	1.1	
Naphthalene	4.45 x 10 ⁴	6.40	5 x 10 ²	2.3	
Anthracene	1.55 x 10 ⁶	8.5	1.2 x 10 ²	0.6	
Perfluorocyclo- hexane	2.58 x 10 ⁷	10.2	3.5 x 10 ²	1.60	
Perfluorodecalin	1.11 x 10 ¹¹	15.2	4.6 x 10 ²	2.06	22.4
Benzoquinone	6.35 x 10 ³	5.2	2.8 x 10 ²	1.28	25.8
Anthraquinone	2.88 x 10 ⁸	11.6	3.6 x 10 ²	1.65	26.3
Chloranil	3.05 x 10 ⁹	13.0	-	-	44.1
Oxygen	5.4 x 10 ³	5.12	5.7 x 10 ²	2.5	10.15 ⁽⁹⁶⁾

TABLE 4.1

Since m_{BQ} is large compared with m_e equation 4.55 may be rewritten

$$\frac{n_{BQ} \cdot n_e \sigma_{BQe}^2}{n_{BQ^-} n_A \sigma_{BQ^-A}^2} \left[\frac{1}{m_e} \cdot \frac{m_{BQ^-} \cdot m_A}{m_{BQ^-} + m_A} \right]^{1/2} \exp E/RT = 1 \quad \dots \dots (4.56)$$

Taking σ_{BQ^-A} as the sum of the covalent radii and equal to 9.6 \AA and since

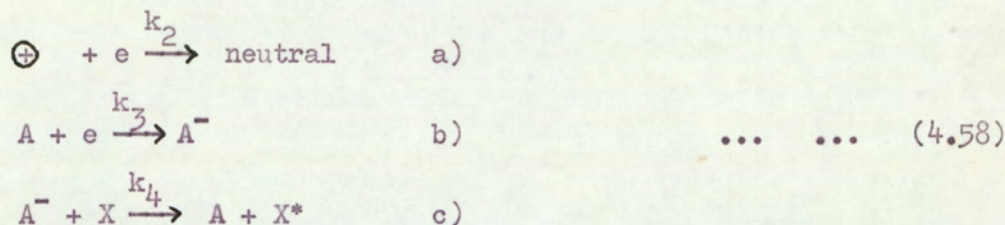
$$\frac{n_{BQ} \cdot n_e}{n_{BQ^-}} = \frac{\epsilon X}{(\epsilon_0 - \epsilon)} = 1/K$$

which from table 4.1 for benzoquinone is $(6.35 \times 10^3)^{-1}$ atmospheres⁻¹

$$\sigma_{BQ.e}^2 (0.18 \times 10^{-5}) \exp E/RT = 1 \quad \dots \dots (4.57)$$

The electron affinity of benzoquinone was found to be 31.4 kcal/mole using the magnetron technique (section 3.7). Substituting this value into equation 4.57, $\sigma_{BQ.e}^2$ may be calculated to be $3.5 \times 10^{-2} \text{ \AA}^2$ at 20°C, and $3.5 \times 10^3 \text{ \AA}^2$ at 100°C. The collision cross section would not be expected to vary with temperature over such a wide range. However, an expected value of a few tens of \AA^2 does lie within the above limits. With Brieglebs value⁽⁴⁴⁾ of 13.8 kcal/mole for the electron affinity of benzoquinone the collision cross sections calculated are $3.47 \times 10^{11} \text{ \AA}^2$ at 20°C and $5.5 \times 10^{13} \text{ \AA}^2$ at 100°C which are much higher than could reasonably be expected. Thus it is seen that a mechanism of balanced reactions as represented by equations 4.47 and 4.48 does not adequately account for the observed results.

A third possible mechanism may be suggested, that is, that electron capture is proportional to the cross sectional area of the molecules. Some of the reactions occurring within the cell may be represented by the following equations



In the presence of the carrier gas only, the rate of production of electrons is given by

$$d[e]/dt = k_1 a(G+1) - k_2 [e][\oplus] - u[e] \quad \dots \quad \dots \quad (4.59)$$

where k_1 is the rate of production of β -particles per unit area of the foil of area a , and each β -particle forms G ion pairs and u is the flow rate of the gas. With a capturing species A present

$$d[e]/dt = k_1 a(G+1) - k_2 [e][\oplus] - u[e] - k_3 [A][e] + k_4 [A^-][X] \quad \dots \quad \dots \quad (4.60)$$

Under steady state conditions $d[e]/dt = 0$. Therefore, equating equations 4.59 and 4.60 and setting the electron concentration with only carrier gas present as ϵ_0 and that with the acceptor present as ϵ , one obtains

$$-k_2 \epsilon_0 [\oplus] - u \epsilon_0 = -k_2 \epsilon [\oplus] - u \epsilon - k_3 [A] \epsilon + k_4 [A^-][X] \quad \dots \quad \dots \quad (4.61)$$

If $[A^-]$ is much smaller than $[A]$ then

$$k_3 = \frac{\epsilon_0 - \epsilon}{\epsilon [A]} (k_2 [\oplus] + u + k_4 [X]) \quad \dots \quad \dots \quad (4.62)$$

$$= \frac{K}{A} (k_2 [\oplus] + u + k_4 [X]) \dots \dots (4.63)$$

If $k_2 [\oplus] + u + k_4 [X]$ is a constant then the slope of a graph of K against A will be proportional to k_3 , which if the detector responds to cross sectional areas should be directly proportional to the area of the molecule concerned in the capturing process. In figure 4.23 a graph is plotted of $\log K$ against the \log of the area of cross section calculated from data on covalent bond radii (97). The area taken was that within the geometrical figure obtained from joining the outer atoms through their covalent radii. The graph shows that within a group of compounds of the same type the area does indeed appear to be proportional to the equilibrium constant K but the different compounds lie on different lines. This is because the effective cross sectional area for electron attachment of the molecule with a positive electron affinity is greater than the geometrically calculated area so that, for example benzoquinone has a geometrical area of about 50 \AA^2 but from figure 4.23 it is seen to have an effective area of 70 \AA^2 relative to the series of hydrocarbons.

It was suggested above that

$$(k_2 [\oplus] + u + k_4 [X])$$

was a constant for all compounds which were studied. The flow rate u was in fact kept constant for all the experiments and $k_2 [\oplus]$ does not depend to any large extent on the presence of a capturing species since the positive ion concentration is much greater than

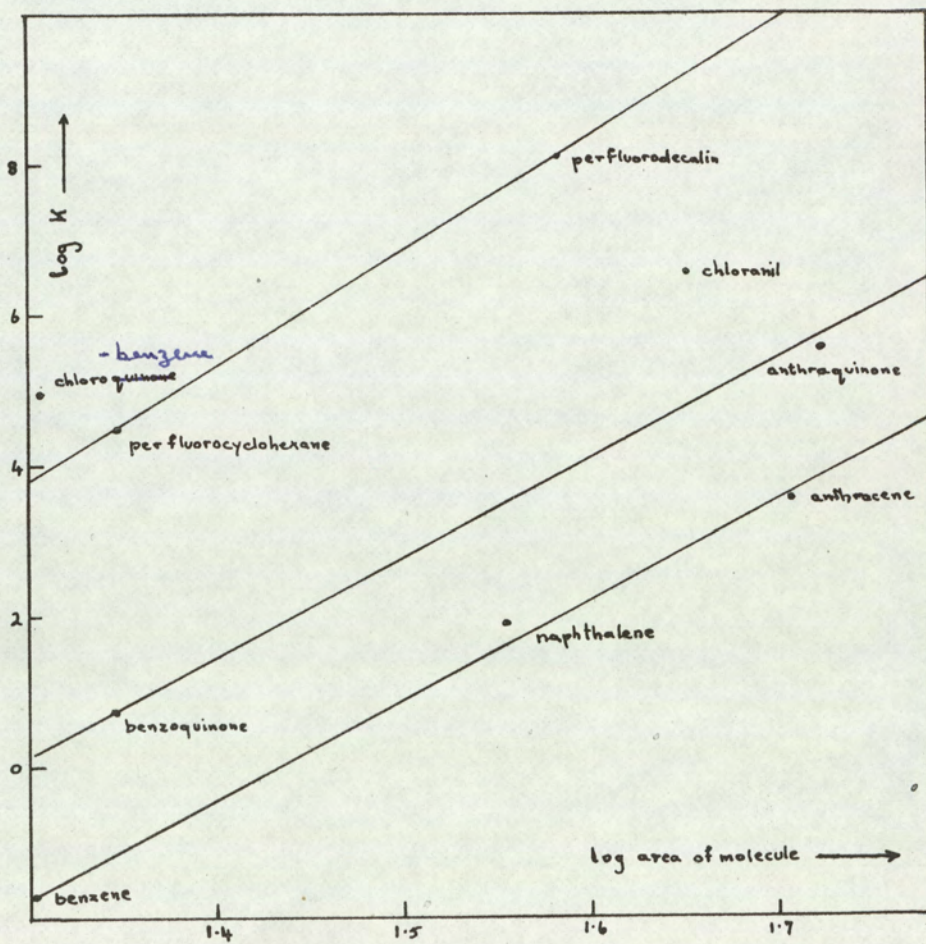


Fig 4.23 .Log K against log area of molecule.

the ion or electron concentration and therefore may be taken to be constant. $k_4 [X]$ however does depend on the electron affinity of the molecules present in the cell since the rate k_4 depends on the activation energy necessary to detach an electron from the negative ion. This effect seems to be small compared with the increase in cross sectional area since within groups of the same type of compound a linear relationship between K and cross sectional area appears to hold.

Thus it is seen that the response of the electron capture detector does not vary directly with the electron affinity of the molecules which are introduced into the gas stream but rather with their cross sectional area for electron capture. Since this depends on the geometrical area and the electron affinity of the molecules it is not possible to predict the contribution to this capture cross section made by particular substituents and the two effects may not therefore be separated. Until the relationship between the actual size and the electron collision cross section is known it will not therefore be possible to obtain electron affinities from measurements made in the electron capture cell.

Chapter 5. Values of electron affinities obtained by other methods.

5.1 Introduction

In the previous chapters, two methods have been described which offered the possibility of obtaining electron affinities of relatively large molecules. By the magnetron technique it was possible to measure the stability of a number of ions, but it was found that the electron capture detector could not be used to measure the same energies for purposes of comparison. It is now intended to discuss briefly some other methods available for estimating electron affinities and to compare any relevant data with the measurements discussed earlier.

A number of methods, potentially useful in measuring electron affinities, were reviewed by Pritchard ⁽⁹⁸⁾ in 1953. Most of these however were very limited in their application. The study of electron attachment and electron impact phenomena by such techniques as mass spectrometry had been mainly restricted to the halogens and a few other simple molecules. Equilibrium measurements in flames and at heated metal surfaces were also discussed but again the measurements had been limited mainly to the halogens.

Electron affinities had also been obtained from the Born-Haber cycle, from thermochemical data and lattice energies. These latter had been calculated using the Born Mayer equation relating the lattice energy to the ionic charges and the distance between them. Alternatively they had been obtained from equilibrium measure-

ments on the dissociation of crystals in a furnace, or on a heated metal surface, but again most of the work had concerned the halogens.

The possibility of obtaining electron affinities from the heats of solvation of ions and from the kinetics of electrode processes were also discussed in the review by Pritchard. This last method has been further developed and will be discussed below. Finally, some semi-empirical methods were discussed such as attempts to derive electron affinities from spectroscopic data, by extrapolation techniques, and by quantum mechanical calculations. These did not give very reliable data and were again limited in their application.

Since Pritchard's review, some of the techniques mentioned have been modified and other, new methods, have been developed. The theory and technique of the magnetron as used by Sutton and Mayer (17) has been developed by Page, and used to measure a large number of electron affinities (26 - 40). This method was used to study several groups of organic compounds discussed in Chapter 2 of this dissertation. The newer methods include the photodetachment studies of Branscomb (53) and Berry (52) who, independently, measured the electron affinities of the halogens by spectroscopic analysis of the photodetachment of electrons.

Their results are in excellent agreement with the lattice energy calculations on the alkali halides by Cubicciotti (99). Another recently developed method using the electron capture detector

which was described in chapter 4 has a potentially wide application to the measurement of the electron affinities of polyatomic molecules. It has been claimed that the electron affinities of a number of hydrocarbons have been obtained by this method (79). Other currently used methods for estimating electron affinities include charge-transfer measurements and polarography. Theoretical calculations have also been made using molecular orbital theory to find the energy of the lowest unfilled orbital of a molecule and hence its electron affinity. These methods will now be discussed and the values obtained compared.

5.2 Calculated values of electron affinities

There have been various attempts to calculate ionisation potentials and electron affinities using Molecular Orbital theory. According to simple Huckel theory, the ionisation potential, I , of a molecule is the energy of the highest occupied molecular orbital and is given by

$$-I = \alpha_0 + f\beta \quad \dots \quad (5.1)$$

where α_0 is the Colomb integral, β the resonance integral for two neighbouring atoms and f is the Huckel coefficient which expresses the contribution of β to the total energy I . The electron overlap integral is assumed to be zero and electron repulsion is neglected. Since electron affinities are the ionisation potentials of the corresponding negative ions, it should be possible to calculate electron affinities using a similar equation.

Hedges and Matsen (25) have used the approximate anti-symmetrised molecular orbital expressions derived by Pople (12) for

the electronic energy of a conjugated system and have calculated electron affinities and ionisation potentials of some aromatic compounds. The values obtained are shown in column 1 of table 5.1. Hoyland and Goodman ⁽¹³⁾ have improved on the calculations by allowing for atomic orbital deformation when an extra electron is added. Their calculated values which do not require scale factors as the other method does, are also included in table 5.1 in column 2.

For polycyclic hydrocarbons where all the Hückel π centers are the same, Ehrenson ⁽²³⁾ has proposed the use of the ω technique and developed an expression by the self-consistent field method for the ionisation potential which is

$$I = -\alpha_0 - \left(f - \frac{n-1}{n} \omega \right) \beta \quad \dots \quad (5.2)$$

where n is the total number of π electrons in the system and f is a semi-empirical constant reflecting the sensitivity of the coulomb integral to changes in the charge density. The electron affinity, the energy of the lowest unoccupied orbital, is similarly given by

$$A = -\alpha_0 - \left(f - \frac{n+1}{n} \omega \right) \beta \quad \dots \quad (5.3)$$

Ehrenson found that equation 5.2 gave satisfactory values for the ionisation potentials of aromatic hydrocarbons using values for α_0 and β of -9.878 and -2.11 eV respectively and 1.4 for ω . He then applied these parameters to the calculation of electron affinities and the values obtained are shown in column 3a of table 5.1.

By comparison with the other calculated values, and with the experimental values obtained by Wentworth and Becker ⁽⁴³⁾ shown in column 4, Ehrenson's figures are seen to be high by about 4 eV. He pointed out that if a larger value of 3.8 was used for ω better correlation with the other methods was obtained, as is seen from column 3b. (This value of ω is such that it gives the electron affinity and ionisation potential of graphite to be symmetrical about its work function ⁽²³⁾). No theoretical explanation appears to be available for the fact that calculations of ionisation potentials and electron affinities require different values of ω .

Scott and Becker ⁽²⁴⁾ by comparison of their calculated values (column 5, table 5.1) with the measurements of Wentworth and Becker ⁽⁴³⁾ found that ω equal to 3.80 gave good correlation between the self-consistent field method of Ehrenson and the experimental values except in a few cases (phenanthrene, 3,4-benzopheanthrene, and triphenylene) when ω equal to 3.73 gave much better agreement. They suggested that future calculations of electron affinities of alternant hydrocarbons using the ω -technique should use a value of 3.77 for ω until experimental work indicated an alternative value.

Becker and Wentworth ⁽⁷⁹⁾ have found that for four hydrocarbons for which electron affinities and ionisation potentials are known the electronegativity, based on the Mulliken definition, is approximately constant and equal to 4.07 ± 0.05 . The electron affinities used were those obtained from electron capture phenomena by Wentworth and Becker ⁽⁴³⁾ and the ionisation potentials were

experimental values obtained from various sources. Using this mean value for the electronegativity and measured ionisation potentials the electron affinities of several other hydrocarbon molecules were predicted - the values for benzene and naphthalene are included in column 4 of table 5.1

From table 5.1 it is seen that most of the theoretical and semi-empirical methods discussed earlier predict similar electron affinities for benzene, naphthalene and anthracene much lower than the limit of measurement of the magnetron where direct capture was not observed for these compounds (section 3.2). The higher polycyclic hydrocarbons have higher predicted affinities ⁽⁴⁴⁾ for example benzo [a] tetracene 1.1 eV and benzo [a] pentacene 1.45 eV. Had their vapour pressure been high enough it should have been possible to measure these energies using the magnetron technique and to compare the two values. This, however, was not attempted since the vapour pressure of the tricyclic hydrocarbons in the magnetron was not great enough and it was therefore unlikely that the larger molecules would be sufficiently volatile.

Table 5.1 Calculated electron affinities

Compound	Hedges and Matsen (25)	Hoyland and Goodman (13)	Ehrenson (23)		*Wentworth and Becker (79)	Scott and Becker (24)
			a	b		
Benzene	-1.63	-1.40	4.32	-1.62	(-1.1)	-1.59
Naphthalene	-0.38	-0.2	5.32	-0.25	-0.12	-0.25
Anthracene	0.49	0.61	5.84	0.43	(0.42)	0.42
Tetracene	0.82					0.79
Phenanthrene	-0.20	0.25	5.44	0.0	(0.20)	0.01
Pyrene	0.68	0.55				0.42

* values in brackets are experimental values

5.3 Charge transfer spectra and electron affinities

The molecular complexes which are formed between electron acceptor and electron donor molecules show characteristic absorption bands which have no counterpart in the absorption spectra of the separate substances. The first satisfactory quantum mechanical treatment of these molecular complexes was given by Mulliken⁽¹⁰²⁾. He considered the formation of weak complexes to be due to the interaction of a no bond ground state whose wave function may be represented as $\psi(D_1A)$, and an ionic excited state $\psi(D^+A^-)$ which produced a stabilised ground state with a wave function

$$\psi_0 = \psi(D, A) + a \psi(D^+ - A^-) \quad \dots \quad \dots \quad (5.4)$$

and an excited state having a wave function

$$\psi_1 = b \psi(D, A) + \psi(D^+ - A^-) \quad \dots \quad \dots \quad (5.5)$$

The energy of ψ_0 is less than the energy of either $\psi(D, A)$ or $\psi(D^+ - A^-)$ so the interaction provides an explanation of the stability of the complex, and the electronic transition $\psi_0 \rightarrow \psi_1$ is associated with the characteristic absorption band of the complex. The energy associated with the charge transfer is given by Mulliken⁽¹⁰⁰⁾ and if the interaction of the no bond ground state and ionic excited state is small (that is a and b in equations 5.4 and 5.5 are much less than unity) then

$$h\nu = I - E - C \quad \dots \quad \dots \quad (5.6)$$

where I is the ionisation potential of the donor, E is the electron affinity of the acceptor and C is the interaction energy of the excited state relative to the ground state.

This equation and its related form⁽¹⁰¹⁾ have been used to

determine ionisation potentials by measuring the charge transfer energies of a series of donors of known ionisation potentials, with one acceptor and by assuming that C in equation 5.6 is constant. Values of ionisation potentials interpolated from these data agree well with those obtained from photoionisation and electron impact studies and this assumption therefore seems to be valid. The data on electron affinities are however so scarce that it has not been possible to justify experimentally the assumption that C is a constant for a series of acceptors with the same donor. Jortner and Sokolov⁽¹⁰²⁾ have measured charge transfer spectra of one donor with various acceptors and calculated the electron affinities of the latter from equation

$$h\nu_{\max}^1 - h\nu_{\max}^2 = E_2 - E_1 \quad \dots \quad \dots \quad (5.7)$$

where 1 and 2 refer to different acceptors with the same donor.

The constant C was assumed to be the same in both cases. Hence, if the electron affinity of one acceptor were known, others might be calculated. Jortner and Sokolov calculated the electron affinity of the iodine molecule to be 1.8 eV from the known value for atomic iodine and used this to estimate other electron affinities. Batley and Lyons⁽¹⁰³⁾ found the electron affinities of a number of molecules relative to iodine, from charge transfer data of each acceptor with about a dozen donors. The spread of the values so determined was about 0.2 eV. for each acceptor which lends some support to the fact that the difference between the interaction energies of different donors with one acceptor is small. They assumed this to be zero and compiled a table of electron affinities of molecules which act as

acceptors in charge transfer spectra. The " I_2 standard technique" has recently been applied to a series of quinones with two donors and mean electron affinities obtained (104).

Briegleb (44) has discussed a number of semi-empirical methods combining charge transfer measurements with other data, such as ionisation potentials calculated by equation 5.2, and first excitation energies of donor molecules, and has produced an extensive table of relative electron affinities. Some of the mean values he obtained are shown in table 5.2 row 1. The second row of this table shows the electron affinities obtained by the magnetron method and it is seen that these are considerably higher than those values obtained from charge transfer measurements. This is probably due to the neglect of the interaction energy term in the latter method.

By assuming that the energy of the excited state of the complex is entirely electrostatic in origin and resolving it into its component charge-charge and charge-dipole contributions it has been shown (50) that interaction energies are more important when estimating electron affinities from a series of charge transfer spectra of a donor with several acceptors, than in obtaining ionisation potentials from spectra of an acceptor with several donors, where the interaction energy is likely to be small. Since it is not possible to calculate the interaction energies involved due to lack of data on the dimensions of the complex and dipole moments of substituents, it is not possible at present to calculate accurate, absolute electron affinities from charge transfer measurements although it is a useful

method for obtaining relative values.

Table 5.2

Compound	Electron affinity values (eV)								
	BQ	CQ	NQ	AQ	TCNE	B	N	AN	AZ
From charge transfer (44)	0.6	1.37	0.7	0.5	1.8	-1.5	-0.3	0.5	0.5
From magnetron (Chapter 3)	1.12	1.91	-	1.14	2.88 (50)				2.6 (?)

BQ = benzoquinone CQ = chloranil NQ = naphthaquinone

AQ = anthraquinone TCNE = tetracyanoethylene B = benzene

N = naphthalene AN = anthracene AZ = azulene

5.4 Polarographic half wave reduction potentials and electron affinities

It has been shown by Matsen ⁽¹⁰⁵⁾ that the polarographic half wave reduction potential represents a reversible one electron transfer at the mercury cathode and it can be related to the electron affinity of the reduced species by the equation

$$-e_{1/2} = E + \Delta H_{(Sol)} - \chi_{Hg} - e_0 \quad \dots \quad (5.8)$$

where $e_{1/2}$ is the half wave reduction potential, E the electron

affinity of the species reduced, $\Delta H_{(Sol)}$ the difference in the heats of solution of the ion and molecule, χ_{Hg} the work function of mercury and ϵ_0 the absolute potential of the electrode. If the potentials are measured relative to the saturated calomel electrode then

$$-\epsilon_{1/2} = E + \Delta H_{(Sol)} - 5.07 = E' - 5.07$$

Using this equation Matsen calculated E' for a series of condensed aromatic molecules from measured reduction potentials. Maccoll⁽¹⁰⁶⁾ had suggested that $\epsilon_{1/2}$ should be proportional to the energy of the lowest unoccupied orbital of simple Hückel Molecular Orbital theory, that is to the electron affinity of the molecule. Lyons⁽¹⁰⁷⁾ pointed out that this was valid for the sum of the electron affinity and solvation energy, E' . From Hückel theory the energy of the lowest unoccupied orbital A is given by

$$-A = \alpha + f\beta \quad \dots \quad \dots \quad (5.9)$$

where α is the coulomb integral, β the resonance integral for two neighbouring atoms and f is the Hückel coefficient which expresses the contribution of β to the total energy. It was shown⁽¹⁰⁶⁾ that a linear relationship did in fact hold between $\epsilon_{1/2}$ and f for a series of hydrocarbons where β may be taken to be constant. Matsen⁽¹⁰⁵⁾ has shown that E' is also proportional to f . Absolute electron affinities cannot, however, be directly obtained since the term E' contains the solvation energy terms, $\Delta H_{(Sol)}$, for which there is no

adequate estimate available at the present. Lyons⁽¹⁰⁷⁾ originally calculated the free energy of solvation of the negative ion using the Born equation which involves a knowledge of the radius of the ion and the dielectric constant of the solvent in the immediate neighbourhood of the ion, which is difficult to estimate. Attempts have been made to elaborate the original equation⁽¹⁰⁸⁾ but the reliability of these calculations is difficult to assess. The major part of $\Delta H_{(Sol)}$ is the solvation energy of the anion, that of the neutral molecule being negligible. Peover measured $\epsilon_{1/2}$ for a number of acceptors⁽¹⁰⁹⁾ and showed that $\Delta H_{(Sol)}$ for the anion was nearly constant. Using the average value of -3.66 eV for ΔH_{Sol} from these results, Briegleb⁽⁴⁴⁾ estimated the electron affinities of several compounds for which there were only polarographic data. This was done for some methyl substituted quinones for which there are no comparable data, and also for some organic anhydrides for which the values agreed fairly well with those obtained from charge transfer measurements. Peover⁽¹⁰⁹⁾ has combined the techniques of charge transfer spectroscopy and polarography with the direct measurement of the gas phase electron affinity. He used the value of the electron affinity of benzoquinone as found by the magnetron technique⁽⁵⁰⁾ as a reference value to establish the electron affinities of a number of monosubstituted benzoquinones, from polarographic half wave reduction potentials and charge transfer data. These values were lower than the values found by the magnetron⁽⁵⁰⁾, again probably due to the

assumption of constant interaction energies. Because of the difficulty of estimating the solvation energies it is not possible to obtain electron affinities directly from polarographic data, but rather calculated electron affinities or those obtained from charge transfer spectroscopy are used to estimate solvation energies.

Although absolute values for electron affinities may not at present be obtained from polarographic data, relative values can usefully be found as they can also from charge transfer spectra

5.5 Dipole moments and electron affinities

Since the electron affinity of a molecule may be defined as the work done in bringing up an electron from infinity to the lowest unoccupied orbital, it should be possible to calculate this energy from the amount of work done against the field produced by assembly of bond dipoles forming the molecule. The potential at a point is equal to the work done in bringing unit charge from infinity to that point and hence the potential at the centre of the molecule may be taken to be its electron affinity. For one dipole of moment μ whose centre is at a distance r from the centre of the molecule, this potential is given by electrostatic theory as $\mu \cos \theta / r^2$ where θ is the angle between the axis of the dipole and the line of distance r . This may be summed over all the dipoles to give the electron affinity of a molecule as $\sum (\mu \cos \theta / r^2)$. The point of action of the dipole is difficult to ascertain because of the uneven distribution of charge but it has been suggested that about three-quarters of the way

along the bond between the molecule and substituent may be taken as a useful guide⁽¹¹¹⁾. The contribution due to several substituents in the benzene ring has been calculated and is tabulated in column 3 of table 5.3. The total electron affinity of substituted benzene is due to the sum of the contributions of the substituents and the contribution of the ring itself, or 'ring affinity'. This ring affinity, RA, obtained from the difference in the measured and calculated values of the electron affinity of the molecules is tabulated in column 2 of table 5.4., and is seen to be variable and of rather a large negative value giving benzene an electron affinity of the order of -70 kcal/mole which seems an unreasonably large negative value.

An alternative approach is to regard the dominant contribution of a dipole to be due to the interaction of its field with the excess electron density at every carbon atom except that to which the group is attached⁽¹¹²⁾. If one assumes a uniform charge distribution in the molecule and the extra electron to be distributed equally at each of the other five carbon atoms the contribution to the electron affinity due to each dipole is

$$1/5 \sum (\mu e \cos \phi / l^2)$$

l is the distance between the centre of action of the dipole and another carbon atom, and ϕ is the angle between the line of length l and direction of the dipole.

As is seen from column 4 of table 5.3 the values obtained using this model are slightly less than those from the electron at the centre model but they still give variable and large values for

the ring affinity (column 3, table 5.4).

Compton (113) has found temporary negative resonance for some fluoro-substituted negative ions and has found the electron affinity values to lie on a line whose equation is

$$E.A. = -35.6 + 10.6n \text{ kcal/mole} \quad \dots \quad (5.10)$$

where n is the number of fluorine atoms substituted in the benzene ring. This would predict a difference of 10.6 kcal/mole between the electron affinity contribution due to the hydrogen and fluorine substituents, but from the figures in column 3, table 5.3, it is seen to be of the order of 20 kcal/mole. Also the electron affinity of benzene from equation 5.10 is -35.6 kcal/mole so that if the hydrogens have a contribution of -5 kcal/mole, the ring affinity should be about 7 kcal/mole which is much smaller than the values in table 5.4, columns 2 and 3. This discrepancy could be due to the neglect of dipole interactions. Each dipole produces a field at the other dipoles and hence the effective field is the algebraic sum of these fields. Reduced dipoles are therefore calculated for the molecules in table 5.4. The reduced dipoles μ_{red} were then used to re-calculate a new reduced dipole and the procedure repeated three times when reasonable consistency was obtained. Electron affinity contributions were then calculated using the reduced dipoles from the expression

$$E. = 1/5 \sum (\mu_{\text{red}} e \cos \phi / r^2)$$

and added to obtain the molecular electron affinities in column 4, table 5.4. The values of the ring affinity were calculated as before

from the difference in measured and calculated values. The results are in fairly good agreement with the data obtained by Compton since the difference between the contribution from a hydrogen and fluorine atom is 13.8 kcal/mole compared with a value of 10.6 from equation 5.10. Also the electron affinity of benzene (taking the mean of the ring affinities 6.3 kcal/mole) is -32.7 kcal/mole compared with a value of ~~-35.6~~ kcal/mole from equation 5.10. The reason for the anomalous result from hexafluorobenzene is not clear but may be due to the fact that an even greater reduction of the dipoles occurs with complete fluorine substitution. On the basis of equation 5.10, the measured electron affinity and the mean value of the ring affinity, the reduced C - F dipole in C_6F_6 may be found to be 0.5 D which is about half the calculated dipole.

From the measurements made by Compton ⁽¹¹³⁾ on C_6H_6 , C_6H_5F , and $C_6H_4F_2$ and $C_6H_3F_3$ the extrapolated value for the electron affinity of C_6F_6 is 26.6 kcal/mole which is in excellent agreement with the present magnetron result of 26.0 kcal/mole.

In view of the crude approximations used the agreement between the calculated and measured values of the 'substituent contributions' is good, provided dipole-dipole interaction is not neglected, and an additive effect is justified. For more accurate calculations, however, it would be necessary to know the charge distribution around the ring and the precise nature of the interaction between the dipoles.

Table 5.3

bond	1	2	3	4
	bond length o A	bond dipole (D) (111)	$\mu \cos \theta / r^2$ (kcal/mole)	$1/5 \sum (\mu \cos \phi / l^2)$ (kcal/mole)
C - H	1.08	-0.4	-5.65	-4.4
C = O	1.23	2.30	29.3	23.9
C - Cl	1.7	1.32	12.4	10.5
C - F	1.3	1.4	16.8	14.4

Table 5.4

Compound	Energy values (kcal/mole) calculated as in key below						
	1	2		3		4	
	E	E	R.A.	E	R.A.	E	R.A.
Benzoquinone	25.8	36.0	-10.2	30.2	-4.4	34.0	-8.2
Fluoranyl	55.2	135.8	-80.6	105.4	-50.2	60.4	-5.2
Chloranyl	44.1	108.2	-64.1	89.8	-45.7	49.8	-5.7
Perfluoro- benzene	26.0	100.8	-74.8	86.4	-60.4	56.4	-30.4

Key: 1/ Measured by the magnetron technique (chapter 3)

2/ Calculated from $E = \sum (\mu \cos \theta / r^2)$

3/ Calculated from $E = 1/5 \sum (\mu \cos \phi / l^2)$

4/ Calculated from $E = 1/5 \sum (\mu_{\text{red}} \cos \phi / l^2)$

5.6 Conclusion

This study has been an attempt to find a method of measuring the electron affinities of fairly large polyatomic molecules. Using the magnetron technique it was possible to estimate the electron affinities of a few neutral molecules and a number of radicals. The method could not, however, be applied to large aromatic molecules whose vapour pressure was so low that it was not possible to obtain a sufficient concentration of the molecules in the magnetron. The electron capture detector offered another possible method of measuring electron affinities. The compounds which had been examined in the magnetron were studied in the electron capture cell to see if similar values could be obtained by both methods. It was found that the detector responded to electron collision cross sections rather than to the electron affinity of the molecules, and that until the relationship between these two factors is known, electron affinities may not be obtained directly by this method. The values measured using the magnetron technique are higher than those obtained from the study of compounds in solution, that is from charge transfer spectroscopy and polarography. This is possibly due to the neglect of various interaction energies or the assumption that these are constant for a series of compounds.

Although the magnetron technique has been useful in measuring the stability of a number of negative ions it is limited by certain conditions which the compounds studied must satisfy, such as a

suitable vapour pressure and an electron affinity of at least 1 eV. Therefore it will be necessary for further work to be done on the development of new techniques, or the modification of existing ones before it is possible to draw up an extensive table of the electron affinities of polyatomic molecules.

REFERENCES

1. Szent Györgyi, "Introduction to Submolecular Biology", (Academic Press 1960).
2. Nash and Allison, Biochem. Pharmacol., 12 601 (1963).
3. Nash and Allison, Nature, 195 994 (1962).
4. Karreman, Isenberg and Szent Gyorgi, Science, 130 1191 (1959).
5. Lyons and Mackie, Nature, 197 589 (1963).
6. Mason, Nature, 181 820 (1958).
7. Lovelock, Zlatkis and Becker, Nature, 193 540 (1962)
8. Allison and Lightbrown, Nature, 189 892 (1961).
9. Field and Franklin, "Electron impact phenomena", (Academic Press 1957).
10. Lossing, Ingold and Henderson, J. Chem. Phys. 22 621 (1954).
11. Wacks and Dibeler, ibid, 31 1557 (1959).
12. Pople, Trans. Farad. Soc., 49 1375 (1953).
13. Hoyland and Goodman, J. Chem. Phys., 36 21 (1962).
14. Tsuda and Hamill, J. Chem. Phys., 41 2713 (1964).
15. Glocker and Calvin, ibid, 4 492 (1936, 3 771 (1935)).
16. Dukel'skii and Ionov, J. Exptl. Theoret. Phys. (USSR), 10 1248 (1940)
17. Sutton and Mayer, J. Chem. Phys., 2 145 (1934), 3 20 (1935).
18. Branscomb, Smith and Tisona, ibid, 43 2906 (1965).
19. Berry, Mackie, Taylor and Lynch, ibid, 43 3067 (1965).
20. Waddington "Advances in Inorganic Chemistry and Radiochemistry"
Vol 1 (Academic Press 1959).
21. Ladd and Lee, "Progress in Solid State Chemistry" Vol 1
(Pergamon Press 1964).

22. Hush and Pople, *Trans. Farad. Soc.*, 51 600 (1955)
23. Ehrenson, *J. Phys. Chem.*, 66 706 (1961)
24. Scott and Becker *ibid*, 66 2713 (1962)
25. Hedges and Matsen, *J. Chem. Phys.*, 28 950 (1958)
26. Page, *Trans. Farad. Soc.*, 56 1742 (1960)
27. Page, *Nature*, 188 1021 (1960)
28. Page, *Trans. Farad. Soc.*, 57 359 (1961)
29. Page, *ibid*, 57 1254 (1961)
30. Ansdell and Page, *ibid*, 58 1084 (1962)
31. Napper and Page, *ibid*, 59 1086 (1963)
32. Gaines and Page, *ibid*, 59 1266 (1963)
33. Kay and Page, *Nature*, 199 483 (1963)
34. Kay and Page, *Trans. Farad. Soc.*, 60 1042 (1964)
35. Farragher, Page and Wheeler, *Disc. Farad. Soc.*, 37 203 (1964)
36. Gaines, Kay and Page, *Trans. Farad. Soc.*, 62 874 (1966)
37. Farragher and Page, *ibid*, 62 3072 (1966)
38. Kay and Page, *ibid* 62 3081 (1966)
39. Farragher and Page, *ibid*, 63 2367 (1967)
40. Page, "Final Technical Report", U.S. Army Contract No DA-91-591
EUC-3870
41. Morton, *Endeavour*, 24 81 (1965)
42. Lovelock and Lipsky, *J. Amer. Chem. Soc.*, 82 431 (1960)
43. Wentworth and Becker, *ibid*, 84 4263 (1962)
44. Briegleb, *Angew. Chem.*, international edition Vol 3 617 (1964)
45. Moelwyn-Hughes, "Physical Chemistry", 2nd edition
(Pergamon Press 1961)
46. Hayward and Trapnel, "Chemisorption" Butterworth (London 1964)

47. Eley, Disc. Farad. Soc., 8 34 (1950)
48. Hull, Phys. Rev., 18 31 (1921)
49. Parker, "Electronics", (Arnold, London 1963)
50. Farragher - Ph.D. Thesis, University of Aston (1966)
51. Tilney, Barret and Walters, J. Chem. Soc., 3123 (1959)
52. Berry and Reinman, J. Chem. Phys., 38 1540 (1963)
53. Branscombe Burch and Geltmann, Phys. Rev., 111 504 (1958)
54. Cottrell "The Strength of Chemical Bonds", Butterworth (1958)
55. Szwarc and Williams, J. Chem. Phys., 20 1171 (1952)
56. Duncan and Trotman-Dickenson, J. Chem. Soc., 4672 (1962)
57. Skinner and Pilcher, Quat. Revs., 17 264 (1963)
58. Bernstein, Trans. Farad. Soc., 58 2285 (1962)
59. Ladacki and Szwarc, Proc. Roy. Soc., A 219 341 (1953)
60. Herron, Rosenstock and Shields, Nature, 206 611 (1965)
61. Rees, Dip. Tech. Thesis, University of Aston (1964)
62. Finar "Organic Chemistry" Vol. 1 (Longmans 1959 3rd Edition)
63. Speros and Rossini, J. Phys. Chem., 64 1723 (1960)
64. Kovats, Guntherd and Plattner, Helv. Chim. Acta, 38 1912 (1955)
65. Harrison, Honnen, Dauben and Lossing, J. Amer. Chem. Soc.,
82 5593 (1960)
66. Bralsford, Harris and Price, Proc. Roy. Soc., A (258) 459 (1960)
67. Farmer, Henderson, Lossing and Marsden, J. Chem. Phys.,
24 348 (1956)
68. Warren and Craggs, Mass Spectrometry Institute of Petroleum
(London 1952)
69. Dibeler, Rees and Mohler, J. Research Nat. Bur. Standards,
57 113 (1956)

70. Sehon and Szwarc, Proc. Roy. Soc., (A) 209 110 (1951)
71. Rabinovitch and Reed, J. Chem Phys., 22 2092 (1954)
72. Dibeler, Rees and Mohler, J. Chem. Phys., 26 304 (1957)
73. Bibby and Carter, Trans Farad. Soc., 62 2637 (1966)
74. Bayley and Page, (unpublished work)
75. Moss, M.Sc. Thesis, University of Wales (1967)
76. Gillman and Blatt, Organic Synthesis, Collective Vol 1.
77. Schmit and Peters, Facts and Methods for Scientific Research,
Vol. 5 No. 2 (1964)
78. Lovelock, Nature, 187 49 (1960), *ibid*, 188 401 (1960),
ibid, 189 729 (1961)
79. Becker and Wentworth, J. Amer. Chem Soc., 85 2210 (1963)
80. Lovelock, Analytical Chem., 35 474 (1963)
81. Wentworth, Chen and Lovelock, J. Phys. Chem., 70 445 (1966)
82. Wentworth and Chen, J. Gas Chromatography, 170 (1967)
83. Professor S.E. Hunt, University of Aston, Private
Communication.
84. Strominger and Hollannder, Rev. Mod. Phys., 30 585 (1958)
85. Huck, Dip. Tech. Thesis, University of Aston (1965)
86. Massey and Burhop, "Electronic and Ionic Impact Phenomema"
Oxford Clarendon Press 1952.
87. Fox and Hobson, Advisory Group for Aerospace Research and
Development, 30 Propulsion and Energetics Panel Meeting,
Munich(1967).
88. Gaydon and Wolfhard "Flames - Their structure and Properties",
(Chapman and Hall, London 1960).

89. Stuckey and Saylor, J. Amer. Chem. Soc., 62 292 1940
90. Andrews, J. Phys. Chem., 30 1497 1926
91. Mortimer and Murphy, Ind. Eng. Chem., 15 1140 (1923)
92. Private communication from "Imperial Smelting Co. Ltd."
93. Rowlinson and Thacker, Trans. Farad. Soc., 53 1 1957
94. Coolidge and Coolidge, J. Amer. Chem. Soc., 49 100 1927
95. Handbook of Chemistry and Physics, 48th edition (Chemical Rubber Co. 1967)
96. Phelps and Pack, Tenth Combustion Institute 1965
97. Pauling "Nature of the Chemical Bond and the structure of molecules and crystals" (Cornell University Press 1960)
98. Pritchard, Chem. Revs., 52 529 (1953)
99. Cubicciotti, J. Chem. Phys., 31 1646 (1959), 33 1579 (1960), 34 2189 (1961),
100. Mulliken, J. Amer. Chem. Soc., 72 600 (1950) *ibid.*, 74 811 (1952) J. Phys. Chem., 56 801 (1952)
101. Hastings, Franklin, Schiller and Matsen, J. Amer. Chem. Soc., 75 2900 (1953)
102. Jortner and Sokolov, Nature, 190 1 (1961)
103. Batley and Lyons, *ibid.*, 196 573 (1962)
104. Hough, B.Sc. Project thesis, University of Aston (1967)
105. Matsen, J. Chem. Phys., 24 602 (1956)
106. Maccoll, Nature, 163 178 (1949)
107. Lyons, *ibid.*, 166 193 (1950)
108. Eley and Evans, Trans. Farad. Soc., 34 1093 (1938)
109. Peover, J. Chem. Soc., 4540 1962

110. Davis, Hammond and Peover, Trans. Farad. Soc., 61 1516 (1965)
111. Smyth, "Dielectric Behaviour and Structure" (McGraw-Hill 1955)
112. Murrell and Williams, Proc. Roy. Soc., Series A 291 224 (1966)
113. Compton, Private communication to Professor F.M. Page.